UNIVERSITY OF CAPE TOWN
IYUNIVESITHI YASEKAPA • UNIVERSITEIT VAN KAAPSTAD

ANALYSIS AND COMPARISON OF THE SOUTH AFRICAN AND EUROCODE LIVE LOAD MODELS FOR RAILWAY BRIDGES

by

SHERYL DAWN PAULSE

Dissertation submitted in partial fulfilment of the requirements for the degree

Master of Engineering: Structures

in the FACULTY OF ENGINEERING & THE BUILT ENVIRONMENT
DEPARTMENT OF CIVIL ENGINEERING

at the University of Cape Town

Supervisor: Prof P. Moyo

Submitted March 2017

Copyright

The dissertation may not be published either in part (in scholarly, scientific or technical journals), or as a whole (as a monograph), unless permission has been obtained from the University

DECLARATION

I know the meaning of plagiarism and declare that all the work in the document, save for that which is properly acknowledged, is my own. This thesis/dissertation has been submitted to the Turnitin module (or equivalent similarity and originality checking software) and I confirm that my supervisor has seen my report and any concerns revealed by such have been resolved with my supervisor.

Signed by candidate

10/4/2017

Date

ABSTRACT

This dissertation is an analytical study that compares the South African Transport Services (SATS) and Eurocode (EC) live load models for railway bridges. The study is specifically concerned with the critical load effects of shear and bending moment. The load models are simulated as moving loads over the full length of simply supported and continuous railway systems with speeds not exceeding 180km/h. The study is limited to short to medium spans ranging from 5m – 40m analysed in increments of 5m.

The position of the maximum load effects for simply supported systems was determined using the frame analysis module in Prokon. Maximum load effects were determined using the influence line method. Maximum load effects for the continuous systems were determined using the moving load option in STRAP.

It was found that SATS live load models imposed on single span railway bridges, produce conservative load effects for short span bridges but become over conservative with an increase in span, when compared with characteristic values of the EC load model 71 (LM71). For heavy loads (α = 1,10) in LM71, there is a good comparison with that of the EC for static and design moment (for a track with standard maintenance) with values of 5% lower at 10m but become moderately conservative (2% - 5%) with an increase in span. In the case of design bending moment (for a carefully maintained track) the SATS code is moderately conservative (6% - 8%) over the full range of spans for a carefully maintained track.
For heavy loads (α = 1,10) in LM71, there is a good comparison with that of the Eurocode for static and design shear (for a carefully maintained track) with values of 4% lower at 10m but becoming moderately conservative (1% - 5%) with an increase in span. In the case of design shear (for a track with standard maintenance) the SATS code compares well with that of the EC, with values of 5% lower at 10m but becoming moderately conservative (4% - 13%) with an increase in span.

Live traffic loads imposed on equal span (limited to 2) continuous railway bridges, produce conservative static and design shear load effects (for a carefully maintained track) in the mid-range of spans but become moderately conservative with increase in span for heavy loads (α = 1,10) for load model SW/0. There is a good comparison with that of the EC for design shear force (for a carefully maintained track) with moderately conservative (1% - 9%) for short span and long span systems for heavy loads (α = 1,10) for load model SW/0. A similar

comparison occurs for heavy loads (α = 1,21) for SW/0 for static and design shear for a carefully maintained track.
Live traffic loads imposed on equal span (limited to 2) continuous railway bridges produce over conservative static bending moment load effects for short span and long span bridges (2 x 30m – 2 x 40m) for characteristic values and heavy loads (α = 1,10 and α = 1,21) for load model SW/0. Generally, there is not a good comparison with that of the EC for static and design bending moment, for two span continuous railway bridges.

Live traffic loads imposed on equal span (limited to 3) continuous railway bridges produce moderately conservative static shear force effects for heavy loads (α = 1,10 and α = 1,21) for load model SW/0. The only significant value is at the 3 x 5m span (21% higher) and the 3 x 15 – 3 x 20m range of spans (9% - 10% lower) for heavy loads (α = 1,10) and (α = 1,21) respectively. A similar comparison is observed for design shear effects for both types of track for heavy loads (α = 1,10) and (α = 1,21) for a carefully maintained track. Generally, there is not a good comparison with that of the Eurocode for static and design bending moment, for three span continuous railway bridges.

Keywords: Eurocode, SATS, NR load model, LM71 load model, SW/0 load model, moving loads, load effects.

ACKNOWLEDGEMENTS

I wish to thank:

- God for His grace, guidance, wisdom and for being my source of strength and courage to persevere throughout this dissertation.
- My husband, James, for your prayers, patience, encouragement and your faith in me and for the tremendous support you've shown throughout this dissertation. Through times of despair, you have encouraged me to put my faith and trust in God rather than lean on my own understanding.
- Mr Pieter Louw for unselfishly sacrificing time between business trips to Cape Town to train me in the use of the STRAP software. Thank you for availing yourself to attend to all my queries and allowing me the use of the STRAP software for this dissertation.
- Dr Vitalii Artomov for your helpfulness and assistance in the translation of parts of your journal article.
- My colleagues in the civil engineering department for your encouragement.
- To my supervisor, Prof. Pilate Moyo, for being so patient with me during my years of study.

DEDICATION

To my late parents, George Malcolm and Eileen Petronella Smith,
who endured many challenges in their endeavour
to provide me with the best education.

TABLE OF CONTENTS

	Declaration	**ii**
	Abstract	**iii**
	Acknowledgements	**v**
	Dedication	**vi**
	Glossary	**xvii**

CHAPTER ONE: INTRODUCTION

1.1	**Background**	**1**
1.2	**Objectives of the dissertation**	**4**
1.3	**Scope and Limitations of the study**	**4**
1.4	**Organisation of the study**	**5**

CHAPTER TWO: REVIEW OF THE CODES

2.1	**Introduction**	**6**
2.2	**Review of the South African railway bridge loads**	**6**
2.3	**SATS design requirements**	**8**
2.4	**Review of Eurocode**	**9**
2.5	**Structure of Eurocode Rail Traffic Load Models**	**10**
2.6	**Eurocode design analysis requirements**	**12**
2.7	**Summary**	**14**

CHAPTER THREE: METHODOLOGY: APPLICATION OF LIVE LOADS

3.1	**Introduction**	**16**
3.2	**Overview of analysis methods**	**16**
3.2.1	Overview of Prokon	16
3.2.2	Overview of the influence line analysis method	17
3.2.3	Overview of STRAP analysis for continuous beams	18
3.3	**Analysis of single span systems**	**18**
3.3.1	Approximation of position for maximum bending moment	18
3.3.2	Static analysis: Influence line analysis for LM71 and NR load model for evaluating bending moment	20

3.3.3 Static analysis: Influence line analysis applied to LM71 and NR load model for evaluating shear force 24
3.3.4 Requirement for dynamic analysis 26
3.4 Analysis of continuous beams 26
3.4.1 Analysis of South African NR load model for continuous beams 27
3.4.2 Analysis of Eurocode SW/0 load model for continuous beams 28
3.5 Summary 29

CHAPTER FOUR: RESULTS AND DISCUSSION

4.1 Introduction 31
4.2 Results for simply supported beams 31
4.2.1 Approximate position of maximum bending moment 31
4.2.2 LM71 and NR load model positions for maximum bending moment 32
4.2.3 LM71 and NR load model positions for maximum shear 35
4.2.4 Influence line method results for LM71 and NR load model for maximum shear 36
4.2.5 Dynamic analysis test results for load model 71 36
4.3 Results for continuous systems 37
4.3.1 Mmax results for 2 span continuous systems 37
4.3.2 Vmax results for 2 span continuous systems 38
4.3.3 Mmax results for 3 span continuous systems 39
4.3.4 Vmax results for 3 span continuous systems 40
4.4 Discussion of the comparison between the SATS and the Eurocode 41
4.4.1 Simply supported systems 41
4.4.2 Continuous systems 45
4.5 Summary 54

CHAPTER FIVE: CONCLUSIONS AND RECOMMENDATIONS 57

5.1 Conclusions 57
5.2 Recommendations 61

REFERENCES 60

LIST OF FIGURES

Figure 2.1: NR load model 7
Figure 2.2: Type RU loading 7
Figure 2.3: Load model 71 10
Figure 2.4: Load model SW/0 11
Figure 2.5: Flowchart for determining whether a dynamic analysis is required 13
Figure 2.6: Limits of bridge natural frequency n0 [Hz] as a function of L [m] 14
Figure 3.1: Symmetrical arrangement of loading for 10m span: first trial 19
Figure 3.2: Loading positions for trials spans 20
Figure 3.3: Vertical load arrangement for load model 71 in terms of 'x' 20
Corresponding influence line diagram for bending moment at axle load Qvk3
Figure 3.4: Vertical load arrangement for NR loading in terms of 'x' 21
Corresponding influence line diagram for bending moment at axle load Qvk3
Figure 3.5: Influence line diagram for maximum shear for load model 71 25
Figure 3.6: Influence line diagram for maximum shear for SATS NR loading 25
Figure 3.7: Cross section of beam 27
Figure 3.8: Arrangement of NR load model for 2 x 5m continuous beam 27
Figure 3.9: Leading UDL for NR load model on 2 x 5m continuous beam 27
Figure 3.10: Trailing UDL for NR load model on 2 x 5m continuous beam 28
Figure 3.11: Arrangement of SW/0 load model for a 2 x 5m continuous beam 29
Figure 4.1: Position of the loads on 10m, 25m and 40m spans for Mmax 32
Figure 4.2: Load position for Mmax for 5m simply supported system 33
Figure 4.3: Load position for Mmax for 10m simply supported system 33
Figure 4.4: Load position for Mmax for 15m simply supported system 33
Figure 4.5: Load position for Mmax for 20m simply supported system 33
Figure 4.6: Load position for Mmax for 25m simply supported system 34
Figure 4.7: Load position for Mmax for 30m simply supported system 34
Figure 4.8: Load position for Mmax for 35m simply supported system 34
Figure 4.9: Load position for Mmax for 40m simply supported system 34
Figure 4.10: Load arrangement for Vmax for load model LM71 35
Figure 4.11: Ratio of static Mmax (kNm) for LM71 and NR load models 41
Figure 4.12: Ratio of static Vmax (kN) for LM71 and NR load models 42
Figure 4.13: Ratio of design Mmax (kNm) for LM71 and NR load models 43

Figure 4.14: Ratio of design Vmax (kN) for LM71 and NR load models 44
Figure 4.15: Ratio of static Mmax (kNm) for NR and SW/0 load models (2 span systems) 47
Figure 4.16: Ratio of static Vmax (kN) for NR and SW/0 load models (2 span systems) 48
Figure 4.17: Ratio of design Mmax (kNm) for NR and SW/0 load models (2 span systems) 49
Figure 4.18: Ratio of design Vmax (kN) for NR and SW/0 load models (2 span systems) 50
Figure 4.19: Ratio of static Mmax (kNm) for NR and SW/0 load models (3 span systems) 51
Figure 4.20: Ratio of static Vmax (kN) for NR and SW/0 load models (3 span systems) 52
Figure 4.21: Ratio of design Mmax (kNm) for NR and SW/0 load models (3 span systems) 53
Figure 4.22: Ratio of design Vmax (kN) for NR and SW/0 load models (3 span systems) 54

LIST OF TABLES

Table 2.1:	Dynamic factor for NR loading	9
Table 3.1:	Influence line ordinates for load model 71 and NR loading	21
Table 4.1:	Approximate position for maximum bending moment on 10m, 25m and 40m spans	32
Table 4.2:	Natural frequency (n_0) values	36

APPENDICES

Appendix A: **64**

Table A.1: Static Mmax (kNm) for SATS NR and Eurocode LM71 loading 64

Table A.2: Design Mmax (kNm) for SATS NR and Eurocode LM71 loading 64

Table A.3: Static Vmax (kN) for Eurocode LM71 and SATS NR load model 65

Table A.4: Design Vmax (kN) for Eurocode LM 71 and SATS NR loading 65

Appendix B:

B.1 STRAP results – 2 span (SATS) systems 66

Table B.1: NR load model - 2 x 5m system 66

Table B.2: NR load model - 2 x 10m system 66

Table B.3: NR load model - 2 x 15m system 66

Table B.4: NR load model - 2 x 20m system 66

Table B.5: NR load model - 2 x 25m system 67

Table B.6: NR load model - 2 x 30m system 67

Table B.7: NR load model - 2 x 35m system 67

Table B.8: NR load model - 2 x 40m system 67

B.2 STRAP results – 2 span (Eurocode) systems 68

Table B.9: SW/0 load model - 2 x 5m system 68

Table B.10: SW/0 load model - 2 x 10m system 68

Table B.11: SW/0 load model - 2 x 15m system 68

Table B.12: SW/0 load model - 2 x 20m system 68

Table B.13: SW/0 load model - 2 x 25m system 69

Table B.14: SW/0 load model - 2 x 30m system 69

Table B.15: SW/0 load model - 2 x 35m system 69

Table B.16: SW/0 load model - 2 x 5m system 69

B.3 STRAP results – 3 span (SATS) systems 70

Table B.17: NR load model - 3 x 5m system 70

Table B.18: NR load model - 3 x 10m system 70

Table B.19: NR load model - 3 x 15m system 70

Table B.20: NR load model - 3 x 20m system 70

Table B.21: NR load model - 3 x 25m system 71

Table B.22: NR load model - 3 x 30m system 71

Table B.23: NR load model - 3 x 35m system 71

Table B.24: NR load model - 3 x 40m system 71

B.4 STRAP results – 3 span (Eurocode) systems 72

Table B.25: SW/0 load model - 3 x 5m system 72

Table B.26: SW/0 load model - 3 x 10m system 72

Table B.27: SW/0 load model - 3 x 15m system 72

Table B.28: SW/0 load model - 3 x 20m system 72

Table B.29: SW/0 load model - 3 x 25m system 73

Table B.30: SW/0 load model - 3 x 30m system 73

Table B.31: SW/0 load model - 3 x 35m system 73

Table B.32: SW/0 load model - 3 x 40m system 73

Appendix C: 74

C.1 STRAP results – Mmax position for 2 span (SATS) systems 74

Figure C.1: Load position for Mmax for 2 X 5m system (SATS NR load model) 74

Figure C.2: Load position for Mmax for 2 X 10m system (SATS NR load model) 74

Figure C.3: Load position for Mmax for 2 X 15m system (SATS NR load model) 74

Figure C.4: Load position for Mmax for 2 X 20m system (SATS NR load model) 74

Figure C.5: Load position for Mmax for 2 X 25m system (SATS NR load model) 75

Figure C.6: Load position for Mmax for 2 X 30m system (SATS NR load model) 75

Figure C.7: Load position for Mmax for 2 X 35m system (SATS NR load model) 75

Figure C.8: Load position for Mmax for 2 X 40m system (SATS NR load model) 75

C.2 STRAP results – Mmax position for 2 span (Eurocode) systems 76

Figure C.9: Load position for Mmax for 2 X 5m system (SW/0 load model) 76

Figure C.10: Load position for Mmax for 2 X 10m system (SW/0 load model) 76

Figure C.11: Load position for Mmax for 2 X 15m system (SW/0 load model) 76

Figure C.12: Load position for Mmax for 2 X 20m system (SW/0 load model) 76

Figure C.13: Load position for Mmax for 2 X 25m system (SW/0 load model) 77

Figure C.14: Load position for Mmax for 2 X 30m system (SW/0 load model) 77

Figure C.15: Load position for Mmax for 2 X 35m system (SW/0 load model) 77

Figure C.16: Load position for Mmax for 2 X 40m system (SW/0 load model) 77

C.3 STRAP results – Vmax position for 2 span (SATS) systems 78

Figure C.17: Load position for Vmax for 2 X 5m system (NR load model) 78

Figure C.18: Load position for Vmax for 2 X 10m system (NR load model) 78

Figure C.19: Load position for Vmax for 2 X 15m system (NR load model) 78

Figure C.20: Load position for Vmax for 2 X 20m system (NR load model) 78

Figure C.21: Load position for Vmax for 2 X 25m system (NR load model) 79

Figure C.22: Load position for Vmax for 2 X 30m system (NR load model) 79

Figure C.23: Load position for Vmax for 2 X 35m system (NR load model) 79

Figure C.24: Load position for Vmax for 2 X 40m system (NR load model) 79

C.4 STRAP results – Vmax position for 2 span (Eurocode) systems 80

Figure C.25: Load position for Vmax for 2 X 5m system (SW/0 load model) 80

Figure C.26: Load position for Vmax for 2 X 10m system (SW/0 load model) 80

Figure C.27: Load position for Vmax for 2 X 15m system (SW/0 load model) 80

Figure C.28: Load position for Vmax for 2 X 20m system (SW/0 load model) 80

Figure C.29: Load position for Vmax for 2 X 25m system (SW/0 load model) 81

Figure C.30: Load position for Vmax for 2 X 30m system (SW/0 load model) 81

Figure C.31: Load position for Vmax for 2 X 35m system (SW/0 load model) 81

Figure C.32: Load position for Vmax for 2 X 40m system (SW/0 load model) 81

Appendix D:

D.1 STRAP results – Mmax position for 3 span (SATS) systems 82

Figure D.1: Load position for Mmax for 3 X 5m system (NR load model) 82

Figure D.2: Load position for Mmax for 3 X 10m system (NR load model) 82

Figure D.3: Load position for Mmax for 3 X 15m system (NR load model) 82

Figure D.4: Load position for Mmax for 3 X 20m system (NR load model) 82

D.2 PROKON results – Mmax position for 3 span (SATS) systems 83

Figure D.5: Load position for Mmax for 3 X 25m system (NR load model) 83

Figure D.6: Load position for Mmax for 3 X 30m system (NR load model) 83

Figure D.7: Load position for Mmax for 3 X 35m system (NR load model) 83

Figure D.8: Load position for Mmax for 3 X 40m system (NR load model) 83

D.3 STRAP results – Mmax position for 3 span (Eurocode) systems 84

Figure D.9: Load position for Mmax for 3 X 5m system (SW/0 load model) 84

Figure D.10: Load position for Mmax for 3 X 10m system (SW/0 load model) 84

Figure D.11: Load position for Mmax for 3 X 15m system (SW/0 load model) 84

Figure D.12: Load position for Mmax for 3 X 20m system (SW/0 load model) 84

Figure D.13: Load position for Mmax for 3 X 25m system (SW/0 load model) 84

Figure D.14: Load position for Mmax for 3 X 30m system (SW/0 load model) 85

Figure D.15: Load position for Mmax for 3 X 35m system (SW/0 load model) 85

Figure D.16: Load position for Mmax for 3 X 40m system (SW/0 load model) 85

D.4 STRAP results – Vmax position for 3 span (SATS) systems 85

Figure D.17: Load position for Vmax for 3 X 5m system (NR load model) 85

Figure D.18: Load position for Vmax for 3 X 10m system (NR load model) 85

Figure D.19: Load position for Vmax for 3 X 15m system (NR load model) 86

Figure D.20: Load position for Vmax for 3 X 20m system (NR load model) 86

Figure D.21: Load position for Vmax for 3 X 25m system (NR load model) 86

Figure D.22: Load position for Vmax for 3 X 30m system (NR load model) 86

Figure D.23: Load position for Vmax for 3 X 35m system (NR load model) 86

Figure D.24: Load position for Vmax for 3 X 40m system (NR load model) 87

D.5 STRAP results – Vmax position for 3 span (Eurocode) systems 87

Figure D.25: Load position for Vmax for 3 X 5m system (SW/0 load model) 87

Figure D.26: Load position for Vmax for 3 X 10m system (SW/0 load model) 87

Figure D.27: Load position for Vmax for 3 X 15m system (SW/0 load model) 87

Figure D.28: Load position for Vmax for 3 X 20m system (SW/0 load model) 87

Figure D.29: Load position for Vmax for 3 X 25m system (SW/0 load model) 88

Figure D.30: Load position for Vmax for 3 X 30m system (SW/0 load model) 88

Figure D.31: Load position for Vmax for 3 X 35m system (SW/0 load model) 88

Figure D.32: Load position for Vmax for 3 X 40m system (SW/0 load model) 88

GLOSSARY

List of acronyms

EC	Eurocode
FEA	Finite element analysis
FEM	Finite element method
Prokon	Prokon Structural Analysis and Design
RDP	Radio Distributed Power
RU	Railway Upper
SATS	South African Transport Services
STRAP	STRuctural Analysis Program
TFR	Transnet Freight Rail
UDL	Uniformly distributed load

List of symbols

L_ϕ	Determinant length
n_0	Natural frequency
P	Nodal force matrix
Q_{sk}	Characteristic value of nosing force
q_{vk}	Characteristic value of vertical load (uniformly distributed load)
Q_{vk}	Characteristic value of vertical load (concentrated load)
ϕ_3	Dynamic factor

CHAPTER ONE
INTRODUCTION

1.1 Background

Typically live loading dominates all other design considerations in railway bridge design (Arema, 2003). In addition to the usual live loads carried by rail traffic there are dynamic components of rail traffic such as impact, centrifugal, lateral and longitudinal forces that are added to live loads (Arema, 2003:). Each country has its own loading code that is based on the requirements and conditions of that particular country. However, due to the complexity of train loads, all rail traffic live loads are simplified as load models in design loading codes. The load models are depicted as point (axle) loads and/or uniformly distributed loads that represent the predicted external loads, which will be applied to the railway bridge.

In South Africa, railway bridge load models are specified in the SATS bridge code. The live load models in SATS are based on BS 5 400-2:1978 (SATS Bridge Code,1983). South African railway bridge design uses the structure of the RU load model specified in BS 5 400-2:1978. The values for the point (axle) and uniformly distributed loading have however been increased to suit the conditions for South African bridges. In 2010, BS 5400-2:1978 was superseded by Eurocode structural codes for design of new bridges. The structure of the RU load model as well as the load values, remained the same, but the load model was renamed as load model LM71 in the Eurocode standard. Despite the replacement of BS 5400-2:1978 and the standardisation of European countries' design codes into a harmonised national document, South Africa continues to use the SATS bridge loading code for bridge design, in conjunction with the highway bridge loading code TMH7.

The superseding of national design rules applicable to European member states with a set of standardised Eurocode structural design codes, presented many challenges for European member states (EN 1991-2:2003). Implementation of the standardised Eurocode design codes compelled European member states to establish ways to align country specific design codes with those of Eurocode (EN 1991-2:2003). This entailed incorporating additional country specific information to meet the conditions and requirements of each country. Eurocode design codes accommodate any additional information through the introduction of National Annexes. The National Annex document contains country specific information in the form of nationally determined parameters (NDP's), reserved to replace information left open in Eurocode for national choice.

An important challenge to the revised standardised design code was the specification of traffic load models defined in each country and assessing how the effects of these load

models aligned with the standard models defined in the Eurocode. A further challenge was the evaluation of the load bearing capacity of current structures and comparing these with revised design parameters. To address such challenges, some member states embarked on desk study and actual field related research to analyse traffic load models on structures and determine how the different aspects of design standards could be combined (James, 2003; Jonnson and Ljungberg, 2005; Notkus and Kamaitis, 2010; Lukianenko, 2012; Artemov and Raspopov, 2014).

Jonsson and Ljungberg (2005) compared design calculations of an existing single-track steel railway bridge located in Gothenburg, Sweden in their investigation into the transition from the Swedish codes to the Eurocode (EC). A simply supported railway bridge with a free span of 18 m was used in the investigation. The objective of their investigation was to highlight differences between Swedish national codes (Bro 2004, BV BRO, edition 7 and BSK 99) and those of Eurocode (EC). The structure of the BV 2000 live load model for Swedish railway bridges corresponds with load model LM 71 specified in Eurocode. However the magnitude of the UDL and the four axle loads is higher than that of Eurocode with characteristic values of 110 kN/m for the UDL and 330 kN for each axle load. The design analysis only considered the mid span load effect for bending moment. The investigation highlighted differences in the load effects between the two design codes, but no proposal on alignment of the two codes was recorded.

Notkus and Kamaitis (2010) conducted a comparative desk study to investigate the load bearing capacity of railway bridges designed according to the Lithuanian (SNiP code) and the Eurocode load models. The study entailed an analysis of SNiP and Eurocode load models for simply supported railway bridge spans ranging from 2m to 80m, with emphasis on the effects of maximum characteristic (static) and design shear force and bending moment. The objective of the study focussed on the alignment of Eurocode rail traffic load factors to those of SNiP loading provisions and the consequences thereof for rail bridge structures. A further challenge was to establish a comparison between the load effects based on the single load model defined in SNiP and the five load models defined in Eurocode. Notkus and Kamaitis (2010) recorded significant differences in shear force and bending moment incurred by the different load models. They concluded that the possible ways of harmonising the Eurocode and SNiP load models was to adjust the characteristic values given for vertical loads in load model LM71, by applying the factors (α) proposed by Eurocode (Cl 6.3.2 (3P) to convert the characteristic load values to classified load values. However this proposal could only be effective if a particular value of α was applied to specific span intervals.

Artomov and Raspopov (2014) focussed on the mid-span moment in their desk study investigation to determine ways of harmonizing the Ukrainian railway bridge load model (C14) with that of the Eurocode load model LM71. In their investigation they applied analytical methods (influence lines), matrix analysis and computer programming to determine the mid span moments for simply supported bridge spans ranging from 0 to 33m. From their investigation they concluded that for railway bridges for their study range for load models C14 and LM71, there are differences depending on the span and the dynamic coefficients in each code. They concluded that a possible solution to harmonise the Eurocode and SNiP load models was to convert the characteristic values given for vertical loads in load model LM71 to classified vertical loads by applying the highest factor ($\alpha = 1.46$) proposed in Eurocode (Cl 6.3.2 (3P)). The result was proposed as a nationally determined parameter (NDP) in the National Annex to the National Standard of Ukraine NSTU-N EN 1991-2:2010.

Heavy haul railway transport in South Africa was introduced in the mid-1970s for the Iron Ore and the Coal Export lines (Busatta and Moyo, 2015). One such line is the Iron Ore Export Line that has been in operation since 1976 and is currently operating as the 2nd longest heavy haul railway line in the world (Ihha.net, 2015). Busatta and Moyo (2015) carried out visual inspections and conducted dynamic testing on the Olifants River Viaduct, a critical structure crossed by the Iron Ore Export Line. The focal point of the investigation was to develop a vibration monitoring system to assess the dynamic behavior of the viaduct and the vibration response under the new Radio Distributed Power (RDP) freight train introduced in 2007. Currently the RDP train is the longest freight train in the world and three times longer than the Olifants River Viaduct (Busatta and Moyo, 2015). Furthemore, Transnet Freight Rail (TFR) is currently working on the upgrade of the RDP train introduced in 2007 to increase both the number of wagons and the axle load (Busatta and Moyo, 2015). Advances to increase the number of wagons and axle loads on existing bridges may lead to increased traffic loads on existing bridges. Increased traffic loads on existing bridges would compel Transnet to consider whether the current SA code is still relevant. Currently, to the author's knowledge, there is no indication that Transnet intends revising the current SA code.

The significance of the Olifants River Viaduct is that it is crossed by the RDP freight train that currently operates at 300kN/axle. Although the SATS NR loading, based on 280kN/axle load is generally adequate for 300kN/axle load lines once the SATS code dynamic impact factors have been applied, heavier and longer freight trains operating on structures designed according to the current South African code may yield unreliable design results. It will therefore be incumbent on Transnet to engage in regular vibration testing and monitoring programs on existing railway structures that are earmarked to carry heavier loads with the view to consider revisiting the current 34 year code. Furthermore, in the light of advances by

TFR to increase the number of wagons and the axle load, there is no doubt that investigation into a more updated code may be imminent.

This dissertation analyses and compares the load effects of the SATS NR load model and Eurocode LM71 and SW/0 load models for simply supported and continuous railway bridges respectively. European countries analyzed load models in national codes and the resulting load effects for the purposes of alignment and transition to Eurocode standards.

In the light of the superseding of BS 5400:1978 to the Eurocode and the South African code having been based on BS 5400:1978, this dissertation compares the load effects of the South African load model to those of the Eurocode. The reason for addressing this challenge is the similarity in the structure of the load models (for simply supported railway bridges) and the further challenge of the difference in the load models for continuous railway bridges.

1.2 Objectives of the dissertation

The aim of this dissertation is to compare the rail traffic load models defined in the South African Transport Services (SATS) bridge code and those of the Eurocode (EC). A static analysis will be completed using the load models defined in the SATS and the EC bridge codes for single track simply supported and continuous systems. An investigation into whether a dynamic analysis is required for EC simply supported and continuous spans will also be completed. The maximum load effects of the static analysis will be factored and these values will be compared with the results of the dynamic analysis (for EC load models, dependant on whether a dynamic analysis is required). The maximum value will be used to establish whether there is a comparison between the SATS and the EC rail traffic load models.

1.3 Scope and Limitations of the study

This dissertation is a comparative analysis of the maximum load effects due to the application of traffic loads on railway bridges. The analysis is a purely theoretical desk study based on the SATS and EC rail traffic load models. The study is limited to single track simply supported and continuous railway bridges with speeds not exceeding 180km/h. Continuous systems are limited to two- and three equal spans. Maximum load effects of shear force and bending moment are the load effects of interest for purposes of comparison. Medium spans ranging from 5m – 40 m will be analysed in increments of 5m. The chosen span range represents an ideal sample of values to generate meaningful graphs for discussion on the

comparison between the two codes and represent common lengths of South African railway bridges.

The only loads considered in the analysis are the traffic loads. The study is therefore regarded as a conservative analysis where distribution of axle loads to the bridge deck and the sleepers has been excluded. Railway bridges are modelled as two dimensional beams and lateral loads due to nosing, centrifugal forces, traction, braking, impact and derailment are not included in the analysis. The moving load approach is used in the analysis to account for dynamic effects due to impact, oscillations and any other track and wheel irregularities.

1.4 Organisation of the study

Chapter 1 outlines the background into the investigation and a short review of similar research leading to the motivation for this study. The aim and objectives of the study is defined, followed by an outline of the scope and limitations of the study.

Chapter 2 reviews the South African and Eurocode live load models and discusses the design requirements for determining maximum load effects.

Chapter 3 details the analytical methods and software used to determine the critical positions for maximum load effects, for South African and Eurocode load models. It then describes the methods used to determine maximum load effects for shear and bending moment.

Chapter 4 presents the results of the frame analysis for approximating the position for maximum load effects for simply supported trial spans, followed by the results of the influence line analysis method for all simply supported spans in the range of study. Thereafter, the STRAP results for continuous beams will be presented. Lastly, a brief discussion on the comparison between the load effects is provided.
Chapter 5 concludes the study and provides recommendations regarding further research in the STRAP software program. It also provides reasons for recommending further research in railway bridge analysis.

CHAPTER TWO

REVIEW OF THE CODES

2.1 Introduction

Bridge design codes specify traffic loads on railway bridges as ideal load models to standardise and do simple analysis. The characteristic values for these load models are based on normal train loading that is ideally presented as a uniformly distributed load. Some load models include additional heavier point (axle) loads that are positioned at relatively short distances, to simulate individual axles and produce high end shears. Such load arrangements are applied to simply supported bridges for Eurocode load models and all railway bridges for South African load models. Railway bridge models are probabilistic load models suggested to represent the effects of service traffic with the smallest probability that these vertical loads would be exceeded during the design working life of the structure. This chapter reviews the South African and Eurocode live load models and outlines the similarities and differences.

2.2 Review of the South African railway bridge loads

The specification for South African railway bridge design loading is documented in the South African Transport Services (SATS) bridge code (1983). Although reference is made to the TMH 7 design code, specification for bridge loading is covered in SATS 1983. The SATS bridge code comprises two parts. The first part (Part 1) covers the procedures, drawings and design requirements for the construction of railway bridges, road bridges, footbridges, service bridges and culverts. The second part (Part II) covers the specifications for loading on railway bridges, road bridges, footbridges, service bridges and culverts.

Detailed information on principal loads, supplementary loads, load combinations, design live loads, derailment loads and restraint loads are documented in Part II. Principle loads cover the nominal self-weight of the structure, earth pressure on retaining structures and primary rail live loads. Supplementary loads are secondary live loads that account for lateral loads applied by trains to the track (i.e. nosing), centrifugal loads in cases where the horizontal alignment of the bridge is curved, longitudinal loads due to traction and braking, impact loads on bridge supports in the event of derailed vehicles and loads on bridge parapets.

The basis for South African bridge loading is BS 5400-2:1978 which specifies loading on steel, concrete and composite bridges. In 2006, BS 5400-2:1978 was superseded by BS 5400-2:2006. In March, 2010 BS 5400-2: 2006 was withdrawn and replaced by BS EN 1991-

2:2003 ‘Traffic Loads on Bridges’ and BS EN 1990:2005(A1) – Annex A2 ‘Basis of structural design – Application for Bridges’ (Thenbs.com.). However, South African bridge design currently continues using the SATS (1983) bridge loading code.

Primary live loading for South African railway bridge design is described by one single load model, namely, the national rail (NR) load model. The NR load model, shown in Figure 2.1, represents a static load model with normal train loading represented by a uniformly distributed load. To account for occasional, heavy, abnormal loads that may occur on railway bridges, additional axle loads are introduced and represented as point loads over 3 short equally spaced lengths of 1,8m. (BS 5400-2:1978, Appendix D, Clause D.1).

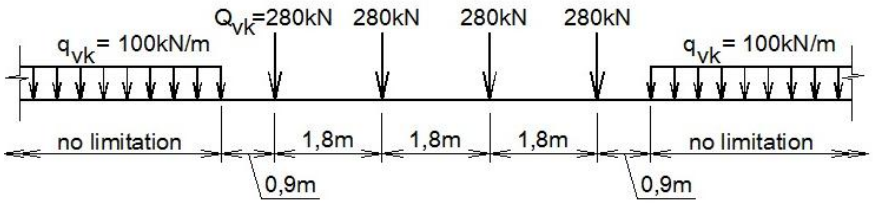

Figure 2.1: NR load model

(Source: SATS bridge code, 1983)

The NR load model applies to both simply supported and continuous bridges and incorporates all possible loading conditions, with no distinction between light, normal or heavy loading. The structure of the NR load model is similar to the RU load model described in BS 5400-2:1978 and shown in Figure 2.2. However, the magnitude of the axle loads and the uniformly distributed loads in the NR load model is 1,12 and 1,25 times higher than the values of RU loading respectively. The higher NR load values accounts for conditions conducive to South African railway bridges.

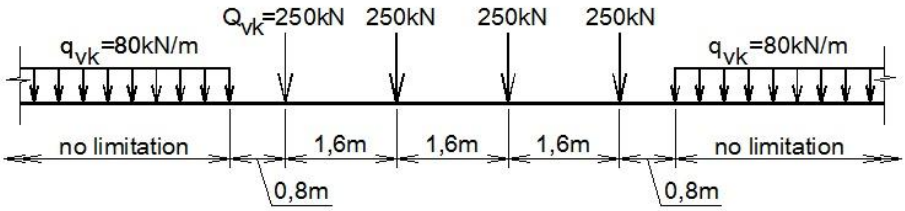

Figure 2.2: Type RU loading

(**Source: BS 5400-2:1978**)

Since the South African load model is based on BS 5400-2:1978 (SATS Clause B1), it can be reasonably concluded that the basis for the NR load model corresponds to that of RU loading. RU loading was derived on the basis of loading on railway bridges in Great Britain

and the continent of Europe at that time, and the values were projected to account for future loading on railway bridges. SATS load models are based on the same principle with adjusted axle and uniformly distributed load values to accommodate the greater locomotive and wagon loadings in the South Africa. The values were based on the wagon types used by South African railways. Class 7E and 7E2, 8E, 9E and 12E electric locomotives with a total mass of 123,5 tonnes (1211 kN); 82 tonnes (804 kN); 166,3 tonnes (1631 kN) and 83,6 tonnes (820 kN) respectively were used for general freight purposes and transportation of South Africa's coal and iron ore. The fully loaded wagon static weight averaged 20,6 t/axle (in the case of wagon class 7E and 7E2, 8E and 12E) and 27,7 t/axle for wagon type 9E locomotives (Web.archive.org, 2018).

To the author’s knowledge there is no documented evidence that the specific values used in the load models were obtained from actual field measurements. However interest in actual field measurements to investigate the structural integrity and dynamic response of existing railway bridges in South Africa has increased (Shibeshi, 2015; Busatta and Moyo, 2015).

2.3 SATS design requirements

To determine the maximum load effects for bending moment and shear, the NR loads are applied as moving loads across the length of the bridge. This results in impact, oscillation and other dynamic effects including those due to track and wheel irregularities (SATS bridge code, 1983. Clause B2.3.2). To account for these dynamic effects, a static analysis is completed and the resulting load effects are factored by the relevant dynamic factor. The formulae defining the dynamic factor are the same as those given in BS 5400-2:1978 and is a function of the span of the bridge for spans 3,6m to 67m. For spans outside the 3,6m to 67m range, constant values as given in Table 2.1 are used. When calculating the dynamic factor for shear or bending moment in simply supported bridge spans between 3,6 and 67m, the actual span length is substituted in the formula defining the dynamic factor. In the case of continuous bridge spans between 3,6 and 67m, ratios of 1,2; 1,3; 1,4 and 1,5 times the mean span for 2, 3, 4 and 5 continuous spans respectively is substituted as the value for “L” in the formula defining the dynamic factor. The dynamic factors for amplifying the static load effects of bending moment and shear are listed in Table 2.1.

Table 2.1: Dynamic factor for NR loading

Dimension L (m)	Dynamic factor for evaluating	
	bending moment	shear
up to 3,6	2,00	1,67
3,6 to 67	$0{,}73 + \frac{2{,}16}{\sqrt{L} - 0{,}2}$	$0{,}82 + \frac{1{,}44}{\sqrt{L} - 0{,}2}$
over 67	1,00	1,00

(**Source: SATS bridge code, 1983.**)

2.4 Review of Eurocode

The Eurocode programme is a development of work started in 1987 by the European Committee for Standardization (CEN). In 1995 a pre-standard, ENV 1991-2 was released and published. Work however continued on ENV 1991-2 by a working group comprising representatives of European countries with the aim of acquiring a full standard. This culminated in a standardized reference document that was published in 2003 (EN 1991–2:2003).

The Eurocode comprises 10 parts (codes). Each part emphasises a standard set of rules for a specific area of design. The areas covered in each specific code are as follows: basis of structural design (EN 1990), actions on structures (EN 1991), design of concrete structures (EN 1992), design of steel structures (EN 1993), design of composite steel and concrete structures (EN 1994), design of timber structures (EN 1995), design of masonry structures (EN 1996), design of aluminium structures (EN 1999), geotechnical design (EN 1997), and design of structures for earthquake resistance (EN 1998). Countries affiliated to Eurocode are compelled to implement these codes in the design of their structures.

Where a country chooses to incorporate alternate parameters that apply to the design of building and civil engineering projects in that particular country, such cases are incorporated in Eurocode through specific clauses written in the relevant sections of each code. Such parameters are referred to as nationally determined parameters (NDP's). Country specific NDP's are documented separately in national annexes. Each country affiliated to Eurocode has its own national annex that is used in conjunction with the Eurocode standard.

EN1991–2 (titled "actions on structures") specifies live load models applicable to the design of road bridges, footpaths and railway bridges. This code (in particular section 6 which

focuses on traffic loads incurred on railway bridges) is the main reference document for analysis in this dissertation.

Eurocode classifies traffic loads on railway bridges as variable loads (traffic and pedestrian loads) and actions for accidental design situations (EN 1991–2:2003, Clause 2.1.2). Although rail carriage weights are measurable parameters, actual rail traffic loads are complex and EN 1991–2 represents these traffic loads as simplified load models. The values of these load models do not reflect the actual values of rail traffic. These values are characteristic values that reflect the worst loading that can occur due to actual and future traffic during the service life of the bridge (Notkus, et al, 2010).

2.5 Structure of Eurocode Rail Traffic Load Models

Eurocode load models are significantly more complex than the SATS bridge code load model, with specific load models for specific rail traffic. EN 1991–2 describes five load models that apply on the standard- and wide track European mainline network. These load models are classified according to bridge support conditions (either simply supported or continuous), traffic loading conditions (normal- or heavy rail traffic or unloaded train) and train speed.

Load Model 71 represents the static effect of normal rail traffic for simply supported bridges. Normal rail traffic refers to standard, low speed (less than 200 km/h) rail traffic operating over the standard-gauge or wide-gauge European mainline-network. The loading arrangement is shown in Figure 2.3. The structure of the load model consists of four 250 kN axle loads, preceded and followed by a distributed load of 80 kN/m. The length of the 80 kN/m uniformly distributed load is unlimited and is left to the discretion of the bridge engineer. Eurocode makes provision for lines carrying rail traffic that is heavier or lighter than normal rail traffic by factoring the characteristic loads given in the load model by a factor “α”, where “α” may be specified in the national annexes. The value given for “α” is given as one of the following values: 0,75; 0,83; 0,91; 1,00; 1,10; 1,21; 1,33; 1,46 (EN 1991–2:2003, Clause 6.3.2(3)) .

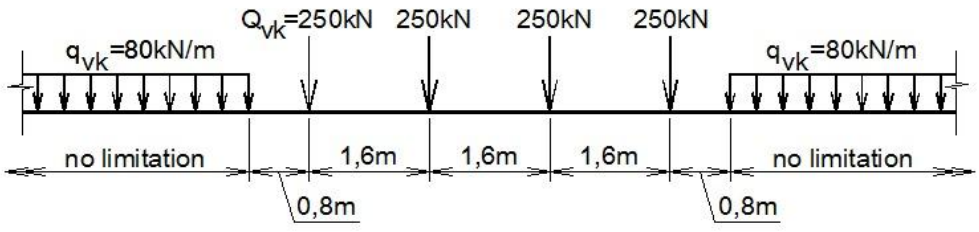

Figure 2.3: Load model LM71

(Source: EN 1991–2:2003: Eurocode 1: Actions on Structures)

Load Model SW/0 represents the static effect of normal rail traffic for continuous bridges. The loading arrangement is shown in Figure 2.4 and consists of two- 15m long uniformly distributed loads (UDL) of 133 kN/m. The UDL's are separated by a distance of 5,3m between them. These loads (as in the case of load model 71) may also be factored by α, in cases where lines carrying rail traffic is heavier or lighter than normal rail traffic.

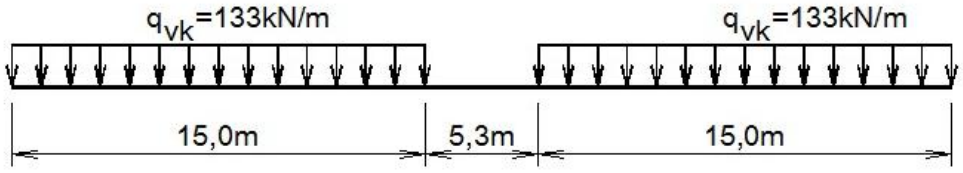

Figure 2.4: Load model SW/0
(Source: EN 1991–2:2003: Eurocode 1: Actions on Structures)

Load Model SW/2 represents the static effect of heavy rail traffic. The loading arrangement corresponds to that shown in Figure 2.4, but consists of two- 25m long uniformly distributed loads (UDL) of 150 kN/m. The UDL's for load model SW/2 are separated by a distance of 7m between them. The relevant national annex defines the line or section of lines over which the heavy rail traffic operates for the assigned project.

Load Model "unloaded train" represents the effect of an unloaded train. This load model is used for checking the lateral stability of single track bridges.

Load Model "HSLM" represents loading from passenger trains moving at speeds exceeding 200 km/h. For the purpose of this dissertation, load model 71 and SW/0 will be used for the analysis of simply supported- and continuous bridges respectively.

Eurocode also makes provision for horizontal forces that have to be combined with the vertical traffic loads in determining design forces on railway bridges. Eurocode equations for determining the magnitude of the centrifugal force in cases where part or the entire length of the bridge is curved are given in (EN 1991-2:2003 Cl 6.5.1 Eqn 6.17 and 6.18). In addition to the centrifugal force, a nominal nosing force equivalent to the value (Q_{sk} = 100 kN) in the SATS bridge code is given in EN 1991-2:2003 Cl 6.5.2(2). Characteristic values for traction and braking forces over the length of the influence lines where these effects occur, are accounted for in the form of uniformly distributed loads. These values are given in EN 1991-2:2003 Cl 6.5.3(2P) for the relevant vertical traffic load models.

2.6 Eurocode design analysis requirements

To determine the load effects for the worst load case in railway bridge design, Eurocode proposes a comparison between the results of an amplified static analysis and a dynamic analysis. This design rule applies to load models LM71, SW/0 and SW/2. A static analysis entails determining the most unfavourable loading position for shear and bending moment as the load models are moved across the length of the bridge. The results of the static analysis are factored by introducing a dynamic factor. The dynamic factor accounts for the magnification of stresses and vibration effects in the structure (EN 1991–2:2003, Clause 6.4.5.1(1)). The dynamic factor is governed by the determinant length as specified in Table 6.2 (EN 1991–2:2003) but, unlike the SATS bridge code, also takes into consideration the quality of track maintenance (EN 1991–2:2003, Clause 6.4.5.2(2)). The equation for the relevant dynamic effect, ϕ referred to in Eurocode is given as follows:

For a carefully maintained track:

$$\phi_2 = \frac{1{,}44}{\sqrt{L_\varphi} - 0{,}2} + 0{,}82 \qquad \text{with} \qquad 1{,}00 \le \phi_2 \le 1{,}67 \tag{2.1}$$

For a track with standard maintenance:

$$\phi_3 = \frac{2{,}16}{\sqrt{L_\varphi} - 0{,}2} + 0{,}73 \qquad \text{with} \qquad 1{,}00 \le \phi_3 \le 2{,}00 \tag{2.2}$$

In addition to the static analysis, Eurocode also specifies the criteria for determining whether a dynamic analysis is required (EN 1991-2:2003 Cl. 6.4.4). The dynamic analysis (which SATS does not take into account) accounts for resonance or excessive vibration of the bridge structure. The criteria for determining whether a dynamic analysis is required are given in the flowchart shown in Figure 2.5. From the flowchart it can be concluded that continuous bridges with train speeds less than 200 km/h as well as simply supported bridges with train speeds less than 200 km/h and where the fundamental natural bending frequency falls within the limits of those given in Figure 2.6, are excluded from a dynamic analysis.

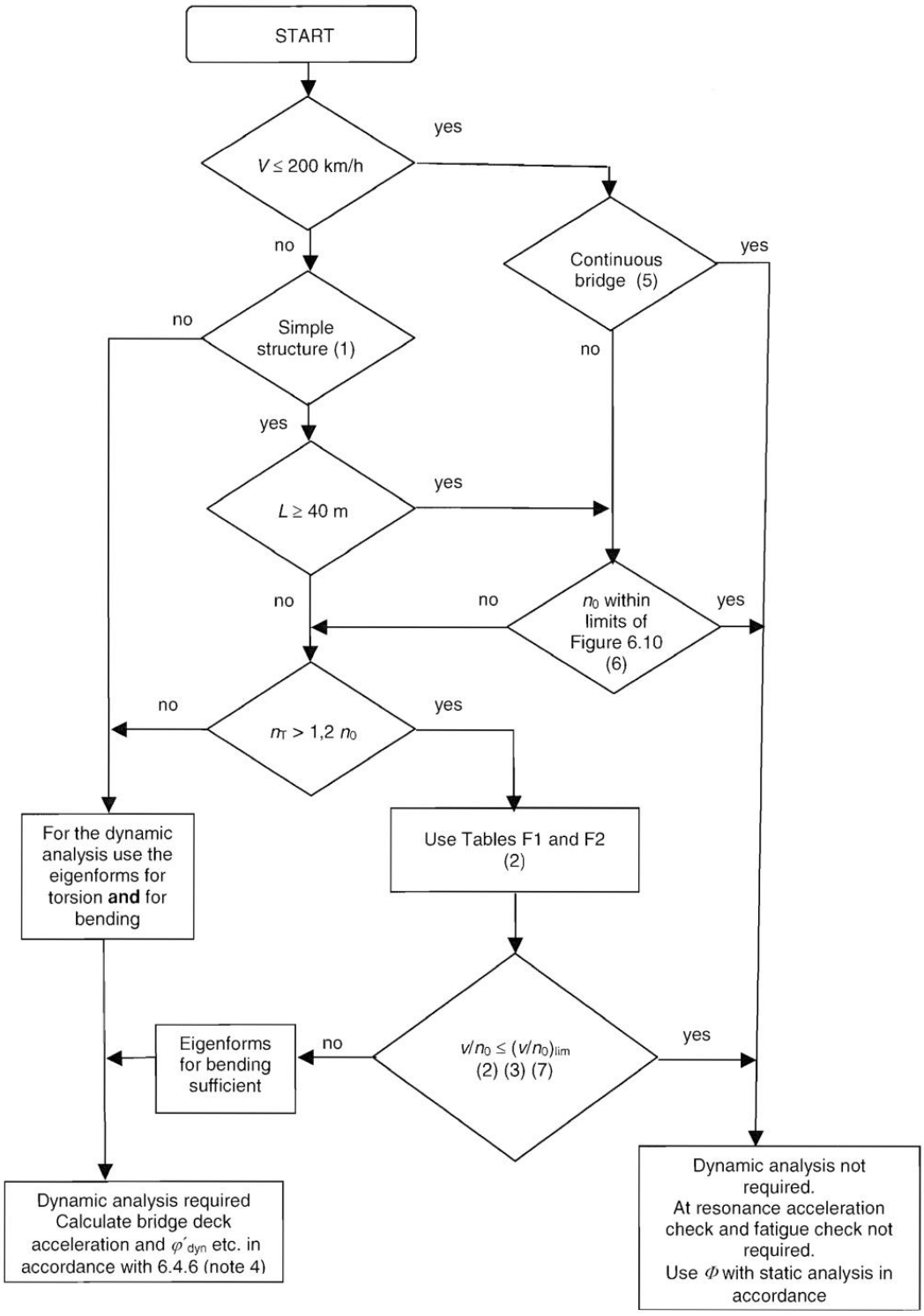

Figure 2.5: Flow chart for determining whether a dynamic analysis is required

(Source: EN 1991–2:2003: Eurocode 1: Actions on Structures)

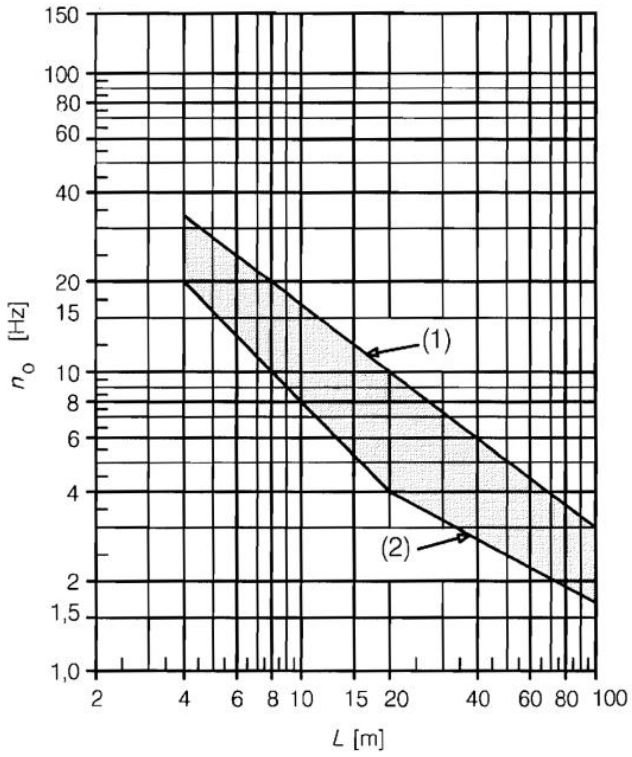

Key
(1) Upper limit of natural frequency
(2) Lower limit of natural frequency

Figure 2.6: Limits of bridge natural frequency n_0 [Hz] as a function of L [m] (Source: EN 1991–2:2003: Eurocode 1: Actions on Structures)

2.7 Summary

Review of the loading codes has demonstrated that Eurocode design procedures are more complex than those of South Africa. In contrast to the five load models specified in Eurocode, the SATS specifies a single load model similar in structure to the Eurocode load model LM71. Furthermore the NR load model specified in the SATS code caters for heavier loads and relatively low speed (< 180km/h) trains. The Eurocode on the other hand makes provision for the conversion of characteristic loads (on load models specifying normal rail traffic) to heavier loads.

The SATS NR load model applies to simply supported and continuous railway bridges. The Eurocode load model on the other hand specifies separate load models based on support conditions (simply supported and continuous bridges), traffic loading conditions (normal- or heavy rail traffic or unloaded train) and train speed. Furthermore, Eurocode makes provision for load models for heavy loads and high speed (exceeding 200 km/h) trains.

Provision for increase of static stresses incurred on railway bridges due to the dynamic effects is specified in both the SATS and the Eurocode. The Eurocode specifies a dynamic factor based on the quality of the track while the SATS specifies a dynamic factor based on the load effect (shear and bending moment) considered. Moreover the dynamic factor for evaluating bending moment for bridges between 3,6m and 67m is equivalent to that of the Eurocode for a track with standard maintenance, while the dynamic factor for evaluating shear force for bridges between 3,6m and 67m is equivalent to that of the Eurocode for a carefully maintained track. The evaluation of the determinant length associated with the dynamic formulae is rather complex in the Eurocode in that it considers various parameters pertaining to the type of deck (closed/open deck with/without a ballast bed; material used, either steel or concrete), structural supports and nature of the main girders. These parameters are not considered in the SATS code and the actual span (simply supported bridges) or factors of the mean span (in the case of continuous bridges) are considered for evaluating the determinant length.

Bridges designed according to the Eurocode high speed load model (train speeds over 200 km/h) may be subjected to large dynamic effects. In such cases a dynamic analysis is required to account for resonance and excessive vibrations. No such provision is made in the SATS bridge codes because the NR load model generally caters for low speeds (train speeds up to 180 km/h).

The complexity of the Eurocode extends to national annexes where country specific information is documented to account for conditions conducive to all member states affiliated to the Eurocode. The SATS bridge code on the other hand, encompasses all aspects of live loading on railway bridges.

CHAPTER THREE
METHODOLOGY: APPLICATION OF LIVE LOADS

3.1 Introduction

To investigate the effects of traffic loads on railway bridges of different spans, critical positions of these loads have to be established. Three analysis methods will be used to determine the load positions that result in maximum load effects. The first method describes the application of the Eurocode LM71 load model on three single span systems, using a trial and error approach and the finite analysis module in Prokon. The results will identify where the loads have to be positioned on the influence line for maximum effects. The second part of the analysis uses influence lines for single span systems to derive a generic equation for all spans in the range of study for both the Eurocode LM71 and SATS NR load models. The equation derived from the influence line method will be used to calculate the load effects for shear and bending moment for the single span systems. The final part of this chapter describes the application of the moving load module in STRAP to determine the maximum load effects for shear force and bending moment for equal span continuous systems.

3.2 Overview of analysis methods

3.2.1 Overview of Prokon

Prokon is extensively used software for analysis and design of structures in South Africa. The software, which consists of a number of modules, was developed by structural engineers in 1989 (Prokon.com, 2016). The basic frame analysis module, one of the many modules in Prokon, will be used in this dissertation to locate the maximum bending moment and shear force position of three single span systems using load model LM71. The relevance of this analysis is to determine where maximum ordinates will be placed on the influence line diagrams.

The frame analysis module performs linear and nonlinear static analysis of two dimensional beams, plane frames and trusses. The input wizard generates models of structural beam and frame elements by entering sets of coordinates that define the structural element and the position of the applied loads.

Prokon uses finite element analysis (FEA) to simulate and analyse the behaviour of structures in order to obtain approximate solutions of ordinary and partial differential equations. The finite element method (FEM) comprises three stages, namely the pre-

processing, solution and post-processing stage. The pre-processing stage produces a finite element mesh by dividing the structure into smaller finite elements. This is called discretization. The solution stage derives the governing equations for each element and assembles the equations as a matrix of equations and applies the nodal coordinates, material properties and loading conditions. For static analysis, the matrix of equations is of the form,

[K] * {d} = {P}

where:

[K] = the structure stiffness matrix

{d} = the unknown nodal displacements

{P} = the applied nodal forces.

The equation applies in the linear elastic range. To solve the matrix of equations, boundary conditions are applied. After solving the equations for the unknown displacements, the program calculates the internal forces and stresses in the beams. The post-processing stage obtains approximate results for the finite element model.

Prokon does not have a moving load analysis module and is therefore not entirely suited for the purpose of this study, as the coordinates that define the position of the loads have to be recalculated and reentered into the input wizard every time the loads are moved to a new position. This can be time consuming for all the load cases being investigated and hence the reason why it is only used as a trial approach to locate the worst position of load effects on three LM71 single span systems.

3.2.2 Overview of the influence line analysis method

Influence lines are extremely useful for determining where to place loads on structures such that the loads cause the maximum possible destructive effect. Using an influence line ensures that no other load position could cause a greater action (reaction, axial force, shear, or moment) at the selected point in the structure. Influence line diagrams allow one to calculate the magnitude of these maximum actions at the selected point in the structure, for use in design.

The influence line method represents a response to a function in the form of a line diagram. Hence, an influence line diagram is a graph that represents the variation in the response function at a particular position of a structural element as a unit load, a train of wheel loads or a uniformly distributed load moves across the length of the element. The response function may be the effect of the support reaction, shear force, bending moment or deflection. This

method is particularly useful in determining the absolute maximum value of the response of a structural element anywhere along the span when a series of loads move across the span. Influence line diagrams for statically determinate structural elements are drawn as straight line graphs. This makes it easy to apply simple mathematical calculations to determine coordinate values at any position on the influence line graph. Influence line diagrams for statically indeterminate structural elements are more complex and analytically tedious as they are represented as curved lines. Selective software would be a more appropriate method for the analysis of load effects due to moving loads for statically indeterminate structural elements.

3.2.3 Overview of STRAP analysis for continuous beams

STRAP, like Prokon, uses the FEA method and the assumption of a linear elastic model and small displacements to solve structural models. Furthermore, STRAP includes an additional moving load analysis feature that creates and analyses a series of moving load cases. The method used positions the loads assigned to the load models at incremental distances starting at one end of the member and moving across to the other end. The loads in the load model will be offset by a constant increment in each successive generated case. The number of positions where the loads are placed along each member is determined by the number of generated cases specified by the user. After the beam has been solved for each load case, the load model is moved to the next position and the process is repeated. The moving load generator allows multiple moving load cases up to a maximum of 995 load cases. Results from the moving load solutions are combined into envelopes of maximums. Similar to the method of solving a model using Prokon software, STRAP solves the model by creating the geometry stiffness matrix and solving for each load case using the inverted stiffness matrix. The position of the load model at maximum moment or shear in a member, is manually calculated using the incremental distance assigned to move the loads together with the number of the load case recorded in the results.

The advantage of the program is the progressive analysis of the maximum positive and negative values of deflection, bending moment, shear, and reaction at each position along the beam for a given load case. A further advantage of the technique is that the load cases are solved relatively fast.

3.3 Analysis of single span systems

3.3.1 Approximation of position for maximum bending moment

To approximate the critical position for maximum bending moment, the Eurocode LM71 load model was moved across a 10m, 25m and 40m single span system. These spans were chosen because they represent the lowest, mid-range and highest spans of the study sample on which all the vertical loads defined in LM71 could be accommodated. In each case the single span system was modelled as a two dimensional beam. The loads were moved in relatively small increments from the left hand side of the beam across towards to the right hand side, along the length of each span. For the first case, the loads were applied symmetrically on a 10m span as shown in figure 3.1, with the uniformly distributed load extending across to the supports. A linear analysis was completed using the frame analysis module in Prokon and the position for maximum bending moment and the corresponding bending moment value was recorded.

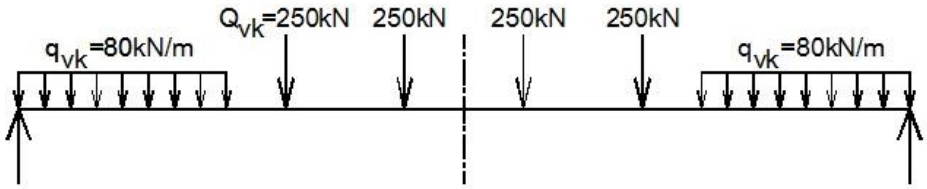

Figure 3.1: Symmetrical arrangement of loading for 10m span: first trial

The loads were then moved further along the 10m span in small increments until the third axle load (Q_{vk3}) reached positions of 0,4m; 0,3m; 0,25m; 0,2m; 0,15m and 0,1m to the left of the centreline. In each case a linear analysis was completed using the frame analysis module and the position for maximum bending moment and the corresponding bending moment value was recorded.

Based on the results of the 10m trial span, the number of trial positions for the 25m single span system was reduced. The first position was chosen with Q_{vk3} positioned at a distance of 0,2m to the left of the centreline. The loads were then moved along the 25m span with Q_{vk3} at varying distances of 0,15m; 0,1m; and 0,05m, measured to the left of the centreline.

In the third case, the loads were applied to the 40m single span beam with the first position for Q_{vk3} at a distance of 0,15m measured to the left of the centreline. The loads were then moved along the 40m span until Q_{vk3} reached positions of 0,1m; and 0,05m measured to the left of the centreline.

Figure 3.2 illustrates the positions of the loads along the 3 simply supported single span systems. The dimension ‘a’ represents the distance between the centreline of the beam and the third axle load (Q_{vk3}) and represent the varying increments through which the loads are moved for each trial span.

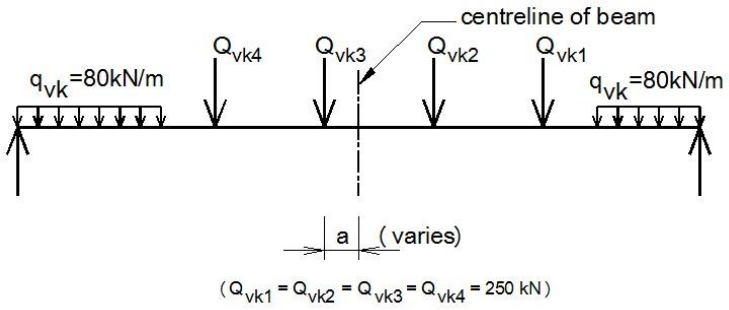

Figure 3.2: Loading positions for trials spans

3.3.2 Static analysis: Influence line analysis for LM 71 and NR load model for evaluating bending moment

The results obtained from the frame analysis module were applied to the influence line diagram for bending moment to determine a generic position for any single span simply supported system.

The Eurocode LM71 loads were positioned on the influence line diagram for bending moment with the maximum ordinate positioned under the axle load identified in the frame analysis results. The load was positioned at an arbitrary distance ('x') measured from the left hand support. The position of the global loads relative to the arbitrary distance ('x') and the corresponding influence line diagram for the Eurocode LM71 loads is shown in figure 3.3.

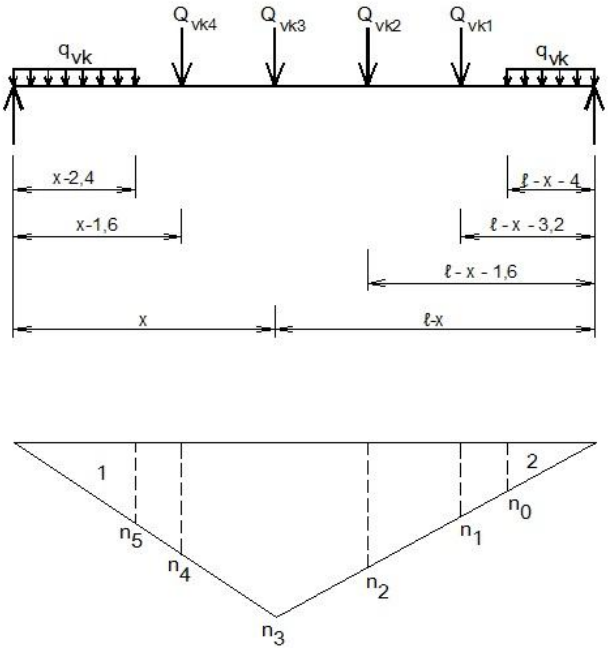

Figure 3.3: Vertical load arrangement for load model 71 in terms of 'x'. Corresponding influence line diagram for bending moment at axle load Q_{vk3}

Similarly, the vertical loads for the SATS NR load model were positioned on the influence line diagram for bending moment with the maximum ordinate positioned under the axle load

identified in the frame analysis results. The position of the global loads relative to the arbitrary distance ('x') and the corresponding influence line diagram for the SATS NR load model is shown in figure 3.4.

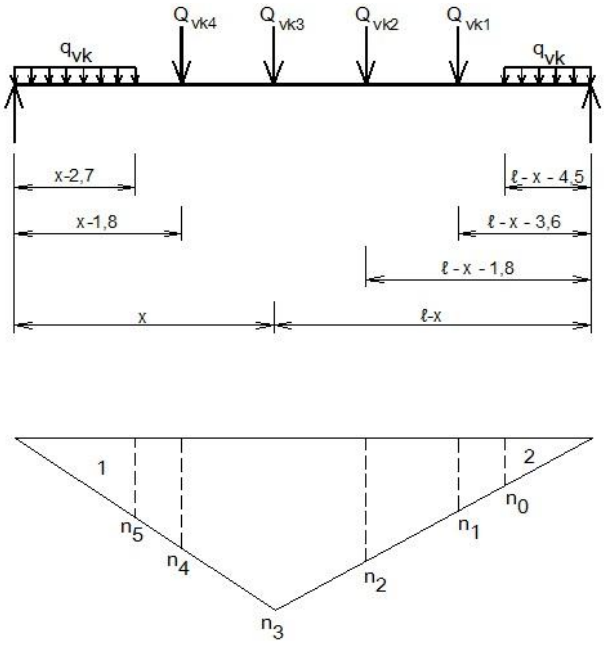

Figure 3.4: Vertical load arrangement for NR loading in terms of 'x'. Corresponding influence line diagram for bending moment at axle load Q_{vk3}

The influence line ordinates n_0, n_1, n_2, n_3, n_4 and n_5 corresponding to the series of loads and the corresponding values for each ordinate for each load model are listed in Table 3.1.

Table3.1: Influence line ordinates for load model 71 and NR loading

Influence line ordinates	
Eurocode load model 71	**SATS NR load model**
$n_0 = \frac{x(\ell - x - 4)}{\ell}$	$n_0 = \frac{x(\ell - x - 4{,}5)}{\ell}$
$n_1 = \frac{x(\ell - x - 3{,}2)}{\ell}$	$n_1 = \frac{x(\ell - x - 3{,}6)}{\ell}$
$n_2 = \frac{x(\ell - x - 1{,}6)}{\ell}$	$n_2 = \frac{x(\ell - x - 1{,}8)}{\ell}$
$n_3 = \frac{x(\ell - x)}{\ell}$	$n_3 = \frac{x(\ell - x)}{\ell}$
$n_4 = \frac{(\ell - x)(x - 1{,}6)}{\ell}$	$n_4 = \frac{(\ell - x)(x - 1{,}8)}{\ell}$
$n_5 = \frac{(\ell - x)(x - 2{,}4)}{\ell}$	$n_5 = \frac{(\ell - x)(x - 2{,}7)}{\ell}$

The maximum ordinate, n_3, is calculated using the standard formula for bending moment $\left(\frac{P \times \ell}{4}\right)$ and ordinates n_0, n_1, n_2, n_4 and n_5 are derived from the expression obtained for n_3 by using basic mathematical concepts of similar triangles.

The maximum moment is evaluated by calculating the algebraic sum of the triangular areas numbered 1 and 2 (in figure 3.3 and figure 3.4) multiplied by the magnitude of the uniformly distributed load. This value is added to the product of the sum of ordinates n_1, n_2, n_3 and n_4 and the magnitude of the concentrated load. This is given by the following mathematical equation:

Moment expression for Eurocode load model 71 (based on normal rail traffic, $\alpha = 1{,}00$):

$$M_x = 80\left(Area_1 + Area_2\right) + 250\left(n_1 + n_2 + n_3 + n_4\right)$$

$$= 80\left(\frac{1}{2}(x - 2{,}4)\left(\frac{(\ell - x)(x - 2{,}4)}{\ell}\right) + \frac{1}{2}(\ell - x - 4)\left(\frac{x(\ell - x - 4)}{\ell}\right)\right)$$

$$+ 250\left(\left(\frac{x(\ell - x - 3{,}2)}{\ell}\right) + \left(\frac{x(\ell - x - 1{,}6)}{\ell}\right) + \left(\frac{x(\ell - x)}{\ell}\right) + \left(\frac{(\ell - x)(x - 1{,}6)}{\ell}\right)\right)$$

$$M_x = \frac{-40x^2\ell + 488x\ell - 169{,}6\ell - 488x^2 - 390{,}4x + 40x\ell^2}{\ell} \quad (\text{simplified}) \qquad (3.1)$$

The differential of the moment expression (given in equation 3.1) with respect to the arbitrary distance ‘x’ yields an expression for shear which is given by the following expression:

$$V_x = \frac{dM}{dx} = \frac{-80x\ell + 488\ell - 976x - 390{,}4 + 40\ell^2}{\ell} \qquad (3.2)$$

For a simply supported beam, maximum bending moment occurs at the position where the shear force is equal to zero. Therefore, setting equation 3.2 equal to zero, yields an expression for the maximum bending moment in terms of the arbitrary distance ‘x’.

$$\frac{dM}{dx} = \frac{-80x\ell + 488\ell - 976x - 390{,}4 + 40\ell^2}{\ell} = 0$$

$$\Rightarrow -80x\ell + 488\ell - 976x - 390{,}4 + 40\ell^2 = 0$$

$$80x\ell + 976x = 488\ell - 390{,}4 + 40\ell^2$$

$$x(80\ell + 976) = 488\ell - 390{,}4 + 40\ell^2$$

$$x = \frac{488\ell - 390{,}4 + 40\ell^2}{(80\ell + 976)} \qquad (3.3)$$

Equation 3.3 represents the general equation for locating the position of Q_{vk3} (measured from the left support) on a simply supported beam for maximum moment for LM 71.

Similarly, the moment expression for SATS NR load model is derived as follows:

$$M_x = 100\,(Area_1 + Area_2) + 280\,(n_1 + n_2 + n_3 + n_4)$$

$$= 100\left(\frac{1}{2}(x - 2{,}7)\left(\frac{(\ell - x)(x - 2{,}7)}{\ell}\right) + \frac{1}{2}(\ell - x - 4{,}5)\left(\frac{x(\ell - x - 4{,}5)}{\ell}\right)\right)$$

$$+ 280\left(\left(\frac{x(\ell - x - 3{,}6)}{\ell}\right) + \left(\frac{x(\ell - x - 1{,}8)}{\ell}\right) + \left(\frac{x(\ell - x)}{\ell}\right) + \left(\frac{(\ell - x)(x - 1{,}8)}{\ell}\right)\right)$$

$$M_x = \frac{-50x^2\ell + 400x\ell - 139{,}5\ell - 400x^2 - 360x + 50x\ell^2}{\ell} \quad (\text{simplified}) \qquad (3.4)$$

The differential of the moment expression (given in equation 3.4) with respect to the arbitrary distance ‘x’ yields an expression for shear which is given by the following expression:

$$V_x = \frac{dM}{dx} = \frac{-100x\ell + 400\ell - 800x - 360 + 50\ell^2}{\ell} \qquad (3.5)$$

Setting equation 3.5 equal to zero yields an expression for the arbitrary distance ‘x’.

$$\frac{dM}{dx} = \frac{-100x\ell + 400\ell - 800x - 360 + 50\ell^2}{\ell} = 0$$

$$\Rightarrow -100x\ell + 400\ell - 800x - 360 + 50\ell^2 = 0$$

$$100x\ell + 800x = 400\ell - 360 + 50\ell^2$$

$$x(100\ell + 800) = 400\ell - 360 + 50\ell^2$$

$$x = \frac{400\ell - 360 + 50\ell^2}{(100\ell + 800)} \qquad (3.6)$$

Equation 3.6 represents the general equation for locating the position of Q_{vk3} (measured from the left support) on a simply supported beam for maximum moment for SATS NR loading.

Equations 3.1, 3.3, 3.4 and 3.6 were set up in an excel spreadsheet and the maximum static moment for spans 10m – 40m were evaluated. Assuming dynamic amplification from imperfections is included in the dynamic factor, the static results were multiplied by the dynamic factor to determine the maximum design moment. In the case of the LM 71 load model, the dynamic factor defined in Eurocode, Cl. 6.4.5.2 (2) applicable to both a carefully maintained track and a track with standard maintenance were considered.

Equations 3.1, 3.3, 3.4 and 3.6 were derived by assuming full loading specified for LM71 and SATS NR positioned on the beam. Since the full loading specified for these load models could not be accommodated on the 5m span, the equations derived from the influence line method could not be used to determine the magnitude for absolute maximum moment. As an alternate method to the influence line method of analysis for the 5m single span system, the frame analysis module in Prokon was used to determine the position for absolute maximum moment for both LM71 and NR load models.

3.3.3 Static analysis: Influence line analysis applied to LM71 and NR load model for evaluating shear force

Similarly, the trial and error method was used to determine the maximum effect for shear force for the 10m, 25m and 40 spans. The loads were moved across the 10m, 25m and 40m spans in relatively small increments from the left hand side towards the right hand side of each single span beam. The result of each trial load case was used to draw the influence line diagram (as illustrated in Figure 3.5 for LM71 and Figure 3.6 for NR) for each load model to

derive an equation for calculating the absolute maximum shear for any single span simply supported system.

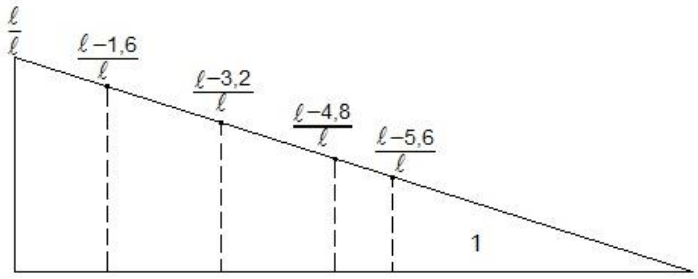

Figure 3.5: Influence line diagram for maximum shear for load model 71

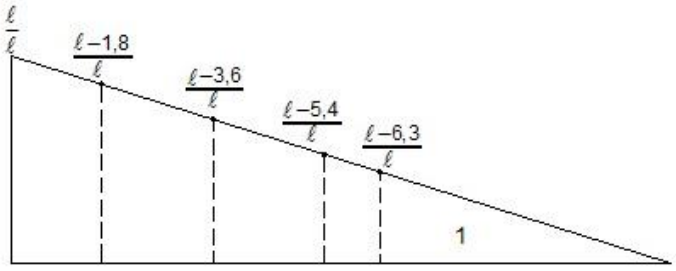

Figure 3.6: Influence line diagram for maximum shear for SATS NR loading

The absolute maximum shear was computed by calculating the algebraic sum of the product of the ordinates under the axle loads and the magnitude of the axle load and adding the product of the triangular area labelled '1' and the magnitude of the uniformly distributed load. The general expression for computing the value for absolute maximum shear for Eurocode load model LM71 is expressed as follows:

$$\begin{aligned} V &= 250\left(\frac{\ell}{\ell}+\frac{\ell-1{,}6}{\ell}+\frac{\ell-3{,}2}{\ell}+\frac{\ell-4{,}8}{\ell}\right)+80\left(\frac{1}{2}\times(\ell-5{,}6)\times\left(\frac{\ell-5{,}6}{\ell}\right)\right) \\ &= 250\left(\frac{4\ell-9{,}6}{\ell}\right)+40\left(\frac{\ell^2-11{,}2\ell+31{,}36}{\ell}\right) \end{aligned} \tag{3.7}$$

and for computing the value for absolute maximum shear for SATS NR loading is as follows:

$$\begin{aligned} V &= 280\left(\frac{\ell}{\ell}+\frac{\ell-1{,}8}{\ell}+\frac{\ell-3{,}6}{\ell}+\frac{\ell-5{,}4}{\ell}\right)+100\left(\frac{1}{2}\times(\ell-6{,}3)\times\left(\frac{\ell-6{,}3}{\ell}\right)\right) \\ &= 280\left(\frac{4\ell-10{,}8}{\ell}\right)+50\left(\frac{\ell^2-12{,}6\ell+39{,}69}{\ell}\right) \end{aligned} \tag{3.8}$$

The absolute maximum shear values were determined by substituting equations 3.7 and 3.8 in each of the spans for the 10m – 40m range. The frame analysis method was applied in the

for the 5m span. The resulting shear values for the SATS NR loading were multiplied by the dynamic factor for shear, defined in the SATS bridge code, Cl.B2.3.2, table 2, for spans 3,6 to 67m. The resulting shear values for Eurocode LM71 were multiplied by the dynamic factor defined in Eurocode, Cl. 6.4.5.2 (2) applicable to both types of track.

3.3.4 Requirement for dynamic analysis.

In accordance with the requirements for a dynamic analysis, the flowchart in Figure 2.5 was applied to check whether a dynamic analysis would be required for Eurocode LM71 load model bridges. For simply supported bridges designed for train speeds less than 200 km/h to be excluded from a dynamic analysis, the requirement is that the fundamental natural bending frequency falls within the limits given in Figure 2.6. This implies that the lower limit and upper limit natural frequency have to be calculated for each simply supported span according to the equations given in Eurocode (EN 1991-2:2003 Cl. 6.4.4). The calculated natural frequencies have to be checked against the graph given in Figure 2.6.

The equation for the upper limit is given by:

$$n_0 = 94{,}76L^{-0{,}748} \qquad (3.1)$$

The equation for the lower limit is given by:

$$n_0 = \frac{80}{L} \quad \text{for} \quad 4\text{m} \le L \le 20\text{m}$$
$$n_0 = 23{,}58L^{-0{,}592} \quad \text{for} \quad 20\text{m} \le L \le 100\text{m} \qquad (3.2)$$

These equations were set up in an excel spreadsheet and the lower limit and upper limit natural frequencies were calculated for the 5m – 40m spans. These results are tabled in Table 4.2.

3.4 Analysis of continuous beams

The plane frame analysis module (in STRAP) was used to model the equal span continuous systems as two dimensional beams. The continuous beams and the applied loads were defined in STRAP in terms of a coordinated node reference system. The moving load option in STRAP was used to move the load models incrementally across from the left to the right hand side of the beam. Small increments were selected for each continuous beam in order to maximize the number of load cases that STRAP could accommodate. The maximum number of generated load cases in STRAP is limited to 998.

Although cross sectional properties have no influence on shear force and bending moment values, beam cross sectional properties have to be defined in order to solve the model in the STRAP program. For this study, a constant concrete cross section (as shown in Figure 3.7) was assigned to all continuous beams.

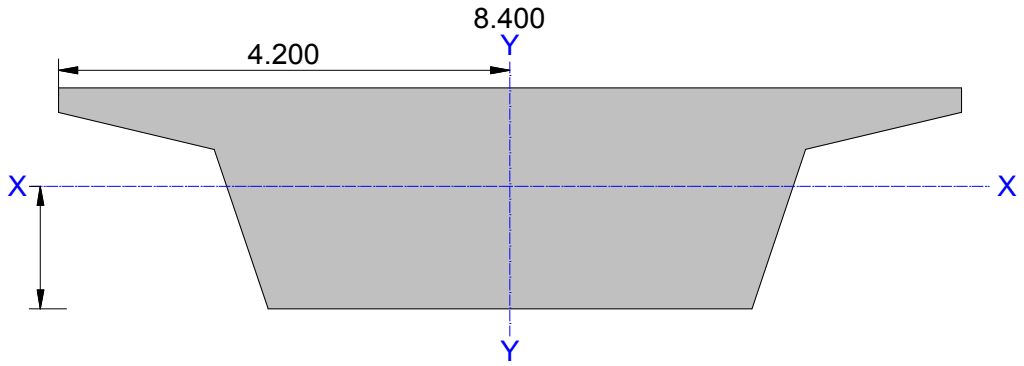

Figure 3.7: Cross section of beam

3.4.1 Analysis of South African NR load model for continuous beams

In the analysis of the South African NR loading model, the length of each UDL was made equivalent to the full length of the beam for each continuous beam. This arrangement ensures that the UDL occupies the full length of the beam before the axle loads move on and off the beam as the load models travel over the full length. This loading arrangement maximizes the applied load to obtain maximum effects for shear and bending moment. An example of a 2 equal span (2 x 5m) continuous beam is shown in Figure 3.8 to illustrate the loading concept. Hence, a leading UDL equal to 10m will occupy the total length of the beam before the first axle load moves onto the beam, as illustrated in figure 3.9.

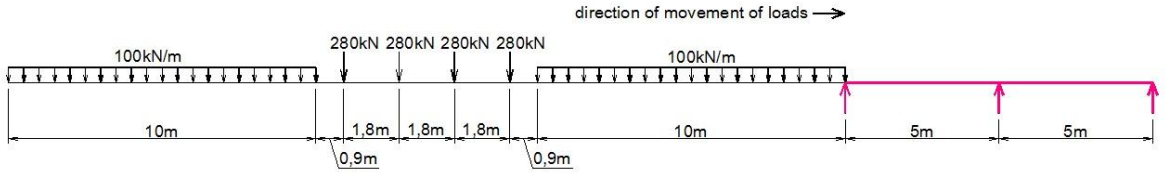

Figure 3.8: Arrangement of NR load model for 2 x 5m continuous beam

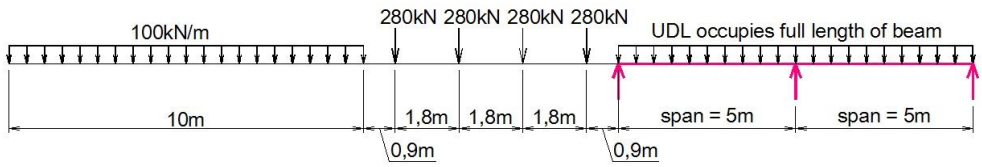

Figure 3.9: Leading UDL for NR load model on 2 x 5m continuous beam

Similarly, the trailing UDL is made equal to the full length of the beam and will occupy the full length of the beam after the last axle load has moved off the beam as is illustrated in figure 3.10.

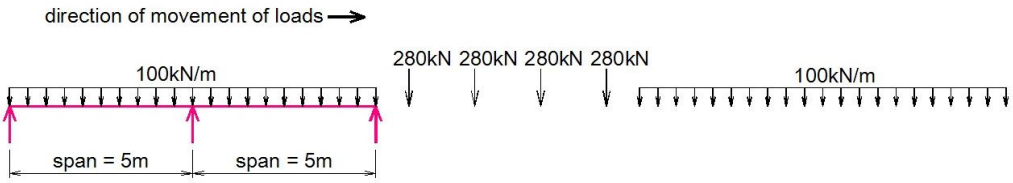

Figure 3.10: Trailing UDL for NR load model on 2 x 5m continuous beam

In the case of the 2 equal span continuous systems, the load cases generated were obtained by moving the NR load models incrementally as follows:

- 1st system (2 x 5m): 50mm intervals;
- 2nd and 3rd systems (2 x 10m and 2 x 15m): 100mm intervals;
- 4th system (2 x 20m): 150mm intervals;
- 5th and 6th systems (2 x 25m and 2 x 30m): 200mm intervals;
- 7th and 8th systems (2 x 35m and 2 x 40m): 250mm intervals.

In the case of the 3 equal span continuous systems, the load cases generated were obtained by moving the NR load models incrementally as follows:

- 1st and 2nd systems (3 x 5m and 3 x 10m): 100mm intervals;
- 3rd system (3 x 15m): 150mm intervals;
- 4th system (3 x 20m): 200mm intervals;
- 5th system (3 x 25m): 250mm intervals;
- 6th system (3 x 30m): 300mm intervals;
- 7th system (3 x 35m): 350mm intervals;
- 8th system (3 x 40m): 400mm intervals.

3.4.2 Analysis of Eurocode SW/0 load model for continuous beams

Similarly, the moving load method in STRAP used to analyse the South African NR load models for maximum load effects of shear and bending moment was applied to move the loads specified in the Eurocode SW/0 model from the left end across towards the right end of the beam. The placement of the loads and the direction of movement are shown in figure 3.11.

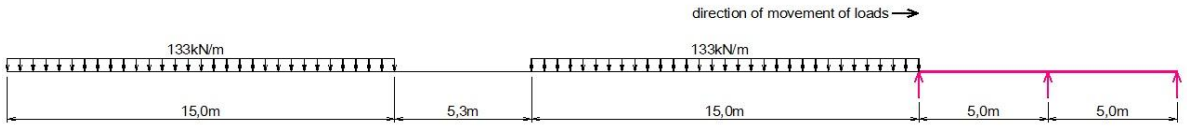

Figure 3.11: Arrangement of SW/0 load model for a 2 x 5m continuous beam

In the case of the 2 equal span continuous systems, the load cases generated were obtained by moving the SW/0 load models incrementally as follows:

- 1st system (2 x 5m): 50mm intervals;
- 2nd, 3rd, 4th, 5th and 6th systems (2 x 10m to 2 x 30m): 100mm intervals;
- 7th and 8th systems (2 x 35m and 2 x 40m): 150mm intervals.

In the case of the 3 equal span continuous systems, the load cases generated were obtained by moving the SW/0 load models incrementally as follows:

- 1st, 2nd, 3rd and 4th systems (3 x 5m to 3 x 20m): 100mm intervals;
- 5th, 6th and 7th systems (3 x 25m to 3 x 35m): 150mm intervals;
- 8th system (3 x 40m): 200mm intervals.

3.5 Summary

This chapter presents analytical and computer methods used to determine the position and magnitude of critical load effects for simply supported and continuous systems over a span range of 5m – 40m. The results obtained from the frame analysis for placement of the loads for maximum load effects simplified the influence line analysis, in that it provided information on where the maximum ordinates had to be placed on the influence line diagram for shear and bending moment.

The moving load module in STRAP was appropriate for the continuous systems, as evaluation of critical load effects would not have been easily achieved by using the influence line method for continuous systems. The moving load cases were generated from the user parameters for each system in a matter of seconds and it was possible to obtain the results in a number of ways (either graphically, displayed in a table or the results could be displayed on a single beam or a line of beams).

Critical positions for shear and bending moment will be illustrated in chapter four. Comparison of the maximum load effects resulting from such placements, will provide information on whether the South African design code is conservative in comparison to the Eurocode.

CHAPTER FOUR
RESULTS AND DISCUSSION

4.1 Introduction

In chapter three the approximation of the position for maximum effects of shear and bending moment for a 10m, 25m and 40m single span system was discussed. From these results it was established under which axle load the maximum bending moment would occur and how the loads are to be positioned for maximum shear. Consequently the results were used as the criteria to derive a generic equation for locating the position for maximum shear and bending moment for the Eurocode LM71 and SATS NR load models. These equations were applied to the single span systems to locate the positions for maximum bending moment. From these positions the magnitude of maximum bending moment were calculated using the equations proposed (Eqn 3.1 and 3.4) for the Eurocode LM71 and SATS NR load models respectively. Similarly the magnitude of maximum shear was calculated from the equations proposed (Eqn 3.7 and 3.8) for the Eurocode LM71 and SATS NR load models respectively.

The results of the maximum shear and bending moment for the single span systems for each code will be presented in this chapter and the comparison of the maximum effects between the codes will be discussed.

In chapter three the moving load option in STRAP to determine the maximum shear and bending moment for the Eurocode SW/0 and SATS NR load models for equal span continuous systems was also discussed. The results of the load cases generated in STRAP for maximum shear and bending moment will be presented for each code and the comparison of the maximum effects between the codes will be discussed.

4.2 Results for single span systems

4.2.1 Approximate position of maximum bending moment

The Prokon frame analysis results for approximating the maximum bending moment position for the 10m, 25m and 40m Eurocode LM71 single span systems are presented in Table 4.1. The maximum bending moment at these positions for each span is highlighted. A significant observation is that for each single span system, the maximum bending moment is located at the third axle load (Q_{vk3}). The significance of this result was to set up the influence line diagram for maximum bending moment with the maximum ordinate positioned at Q_{vk3}.

Table 4.1: Approximate position for maximum bending moment on 10m, 25m and 40m spans

Distance from centre line of beam to Q_{vk3}	Maximum Bending moment			Location of Maximum B.M.
a	10m span	25m span	40m span	
symmetrical loading	1830,00 kNm			
0,40 m	1856,61 kNm			Q_{vk3}
0,30 m	1858,92 kNm			Q_{vk3}
0,25 m	1859,41 kNm			Q_{vk3}
0,20 m	1859,46 kNm	8935,94 kNm		Q_{vk3}
0,15 m	1859,06 kNm	8936,20 kNm	20 515,49 kNm	Q_{vk3}
0,10 m	1858,22 kNm	8936,17 kNm	20 515,65 kNm	Q_{vk3}
0,05 m		8935,83 kNm	20 515,56 kNm	Q_{vk3}

It was observed that for each span the maximum bending moment occurred when the axle load Q_{vk3} had reached the following positions:

- 0,20m to the left of the centerline in the case of the 10m span;
- 0,15m to the left of the centerline in the case of the 25m span and
- 0,1m to the left of the centerline in the case of the 40m span.

It is noted that as the span increases, the distance between the third axle load and the centreline decreases. These positions are shown in figure 4.1.

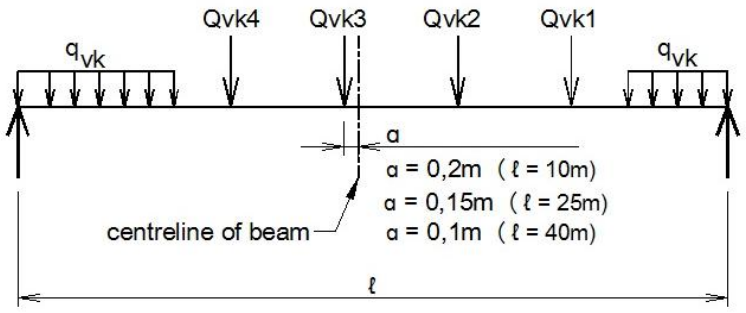

Figure 4.1: Position of the loads on 10m, 25m and 40m spans for Mmax

4.2.2 LM71 and NR load model positions for maximum bending moment

The load positions for maximum bending moment for the Eurocode LM71 and SATS NR load models for the simply supported systems are illustrated in Figures 4.2, 4.3, 4.4, 4.5, 4.6, 4.7, 4.8 and 4.9. These positions were calculated using the equations derived from the influence

line method equations (Eqn 3.3 and 3.6) for the Eurocode LM71 and SATS NR load model respectively.

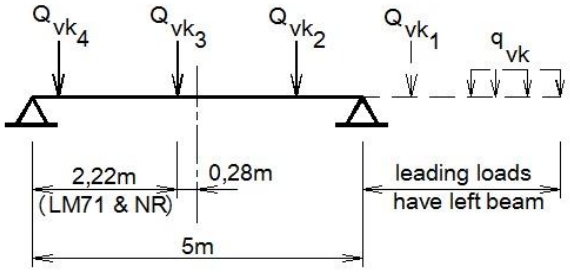

Figure 4.2: Load position for Mmax for 5m simply supported system

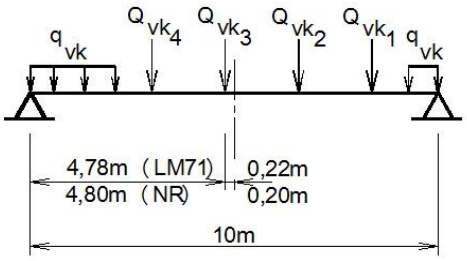

Figure 4.3: Load position for Mmax for 10m simply supported system

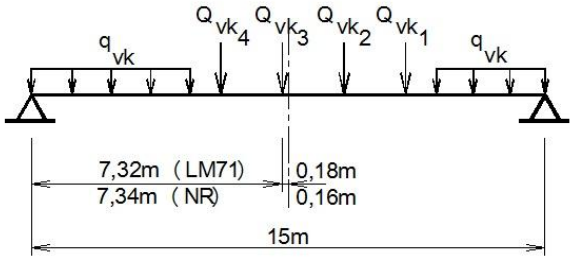

Figure 4.4: Load position for Mmax for 15m simply supported system

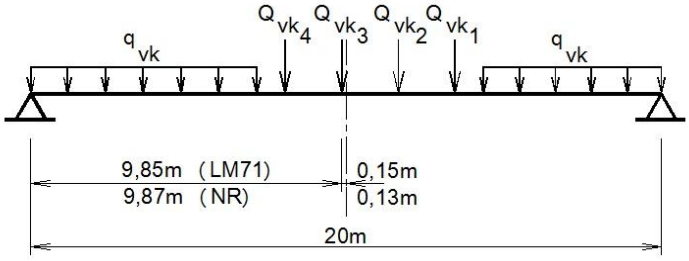

Figure 4.5: Load position for Mmax for 20m simply supported system

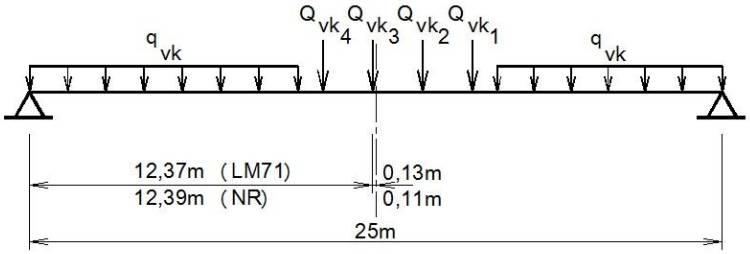

Figure 4.6: Load position for Mmax for 25m simply supported system

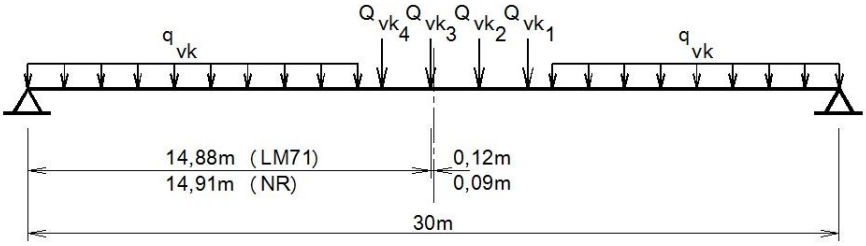

Figure 4.7: Load position for Mmax for 30m simply supported system

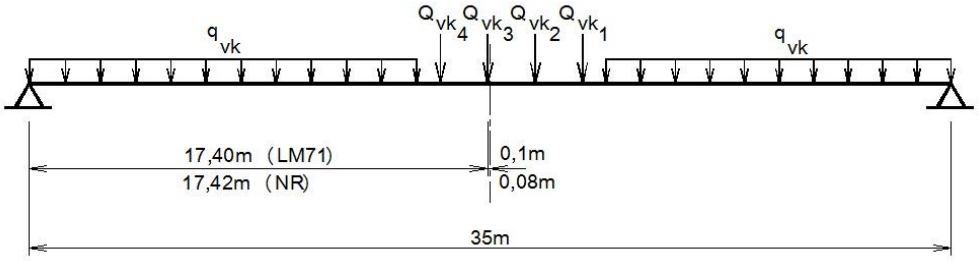

Figure 4.8: Load position for Mmax for 35m simply supported system

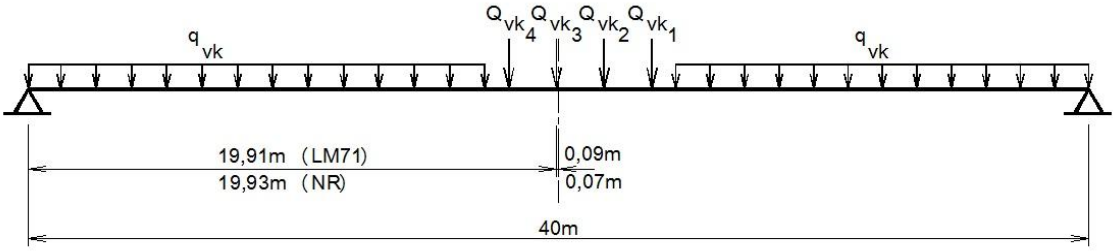

Figure 4.9: Load position for Mmax for 40m simply supported system

There was no significant difference in load position between the frame analysis approximation and the influence line method for the 10m, 25m and 40m spans. Despite the difference in axle load spacing between the two codes, no significant difference was observed between the positions of the loads for the two load models.

In the case of the 5m span, it was noted that the maximum bending moment occurred at the same position in both load models with only the last 3 axle loads positioned on the span. In the case of the remaining spans there was no significant difference in position between the two load models. A further observation was that as the span increased, Q_{vk3} moved closer to the centerline of the beam.

The maximum bending moment values corresponding to the positions for LM 71 and NR loading are tabulated in Table A.1 in the Appendix. Maximum bending moment values for heavier LM71 rail loads (α = 1,10) have been included in Table A.1. The objective of including heavier load moment values is to compare with heavy loads presented in the SATS loading model. The values presented in Table A.1 represent the static effects for bending moment.

Table A.2 in the Appendix represents the maximum design moment after the static moment values have been multiplied by the dynamic factor given in Table 2.1 for SATS NR loading and equations 2.1 and 2.2 for Eurocode LM 71 loading.

4.2.3 LM71 and NR load model positions for maximum shear

The Prokon frame analysis approximation for the maximum shear force position for the 10m, 25m and 40m Eurocode LM71 single span systems show that the maximum shear force occurs at the left hand support, just as the last axle load (Q_{vk4}) was leaving the left hand support.

The load arrangement for this position is shown in figure 4.10.

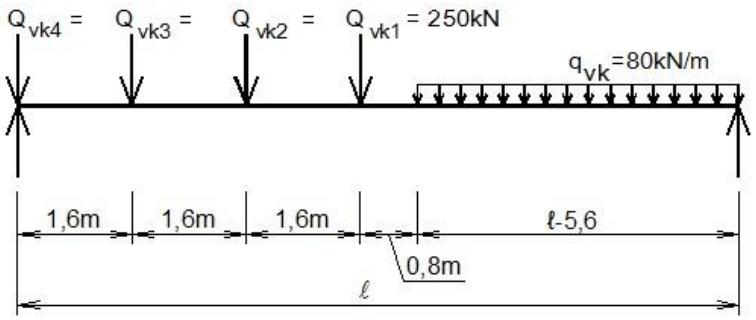

Figure 4.10 Load arrangement for Vmax for load model 71

This load arrangement was transferred to the influence line diagram, from which the generic equation for calculating maximum shear for both the Eurocode LM71 and SATS NR load model was obtained.

4.2.4 Influence line method results for LM71 and NR load model for maximum shear

The maximum shear force values corresponding to the loading position illustrated in Figure 4.10 were calculated using the equations (Eqn 3.7 and 3.8) derived from the influence line diagrams for the Eurocode LM71 and SATS NR load model respectively. These results are tabulated in Table A.3 in the Appendix. Maximum shear force values for heavier LM71 rail loads (α = 1,10) have been included in Table A.3.

Table A.4 in the Appendix represents the maximum design shear after the static shear values have been multiplied by the dynamic factor given in Table 2.1 for SATS NR loading and equations 2.1 and 2.2 for Eurocode LM 71 loading.

4.2.5 Dynamic analysis test results for load model 71

Equations 3.1 and 3.2 were set up in an excel spreadsheet to calculate the upper limit and lower limit natural frequencies respectively, for each of the spans (5m – 40m) in the study range. The results are tabulated in Table 4.2. The calculated results were used to check whether they fall within the limits of graphs (1) and (2) given in Figure 2.6. The results were found to be within the limits given in the graphs (1) and (2) for all spans. This implied that a dynamic analysis for simply supported systems for LM71 with train speeds less than 200 km/h was not required and the static analysis factored with the dynamic factor was adequate for this study.

Table 4.2: Natural frequency (n_0) values

Span (m)	Natural frequency values (n_0)	
	Upper limit frequency	Lower limit frequency
5	28	16
10	17	8
15	12	5
20	10	4
25	9	4
30	7	3
35	7	3
40	6	3

4.3 Results for continuous systems

The results of the STRAP analysis for the SATS NR and Eurocode SW/0 load models for 2 span and 3 span systems are tabled in Appendix B. STRAP tabulates the maximum and minimum values for axial force, shear and bending moment for each continuous beam. In the case of bending moment, maximum values refer to maximum hogging and minimum values refer to maximum sagging moment. For the purpose of this dissertation, maximum absolute values have been considered and used in the discussion.

STRAP allocates a numerical value (indicated in the row labelled “Load”) to each generated load case. The maximum (or minimum in the case of hogging moment or negative shear force) effect at the generated load case, together with the span in which the maximum effect occurs, is displayed in each table. The placement of the load models on each continuous beam to obtain maximum effects for shear and bending moment, are obtained from the number of the load case and the increment assigned to move the global loads across each span.

In the case of the SATS NR load model, the criterion assigned to evaluate the maximum effects of shear and bending moment for all continuous systems, was ensuring that the axle loads are accommodated on the beam with the UDL loading extending all the way to the end supports. The objective of this loading arrangement was to ensure that the axle loads (that are assigned in the code for the purpose of accommodating heavier loads over the axles) were included in the evaluation for maximum effects.

4.3.1 Mmax results for 2 span continuous systems

The load positions generated from the STRAP analysis load cases to obtain the maximum bending moment for the SATS NR load model for the 2-span systems are illustrated in Figures C.1, C.2, C.3, C.4, C.5, C.6, C.7 and C.8 in Appendix C.

It is observed in Figure C.1 that the most unfavourable position for maximum bending moment in the 2 x 5m continuous system occurred when the system was symmetrically loaded. For all other systems the axle loads were concentrated in the 1st span and the UDL spread over the full 2nd span to effect a maximum hogging moment over the centre support.

The load positions generated by the STRAP analysis to obtain maximum bending moment for the Eurocode SW/0 load model for the 2-span systems are illustrated in Figures C.9, C.10, C.11, C.12, C.13, C.14, C.15 and C.16 in Appendix C.

In Figure C.9 it is observed that the maximum bending moment occurred just after a short length of the leading UDL had moved off the beam. In the 2nd system (Figure C.10) the leading UDL was symmetrically positioned over the centre support at maximum bending moment. Due to the length of the beam in each system (2 x 5m and 2 x 10m) the 2nd UDL could not be accommodated on the beam. It is noted that symmetrical loading effected maximum bending moment for the 3rd, 4th, 5th and 6th systems (2 x 15m to 2 x 30m). In the last two systems both UDL's dominated the 2nd span with tail of the trailing UDL approaching the middle support in the 2 x 35m system and just leaving the middle support in the case of the 2 x 40m system.

It was noted that these positions resulted in a maximum hogging moment over the centre support in the cases of the 2 x 5m to 2 x 30m systems. The position of the loads in the 2 x 35m and 2 x 40m systems resulted in maximum sagging moment in the second span.

4.3.2 Vmax results for 2 span continuous systems

The load positions generated by STRAP to obtain the maximum shear force for the SATS NR load model for the 2-span systems are illustrated in Figures C.17, C.18, C.19, C.20, C.21, C.22, C.23 and C.24 in Appendix C.

In Figure C.17 it is observed that the maximum shear force for the 1st system (2 x 5m) occurred just as the 2nd axle load left the centre support. As the span length increased (as was observed in Figures C.18 to C.20 for the 2nd, 3rd and 4th systems), increased UDL loading in the 2nd span resulted in maximum shear force just as the 1st axle load left the centre support. In Figures C.21, C.22 and C.24 it is observed that with further increase in span length, (5th, 6th and 8th systems) the maximum shear force occurred after the axle loads had moved into the second span while the 7th system (2 x 35m) reached maximum shear force before the axle loads approached the centre support

The load positions generated by STRAP to obtain the maximum shear force for the Eurocode SW/0 load model for the 2-span systems are illustrated in Figures C.25, C.26, C.27, C.28, C.29, C.30, C.31 and C.32 in Appendix C.

Similar to the position reached for maximum bending moment for the 1st system, maximum shear force occurred just as the leading UDL was starting to move off the beam while the loading was spread over both spans for the 2nd system in Figures C.25 and C.26 respectively.

As the length of the beam increased in the 3rd, 4th and 5th systems, the maximum shear was recorded as the head of the trailing UDL had just passed the centre support (as observed in Figures C.27, C.28 and C.29), while short lengths of the leading UDL had left the beam in the 3rd and 4th systems. In the case of the 6th and 7th systems the maximum shear force was reached as the tail of the trailing UDL was just approaching the centre support (as observed in Figures C.30 and C.31). In the case of the last system, the head of the leading UDL had just left the centre support to effect maximum shear force.

4.3.3 Mmax results for 3 span continuous systems

The load positions generated by STRAP to obtain the maximum bending moment for the SATS NR load model are illustrated in Figures D.1, D.2, D.3, and D.4 in Appendix D, for the 1st four systems (3 x 5m to 3 x 20m). However, the load cases generated by STRAP in the last four systems (3 x 25 to 3 x 40m) were not consistent with the arrangement specified for the SATS NR load model. Maximum bending moment values were obtained based on only the trailing UDL positioned on the continuous beam. This implied that the leading UDL and the axle loads had already moved off the beam. Due to this discrepancy, the results for these systems were omitted and the systems concerned were analysed using the frame analysis method in Prokon. The load positions generated by Prokon to obtain the maximum bending moments due to the SATS NR load model for these systems are illustrated in Figures D.5, D.6, D.7 and D.8 in Appendix D. These results were regarded as accurate enough and it is noted that the positions of the loads are consistent with the arrangement obtained in STRAP for the 1st four systems.

It is observed that in all cases the axle loads are concentrated in the end span of the continuous system to effect maximum bending moment with the exception of the 1st two systems. In the 1st system the axle loads are symmetrically positioned about the 3rd support. In the 2nd system the axle loads are positioned in the 1st span to effect maximum bending moment.

Load positions generated by STRAP to obtain the maximum bending moment due to the Eurocode SW/0 load model are illustrated in Figures D.9, D.10, D.11, D.12, D.13, D.14, D.15 and D.16 in Appendix D, for spans 3 x 5m to 3 x 40m.

Figure D.9 shows approximately a third of the length of the leading UDL had just moved off the end of the beam to reach maximum moment in the 1st system (3 x 5m) before the 2nd UDL could move on the beam. In the 2nd system the leading UDL had already left the beam leaving the trailing UDL in the 2nd and 3rd spans of the beam. Figure D.11 shows that a short

length of the leading UDL had just moved off the beam to reach maximum bending moment in the 3rd system.

Figures D.12, D.13 and D.14 show that the 4th, 5th and 6th systems reached the maximum moment when the 1st and 2nd UDL loads are positioned in the 1st and 2nd spans respectively on either side of the 2nd support.

In the case of the 7th system the maximum bending moment was recorded as the tail of the trailing UDL was approaching the 3rd support (as observed in Figure D.15) while Figure D.16 shows that the UDL loads dominate the end span in the last system on reaching the maximum moment, just as the tail of the trailing UDL had left the 3rd support.

4.3.4 Vmax results for 3 span continuous systems

The load positions generated by STRAP to obtain the maximum shear force for the SATS NR load model for the 3-span systems are illustrated in Figures D.17, D.18, D.19, D.20, D.21, D.22, D.23 and D.24 in Appendix D.

Figure D.17 shows that the 1st system (3 x 5m) reached the maximum shear force just as the 2nd axle load left the 2nd support. Figures D.18 and D.19 show that as the span increased, the 2nd and 3rd systems (3 x 10m and 3 x 15m) carried heavier UDL loading in the 2nd and 3rd spans and the maximum shear force occurred just as the 1st axle load left the 2nd support.

Figures D.20 to D.24 show that with further increase in span and consequently increased UDL loading over the 2nd and 3rd span and extending into the 1st span, the maximum shear force occurred when all the axle loads were concentrated in the first span.

The load positions generated by STRAP to obtain the maximum shear force for the Eurocode SW/0 load model for the 3-span systems are illustrated in Figures D.25, D.26, D.27, D.28, D.29, D.30, D.30 and D.32 in Appendix D.

A relatively similar load arrangement to that of maximum moment was observed for maximum shear force for the 1st two systems (3 x 5m and 3 x 10m) as illustrated in Figures D.25 and D.26. In the case of the 3rd, 4th and 5th systems (3 x 15m to 3 x 25m) the maximum shear force occurred just as the end of the leading UDL approached the 3rd support as shown in Figures C.27 to C.29 while for the remaining systems, (3 x 30m to 3 x 40m) the maximum shear force occurred just as the tail of the trailing UDL approached the 3rd support.

4.4 Discussion of the comparison between the SATS and the Eurocode

Discussion on the comparison between the codes will be based on the ratio of the most unfavourable load effects due to the SATS code to those of the Eurocode. The ratio will be evaluated as the proportion of the load effects for SATS to those of the Eurocode. This implies that when the ratio is greater than 1, the SATS code is more conservative (or less economic) than the Eurocode.

4.4.1 Simply supported systems

The comparison between the SATS and the Eurocode for simply supported beams is based on the comparison between the NR and LM71 load model. In the case of the load effects for static and design bending moment and shear force, characteristic values (α = 1,00) and heavier loads (α = 1,10) were considered for the Eurocode LM71 load model.

Generally the comparison of the maximum load effects illustrated in Figures 4.11 and 4.12 for static bending moment and shear force between the railway bridge codes are relatively similar. The highest ratios of static shear force and bending moment were observed for the LM71 load model when the characteristic values (α = 1,00) were compared with the NR load model.

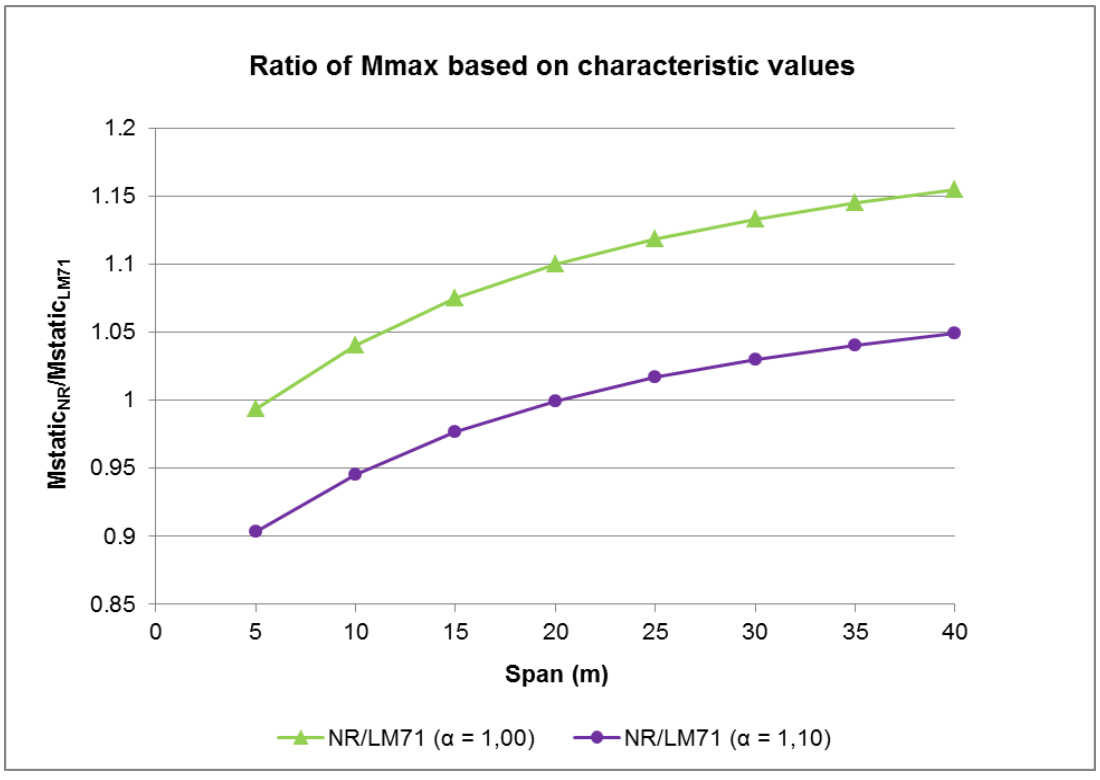

Figure 4.11 Ratio of static M_{max} (kNm) for LM 71 and NR load models

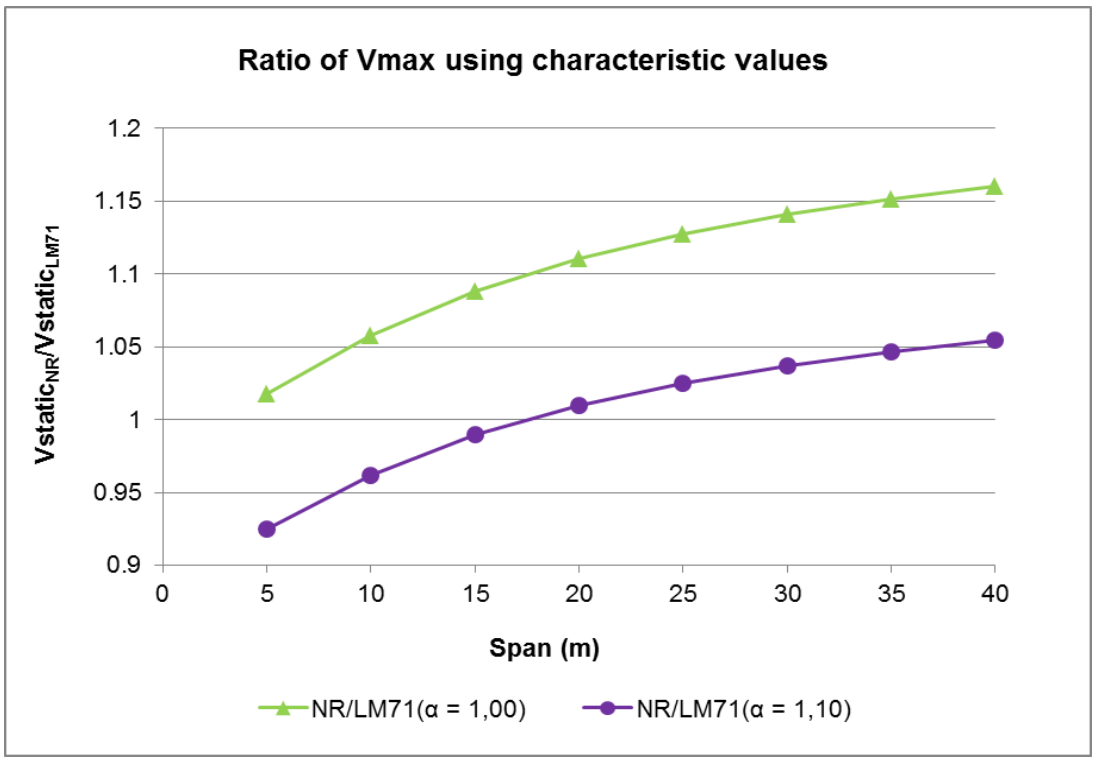

Figure 4.12 Ratio of static V_{max} (kN) for LM 71 and NR load models

The SATS code is observed to be liberal at 5m (i.e. 1% lower for NR) for static bending moment (in the case of characteristic values (i.e. α = 1,00) for the LM71 load model). As the span increases from 10m to 40m the SATS code is observed to be more conservative than the Eurocode. It was noted that the values at these spans were higher by 4% at 10m and increased to a maximum of 15% higher at 40m.

The SATS code is observed to be liberal for simply supported systems spanning 5m to 15m for static bending moment (in the case of heavier loads (i.e. α = 1,10) for the LM71 load model). It was noted that the values were 10% lower at 5m increasing to 2% lower at 15m. As the span increases from 25m to 40m the SATS code is observed to be more conservative than the Eurocode. At 20m it is noted that there is no difference between the two codes but at 25m the value is 2% higher and increases linearly to a maximum of 5% higher at 40m.

In the case of static shear force it is noted that the SATS code is conservative across the full range of spans (where α = 1,00 has been considered for the LM71 load model). The values at these spans were higher by 2% at 5m and increased to a maximum of 16% at 40m.

In the comparison between the NR and LM71 (α = 1,10) load models, it is observed that the SATS code is conservative at 20m to 40m for static shear force. The values at these spans were 1% higher at 20m and increased linearly to 5% higher at 40m. At spans 5m to 20m the values were 7% lower at 5m increasing linearly to 1% lower at 15m.

The formulae in Table 2.1 were used to calculate the dynamic factor applicable to bending moment and shear for NR loading for each span in the study range. Similarly, the formulae given in equations 2.1 and 2.2 were used to calculate the dynamic factor for the LM71 load model for both a carefully maintained track and a track with standard maintenance. These factors are tabled in Appendix A, Table A.2 (for bending moment) and A.4 (for shear force).

The static bending moment and shear force values obtained from the NR and LM71 load models were multiplied by the dynamic factors to obtain the design bending moment and shear force values for the SATS and the Eurocode load models respectively. In the case of the Eurocode load model, the dynamic factor for both a carefully maintained track (equation 2.1) and a track with standard maintenance (equation 2.2) were considered. The design bending moment and shear force values are tabled in Appendix A, Table A.2 and A.4 respectively.

The comparison illustrated in Figures 4.13 and 4.14 shows that the highest ratios of design bending moment and shear force were observed for the LM71 load model when the characteristic values (α = 1,00) were compared with the NR load model. These responses occurred for a carefully maintained track. The lowest ratios were observed for the LM71 load model when the characteristic values were converted to heavier loads (α = 1,10) and a track with standard maintenance was considered..

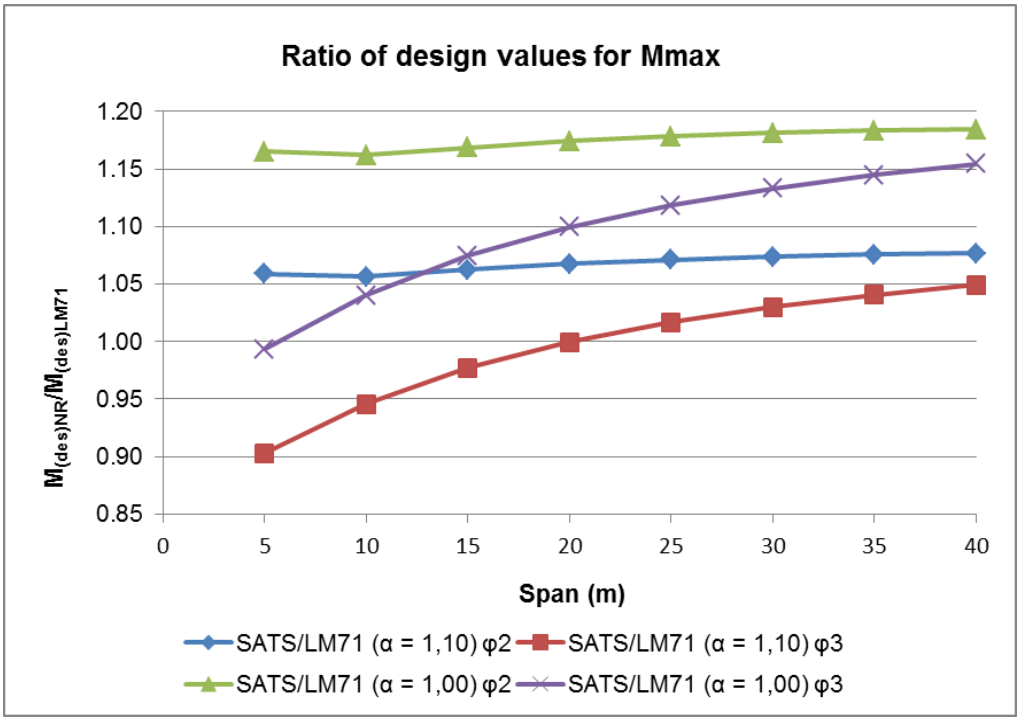

Figure 4.13 Ratio of design M_{max} (kNm) for LM 71 and NR load models

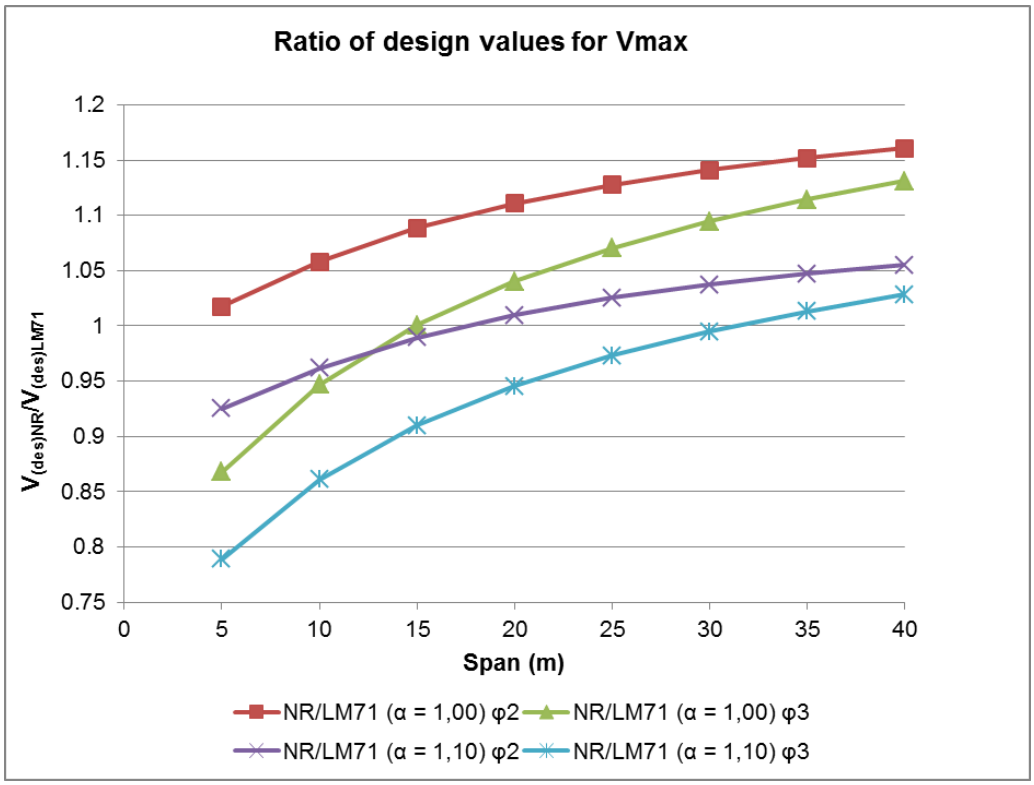

Figure 4.14 Ratio of design V_{max} (kN) for LM 71 and NR load models

A constant ratio for design moment is observed in the comparison between the SATS and the Eurocode (when characteristic values and heavier loads (α = 1,10) were considered for the LM71 load model) in the case of a carefully maintained track. The SATS code is conservative over the full range of spans with an average ratio of 17% higher in the case of characteristic values and an average ratio of 7% higher in the case of heavier loads (α = 1,10) for the LM71 load model.

However in the comparison between the SATS and the Eurocode (when characteristic values were considered for the LM71 load model) for a track with standard maintenance, the SATS code is observed to be conservative at spans 10m to 40m with 4% higher values for SATS at 10m increasing linearly to 15% higher at 40m. In the comparison between the SATS and the Eurocode (when heavier loads (α = 1,10) were considered for the LM71 load model), the SATS code is observed to be conservative at spans 25m to 40m only with 2% higher values for SATS at 25m increasing linearly to 5% higher at 40m. It is noted that there is no difference between the codes at the 20m span.

It is noted that only in the case of the comparison for design shear between the SATS and the Eurocode (when characteristic values (α = 1,00) were considered for the LM71 load model) for a carefully maintained track, the SATS code is observed to be conservative over the full range of spans. In all other cases the SATS code is conservative for certain spans

only for design shear. In the case of the comparison (where heavier loads (α = 1,10) were considered for the LM71 load model) for a carefully maintained track, the SATS code is observed to be conservative at spans 20m to 40m only with 1% higher values for SATS at 20m increasing linearly to 5% higher at 40m. Similarly for a track with standard maintenance the SATS code is conservative at spans 20m (4% higher) to 40m (13% higher) when characteristic values (α = 1,00) were considered for the LM71 load model. In the case of a track with standard maintenance when heavier loads (α = 1,10) were considered for the LM71 load model, the SATS code is conservative at spans 35m (1% higher) and 40m (3% higher) only.

4.4.2 Continuous systems

The comparison between the SATS and the Eurocode for continuous systems is based on the comparison between the NR and SW/0 load models. Static bending moment and shear force values were multiplied by the relevant dynamic factor defined in the SATS bridge code 1983, Cl. B2.3.2 (Table 2) and EN 1991 2: 2003, Cl. 6.4.5 to obtain the design shear force and bending moment values for the SATS and the Eurocode load models respectively. In the case of the Eurocode load model the determinant length specified in Case 5.2 of Table 6.2 (EN 1991 2: 2003) was used to calculate the dynamic factor for both a carefully maintained track and a track with standard maintenance. It is noted that since the equation defined in the SATS code for evaluating the dynamic factor for bending moment, is equivalent to the equation defined for shear and bending moment for a track with standard maintenance in the Eurocode, the comparison between the static and design bending moment will correspond where this type of track is considered in the case of the SW/0 load model. Similarly the equation defined in the SATS code for evaluating the dynamic factor for shear force is equivalent to the equation defined for shear and bending moment for a carefully maintained track in the Eurocode. This implies that the comparison between the static and design shear will correspond where a carefully track is considered in the case of the SW/0 load model.

In the case of the load effects for static and design bending moment and shear force, characteristic values (α = 1,00) and heavier loads (α = 1,10 and α = 1,21) were considered for the Eurocode SW/0 load model. Generally, the highest ratios of static and design shear force and bending moment were observed when the NR load model was compared with the characteristic values for the SW/0 load model (α = 1,00) for all continuous systems.

The following observations were made in the analysis of the 2 equal span continuous systems:

- For effect of static bending moment, the SATS codes is conservative over the 1st two and last four systems when compared with the SW/0 Eurocode load model for characteristic

values (α = 1,00). In the case of heavier loading (α = 1,10 and α = 1,21) considered for the SW/0 load model, the SATS code is conservative at the 1st system (α = 1,10) and last three systems (α = 1,10 and α = 1,21) only. Significantly high ratios are observed at the 1st system (17% higher) and the last three systems (25% - 40%) while moderate values (6% - 8%) are observed at the 2nd and 5th system respectively as illustrated in Figure 4.15. In the case of heavier loading (α = 1,10 and α = 1,21) the ratios are significantly high (27% for α = 1,10) and relatively high (14% - 16% for α = 1,21) at the last two systems.

- It is observed in Figures 4.15 and 4.17 that the ratio of M_{max} for NR and SW/0 load models decrease in the 2 x 10m to 2 x 20m range. This is due to the decrease in the dominance of the axle loading in the 1st span of the continuous system. The large axle loads produce higher bending moment values than the UDL loading. In the 2 x 5m continuous system (Figure C.1) the axle (point) loads for the NR load model dominate the length of the beam. If these axle loads are converted to a UDL, the M_{Max} produced is much lower than the M_{Max} value obtained for axle loads. Therefore, the M_{Max} produced by the NR load model is much higher than that of the SW/0 model for this system. As the continuous system increases, the axle loads dominate the 1st span in the 2 x 10m continuous system (Figure C.2) and the total load moving across the South African beam exceeds that of the Eurocode beam, hence M_{Max} produced by the NR load model is much higher than that of the SW/0 model. However, in the 2 x 15m and 2 x 20m systems (Figures C.3 and C.4), the UDL dominates 52% and 64% of the 1st span resulting in a drop in the M_{Max} produced by the NR load model. Furthermore, with heavier UDL loading across spans in the case of the SW/0 model in comparison to that of the NR load model, a significant drop in M_{Max} value for the NR load model for the 2 x 20m continuous beam was observed. Further increase in spans (2 x 25m to 2 x 40m) produced higher loads moving across the South African beam in comparison to the constant load model in the Eurocode resulting in much higher M_{Max} values produced by the NR load model. Hence the ratio of M_{max} for NR and SW/0 load models increases across this range.

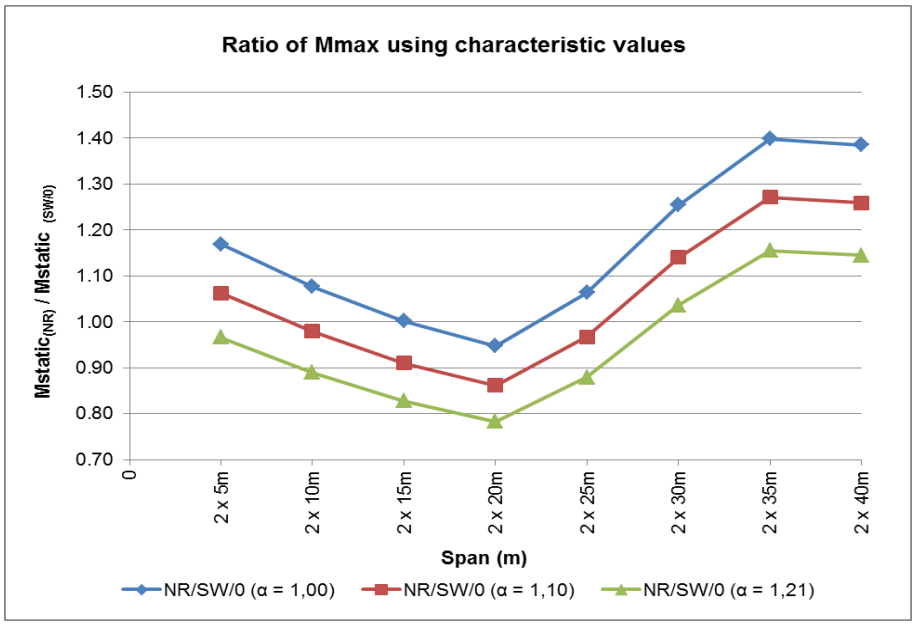

Figure 4.15 Ratio of static M_{max} (kNm) for NR and SW/0 load models (2 span systems)

- For effect of static shear force, the SATS codes is conservative over the full range of spans when both characteristic values (α = 1,00) and heavy loads (α = 1,10) were considered for the SW/0 Eurocode load model. The values are significantly high (22% - 35% at the 1st two spans and 17% - 23% at the last four spans) to relatively high (10% - 11% at the 3rd and 4th systems) in the case of characteristic values. In the case of heavy loads (α = 1,10) the only significant value (22%) was observed at the 1st system while relatively high (10% - 12%) values were observed at the 2nd and last three systems. There was no difference between the codes at the 3rd and 4th systems where the ratio was equal to 1,01 and 1,00 respectively.

  Where heavier loading (α = 1,21) was considered in the case of the Eurocode SW/0 load model, the SATS code was observed to be conservative at the 1st two (2 x 5m and 2 x 10m) systems and at the last three (2 x 30m – 2 x 40m) systems. The only relatively high value was observed at the 1st system (11%) while minimal values (1% - 2%) were observed at the 2nd, 6th and 7th system. There is no difference between the codes at the last span.

- Generally, shear force values decrease linearly over the length of the UDL in comparison to the sudden jump in shear values at positions of point loads. In addition, heavy axle loads close to supports produce large shear force value at the supports. The axle loads in the first 4 SA load systems (Figures C.17 to C.20) are all concentrated close to the centre support. This results in huge shear force values at the centre support. In the case of the first 2 Eurocode load systems (Figures C.25 and C.26), maximum shear was reached with only the 1st UDL positioned across the length of the beam. Consequently the ratio of V_{Max}

$_{(NR)}$ to $V_{Max\ (SW/0)}$ is high in the 1st two continuous systems (Figures 4.16 and 4.18). However, additional loading when both UDL's are positioned on the 2 x 15m to 2 x 20m Eurocode systems (Figures C.27 and C.28) produce higher maximum shear values in comparison to those in the 1st 2 Eurocode systems. Consequently, although the SA shear values exceed those of the Eurocode values, the ratio of $V_{Max\ (NR)}$ to $V_{Max\ (SW/0)}$ are slightly lower for these systems (Figures 4.16 and 4.18). For the remaining systems, the load positions are fairly consistent in both the SA and Eurocode systems as the length of the system increases. This implies that although the maximum shear force values increase proportionately for each load model, the ratio of $V_{Max\ (NR)}$ to $V_{Max\ (SW/0)}$ remain fairly consistent.

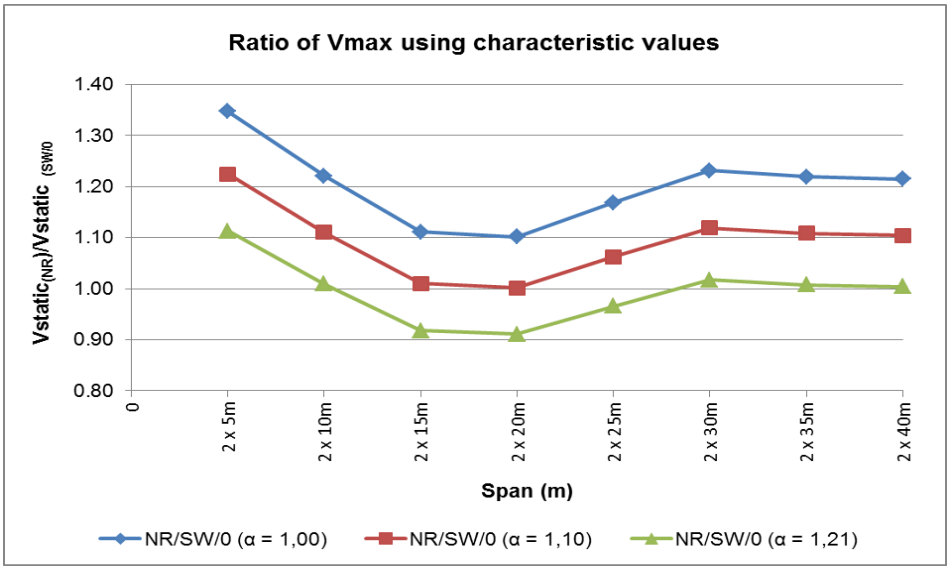

Figure 4.16 Ratio of static V_{max} (kN) for NR and SW/0 load models (2 span systems)

- In the case of design bending moment, the SATS codes is conservative over the full range of spans when compared with the SW/0 Eurocode load model for characteristic values (α = 1,00) and a carefully track. Significantly high ratios are observed at the 1st two systems (19% - 35%) and the last three systems (29% - 43%) and moderate ratios (8% to 11%) at the 3rd and 5th system respectively as illustrated in Figure 4.17. In the case of a track with standard maintenance the comparison is equivalent to that of static moment when compared with the SW/0 Eurocode load model for characteristic values (α = 1,00).

  Where heavier loading (α = 1,10) was considered in the case of the Eurocode SW/0 load model, the SATS code was observed to be conservative at the 1st two and last four systems (in the case of a carefully maintained track). Significantly high ratios are observed at the 1st system (23% higher) and the last three systems (18% - 30%) as illustrated in Figure 4.17 while the comparison for a track with standard maintenance is equivalent to

that of static moment when compared with the SW/0 Eurocode load model for heavy loads (α = 1,10).

Where heavier loading (α = 1,21) was considered in the case of the Eurocode SW/0 load model, the SATS code was observed to be conservative at the 1st (2 x 5m) system only for a carefully maintained track and at the last three (2 x 30m – 2 x 40m) systems for both types of track. Relatively high values are observed at the 1st systems (12%) and the last two systems (16% - 18%). The comparison for a track with standard maintenance is equivalent to that of static moment when compared with the SW/0 Eurocode load model for heavy loads (α = 1,10).

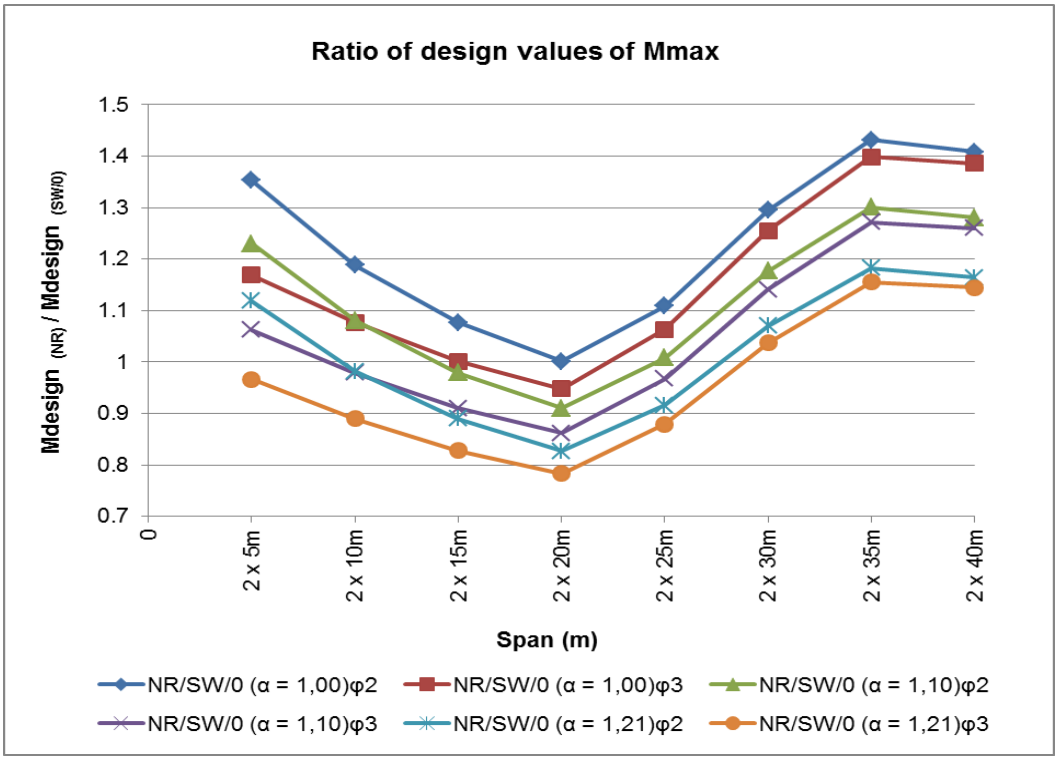

Figure 4.17 Ratio of design M_{max} (kNm) for NR and SW/0 load models (2 span systems)

- In the case of design shear force, the comparison for a carefully maintained track for characteristic values and heavy loads is equivalent to that of static shear force when compared with the SW/0 Eurocode load model with the same loading considerations. In the case of a track with standard maintenance, the SATS codes is conservative over the full range of spans when compared with the SW/0 Eurocode load model for characteristic values (α = 1,00). Relatively high ratios are observed at the 1st two systems (11% - 16%) and the last four systems (12% - 19%) and minimal ratios (3% to 4%) at the 3rd and 4th system respectively as illustrated in Figure 4.82. In the case of a track with standard maintenance for heavy loads (α = 1,10), the SATS codes is conservative at the

1st two and last four systems. Moderate ratios are observed at the 1st and 2nd system (1% - 6%) and the last four systems (2% - 9%).

Where heavier loading (α = 1,21) was considered in the case of the Eurocode SW/0 load model for a track with standard maintenance, the SATS code was observed to be liberal over the full range of spans.

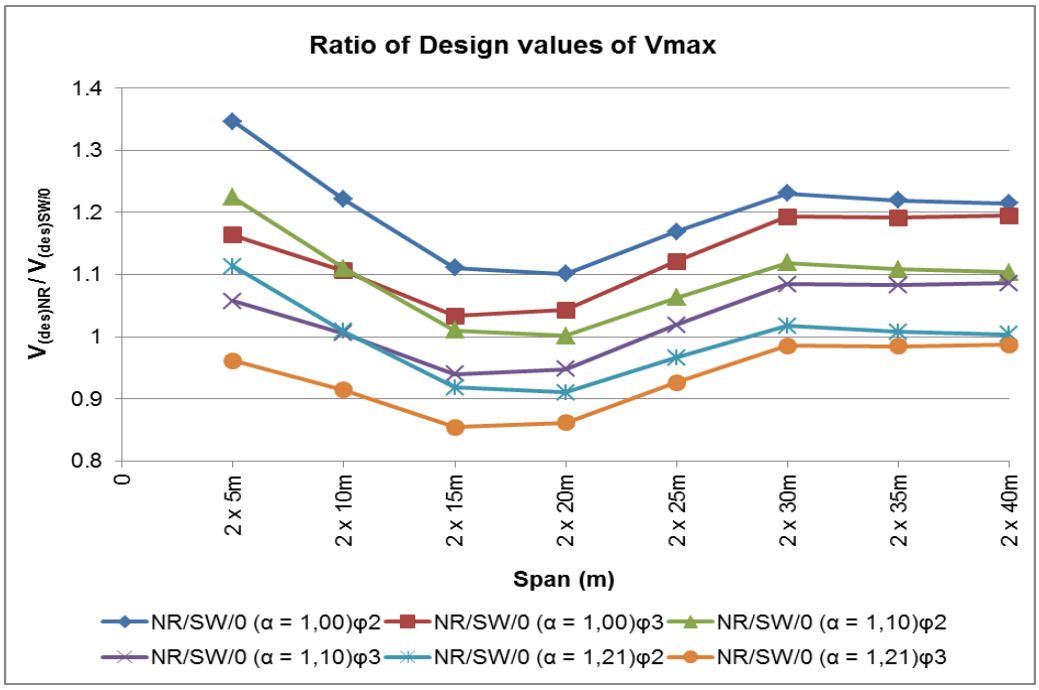

Figure 4.18 Ratio of design V_{max} (kN) for NR and SW/0 load models (2 span systems)

The following observations were made in the analysis of the 3 equal span continuous systems:

- For effect of static bending moment, the SATS codes is conservative over the 1st and last three systems when compared with the SW/0 Eurocode load model for characteristic values (α = 1,00). In the case of heavier loading (α = 1,10 and α = 1,21) considered for the SW/0 load model, the SATS code is conservative at the last two systems (α = 1,10) only. Moderate ratios are observed at the 1st system (7% higher) and the last two systems (15% - 16%) while a moderate value (8%) is observed at the 6th system for characteristic values as illustrated in Figure 4.19.

- Similar loading positions to that of the 2 span continuous systems for M_{Max} are observed in the 3 span continuous systems (Figures D.1 to D.8). In the case of the 3 x 5m continuous system (Figure D.1), the axle loads are dominant over the 2nd and 3rd span and their position, symmetrical about the 3rd support, results in a higher M_{Max} produced by the NR load model in comparison to that of the SW/0 model. However in the 3 x 10m system

(Figure D.2) the axle loads dominate the 1st span, hence the M_{Max} sagging produced by the axle loads in the 1st span is almost equal to the M_{Max} hogging at the 2nd support. In addition, the UDL loading (in the NR load model) in the 2nd and 3rd spans is lower than that of the SW/0 load model that dominates these spans. This results in a higher M_{MAX} over the 3rd support in the SW/0 load model. This therefore results in a drop in the graph in Figure 4.19 and 4.21. A similar loading arrangement occurs in the case of the 3 x 15m to 3 x 25m systems (Figures D.11 to D.13), but in these cases both UDL loads are now positioned over 2 of the spans and symmetrical over one of the central supports, resulting in a higher M_{MAX} over the particular support. This therefore accounts for the drop in the graph in Figure 4.19 and 4.21.

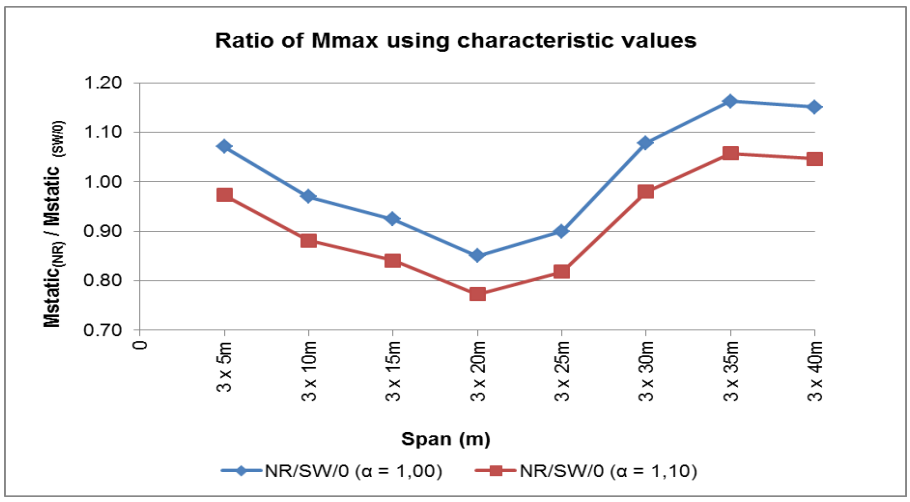

Figure 4.19 Ratio of static M_{max} (kNm) for NR and SW/0 load models (3 span systems)

- For effect of static shear force, the SATS codes is conservative over the full range of spans with the exception of the 4th system (3 x 20m) when heavy loads (α = 1,10) were considered for the SW/0 Eurocode load model. The only significant value (21%) was observed at the 1st system while relatively high (8% - 10%) values were observed at the 2nd and last four systems. There was no difference between the codes at the 3rd and 4th systems where the ratio was equal to 1,00 and -1,00 respectively.

  Where heavier loading (α = 1,21) was considered in the case of the Eurocode SW/0 load model, the SATS code was observed to be conservative at the 1st (2 x 5m) system only.

- Similar loading positions to that of the 2 span continuous systems for V_{Max} are observed in the 3 span continuous systems (Figures D.17 to D.24), hence the graphs in Figures 4.20 and 4.22 show a drop in the ratios for the 3 x 15m and 3 x 20m systems. However, the ratio of $V_{Max(NR)}$ to $V_{Max(SW/0)}$ is fairly consistent in the remaining 3 span systems, with the 3 x 5m system being the only outlier. This again is due to the position of the axle loads in

the 1st span and close to the 2nd support (Figure D.17) in comparison to only 75% the 1st UDL positioned across the 2nd and 3rd spans (Figure D.25). The NR load model therefore produces a higher V_{Max} than the SW/0 load model.

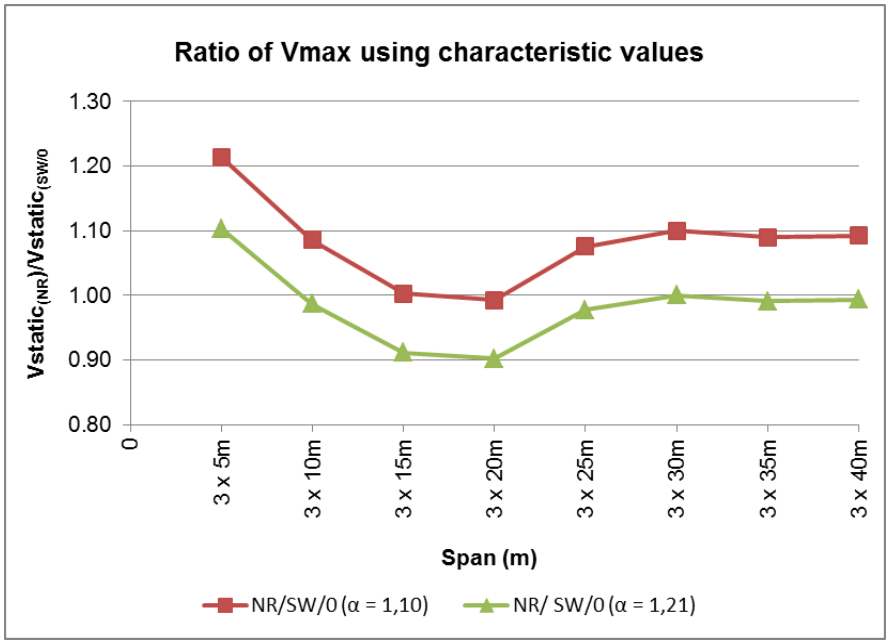

Figure 4.20 Ratio of static V_{max} (kN) for LM 71 and SW/0 load models (3 span systems)

- In the case of design bending moment, the comparison for a track with standard maintenance for characteristic values and heavy loads is equivalent to that of static bending moment when compared with the SW/0 Eurocode load model with the same loading considerations.
  In the case of a carefully maintained track, the SATS codes is conservative at 1st two systems and the last three systems when compared with the SW/0 Eurocode load model for characteristic values (α = 1,00). The ratio at the 1st system was observed to be significantly high (23%) and the last two systems (16% - 19%) with relatively moderate ratios (6% to 11%) at the 2nd and 6th system respectively as illustrated in Figure 4.21. In the case of a carefully maintained track for heavy loads (α = 1,10), the SATS codes is conservative at the 1st and last three systems. A relatively high ratio is observed at the 1st system (12%) and moderately low ratios at the last three systems (1% - 8%).

  Where heavier loading (α = 1,21) was considered in the case of the Eurocode SW/0 load model for a carefully maintained track, the SATS code was observed to be conservative at the 1st system (2%) only.

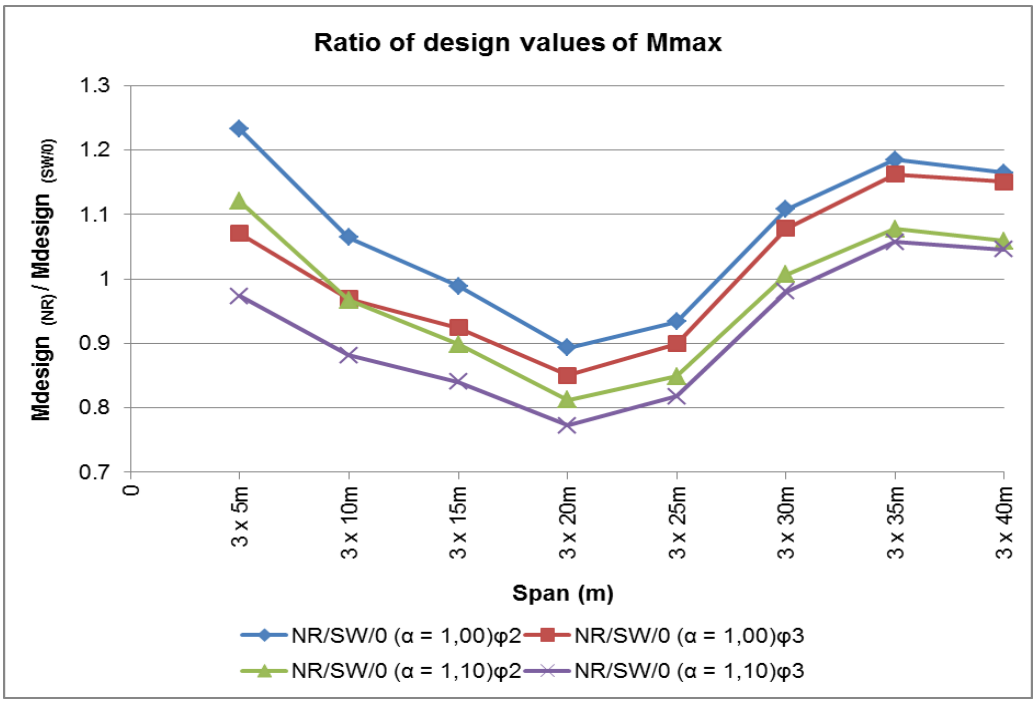

Figure 4.21 Ratio of design M_{max} (kNm) for NR and SW/0 load models (3 span systems)

- In the case of design shear force, the comparison for a carefully maintained track for characteristic values and heavy loads is equivalent to that of static shear force when compared with the SW/0 Eurocode load model with the same loading considerations.
  In the case of a track with standard maintenance for heavy loads (α = 1,10), the SATS codes is conservative at the 1st and last four systems. Moderate ratios are observed at the 1st system (5%) and the last four systems (4% - 8%).
  Where heavier loading (α = 1,21) was considered in the case of the Eurocode SW/0 load model for a track with standard maintenance, the SATS code was observed to be liberal over the full range of spans.

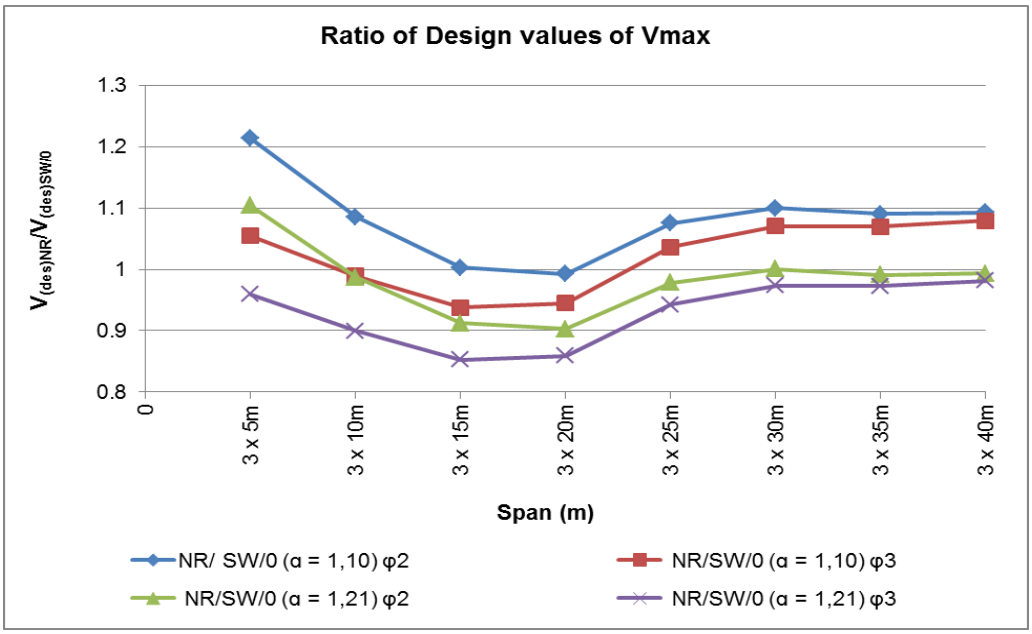

Figure 4.22 Ratio of design V_{max} (kN) for NR and SW/0 load models (3 span systems)

4.5 Summary

Simply supported and continuous systems (limited to 2 and 3 equal spans) were analysed and compared for static effects (limited to shear force and bending moment). Short to medium spans ranging from 5m – 40m were considered. Dynamic effects were taken into account by applying the dynamic factor to the static effects. Ratios of the static and design effects between the codes were evaluated and used as a basis for discussion for the comparison of the codes.

The findings from the influence line analytical method for simply supported systems, showed a fairly conservative comparison (within 5% maximum) between the codes for maximum static effects for spans ranging from 10m - 40m when heavy loads (α = 1,10) were applied in the Eurocode LM71 load model. The findings of the design effects were equivalent over the same range of spans for bending moment in the case of a track with standard maintenance and for design shear in the case of a carefully maintained track. In all cases the only significant value was at the 5m span where SA values were much lower that the Eurocode LM71 values.

As a result of the difference in the structure of the load models for continuous systems, the findings of the STRAP analysis showed conservative comparisons at specific spans for specific rail traffic considerations. Generally the ratios are significantly high at the end range of spans due to the fixed length of the UDL loading for the SW/0 model in comparison to the flexibility of the length of the UDL loading for the NR load model.

The findings for continuous systems (limited to 2 equal spans) showed a fairly conservative comparison (within 8% maximum) for maximum static bending moment and design bending moment (limited to a track with standard maintenance) effects at the 10m span for characteristic loads (α = 1,00). In the case of heavy loads (α = 1,10) a fairly conservative comparison (within 6% maximum) for maximum static bending moment effects was identified at the 5m span while for heavy loads (α = 1,21) a conservative comparison (within 4% maximum) was identified at the 30m span. Isolated cases of conservative comparisons (within 8% maximum) were identified at 15m (for characteristic loads), 10m and 25m (8% and 1% respectively) and at 30m (7% maximum) when a carefully maintained track was considered.

The findings for continuous systems (limited to 2 equal spans) for maximum static shear force effects show a conservative comparison at the middle range of spans (15m – 25m: 1% - 6% maximum) for heavy loads (α = 1,10), while the comparison is fairly conservative at the end range of spans (30m – 40m: 1% - 2% maximum) and at the 10m span (1%) for heavy loads (α = 1,21). The findings were equivalent for maximum design shear force effects when carefully maintained track was considered. Isolated cases of conservative comparisons (within 6% maximum) were identified at the mid-range of spans (15m – 25m) for heavy loads (α = 1,10) and at the end range of spans (30m – 40m: 2% maximum) and at 10m (1%) when a track with standard maintenance was considered.

The findings for continuous systems (limited to 3 equal spans) showed a fairly conservative comparison (within 8% maximum) for maximum static bending moment and design bending moment (limited to a track with standard maintenance) effects at the 5m and 30m spans for characteristic loads (α = 1,00). In the case of heavy loads (α = 1,10) a fairly conservative comparison (within 6% maximum) for maximum static bending moment effects was identified at the last two systems while for heavy loads (α = 1,21) the SATS code was liberal over the full range of spans. Isolated cases of conservative comparisons (within 6% maximum) were identified at 10m (for characteristic loads), 30m to 40m (1% to 8% respectively) when a carefully maintained track was considered for heavier SW/0 loads (α = 1,10).

The findings for continuous systems (limited to 3 equal spans) for maximum static shear force effects show a conservative comparison at the 1st two systems (10m – 15m: 0% - 9% maximum) for heavy loads (α = 1,10) while the comparison is fairly conservative at the end range of spans (30m – 40m: 9% - 10% maximum). The findings were equivalent for maximum design shear force effects when a carefully maintained track was considered. Conservative comparisons were identified at the 1st (5m: 5%) for heavy loads (α = 1,10) and

at the end range of spans (20m – 40m: 8% maximum) when a track with standard maintenance was considered.

CHAPTER FIVE
CONCLUSIONS AND RECOMMENDATIONS

5.1 Conclusions

The objective of this study was to review the South African and Eurocode Railway Bridge loading codes. The emphasis was on rail traffic live loads only. The analysis entailed using appropriate methods to simulate maximum load effects (limited to shear force and bending moment) for a 5m to 40m range of spans. An analytical approach (influence line analysis method) was used for single span systems and computer software (limited use of Prokon and extensive use of STRAP) was used for continuous spans.

The challenge faced was the specification of a single heavy load model for South African loading in contrast to the five load models specified in the Eurocode. A further challenge was the difference in the structure of the load models for continuous beams.

The influence line analysis method proved an effective technique for the analysis of the load effects for simply supported beams. This was largely attributed to the simplicity of the method for analyzing single span systems and the similarity in the structure of the load models specified in both codes. Despite the limitations of the frame analysis module, the moving load approach (although time consuming) identified the position for maximum load effects. The advantage of the frame analysis was that the positions could be directly applied to the appropriate influence lines from which the maximum load effects could be easily evaluated. The advantage of the moving load option in STRAP was the speed at which the load cases were generated and the numerous load cases that could be generated by the software. The STRAP method however produced unsatisfactory results for maximum bending moment for the last four systems of the NR load model. This was difficult to account for and access to information on how and what is written into the software is limited.

In contrast to the fixed length of the UDL's in the SW/0 load model, the NR load model has the freedom of optimizing the load effects by extending the length of the UDL's until they reach the end supports. This was acceptable for the spans in this study range since the maximum length of most South African trains range from approximately 80m – 110m. This, together with the additional axle loads present in the NR load model, naturally results in increased shear and moment values with increased spans.

It was found that live traffic loads imposed on single span railway bridges produce conservative load effects over certain range of spans. For characteristic values of LM71, the

SATS code is moderately to over conservative (4% - 15%) over the 10m – 40m range for effects of static and design bending moment (for a track with standard maintenance). However, for heavy loads (α = 1,10) for LM71 the SATS code is moderately conservative (2% - 5%) over the 20m – 40m range. In the case of design bending moment (for a carefully maintained track) the SATS code is over conservative over the full range of spans (16% - 18%) for characteristic values of LM71. Furthermore, when heavy loads (α = 1,10) are considered for LM71, the SATS code is moderately conservative (6% - 8%) over the full range of spans for a carefully maintained track.

In the case of static and design shear (for a carefully maintained track) the SATS code is moderately to over conservative over the full range of spans (2% - 16%) for characteristic values of LM71. For heavy loads (α = 1,10) for LM71 the SATS code is moderately conservative (1% - 5%) over the 20m – 40m range. In the case of design shear for a track with standard maintenance the SATS code is moderate to over conservative (4% - 13%) over the 20m – 40m range, and moderately conservative (1% - 3%) over the 35m – 40m range for heavy loads (α = 1,10) for LM71.

It was found that live traffic loads imposed on equal span continuous (limited to 2 spans) railway bridges produce over conservative (10% - 35%) static and design (for a carefully maintained track) shear force effects over the full range of spans when characteristic values are considered for the SW/0 load model. Where heavy loads (α = 1,10) were considered for the SW/0 load model, the SATS code was found to be relatively conservative (6% - 11%) over 2 x 10m – 2 x 40m spans, and over conservative (22%) at 2 x 5m. For characteristic values of SW/0, the SATS code is moderately to over conservative (3% - 19%) for design shear over the full range of spans for a track with standard maintenance. Where heavy loads (α = 1,10) were considered for the SW/0 load model, the SATS code is moderately conservative (1% - 6%) over the 2 x 5m – 2 x 10m and (2% - 9%) over the 2 x 25m – 2 x 40m range of spans.

Furthermore, live traffic loads imposed on 2 equal span continuous railway bridges produced over conservative (17%) at 2 x 5m and (25% - 40%) at 2 x 30m – 2 x 40m range of spans for static and design (for a track with standard maintenance) bending moment effects when characteristic values are considered for the SW/0 load model. The SATS was found to be over conservative (14% - 27%) at 2 x 30m – 2 x 40m range of spans for static and design (for a carefully maintained track) bending effects when heavy loads (α = 1,10) are considered for the SW/0 load model.

In the case of static and design bending moment (for a carefully maintained track) the SATS code is moderately to over conservative over the full range of spans (8% - 35%) for characteristic values of SW/0. For heavy loads (α = 1,10) for LM71 the SATS code is moderately conservative (1% - 5%) over the 20m – 40m range. In the case of design bending moment for a carefully maintained track the SATS code is over conservative (23% and 18% - 30%) at the 2 x 5m and the 30m – 40m range of spans for heavy loads (α = 1,10) for SW/0 load model. Furthermore the SATS code is over conservative (12% and 16% - 18%) at the 2 x 5m and the 35m – 40m range of spans for heavy loads (α = 1,20) for SW/0 load model.

It was found that live traffic loads imposed on 3 equal span continuous railway bridges produce a moderately conservative value (7%) at the 3 x 5m span and moderate to over conservative values (7% - 16%) at 3 x 30m and 3 x 40m spans for static and design (for a carefully maintained track) shear force effects when characteristic values are considered for the SW/0 load model. Where heavy loads (α = 1,10) were considered for the SW/0 load model, the SATS code was found to be relatively conservative (5% - 6%) at the 2 x 35m – 2 x 40m range of spans. Where heavy loads (α = 1,10) were considered for the SW/0 load model, the SATS code is moderately conservative (9% - 10%) at the 3 x 10m and 3 x 25m – 3 x 40m range of spans for design shear for a carefully maintained track but moderately conservative (4% - 8%) at the 3 x 5m and 3 x 25m – 3 x 40m range of spans for design shear for a track with standard maintenance.

In the case of static and design bending moment (for a carefully maintained track) the SATS code is moderately conservative (7% - 8%) at the 3 x 5m and 3 x 30m span and over conservative (15% - 16%) at the 3 x 35m – 3 x 40m spans (8% - 35%) for characteristic values of SW/0. For heavy loads (α = 1,10) for SW/0 the SATS code is moderately conservative (5% - 6%) at the 3 x 35m – 3 x 40m spans. In the case of design bending moment for a carefully maintained track the SATS code is over conservative (23% and 11% - 19%) at the 3 x 5m and the 3 x 35m – 3 x 40m range of spans for characteristic values of SW/0. For a track with standard maintenance the SATS code is moderately conservative (7% and 8% - 16%) at the 3 x 5m and the 3 x 35m – 3 x 40m range of spans.
For heavy loads (α = 1,10) for SW/0 load model for a carefully maintained track the SATS code is moderately conservative (12% and 6% - 8%) at the 3 x 5m and the 3 x 35m – 3 x 40m range of spans. Furthermore the SATS code is moderately conservative (5% - 6%) at the 3 x 35m – 3 x 40m range of spans for a carefully maintained track.

5.2 Recommendations

The study has identified significant areas that are worth further investigation. The following are recommendations for further research:

5.2.1 Increased research addresses the structural integrity of many bridge structures with the emphasis on identifying defects. James (2003) alludes to absence of previous work on actual field measurements, to qualify current rail traffic models and their associated load effects. To the author's knowledge no such research has been published for South African railway bridges and this could be an area where further work may be required.

5.2.2 The South African load model caters for heavy loads with speeds of up to 180km/h. It would be interesting to conduct further research on the feasibility of increased train speeds for South African railway bridges. This could provide an opportunity to investigate the aspects of dynamic analysis and whether provision should be made for inclusion in the SATS design code.

5.2.3 The dynamic factor is generally based on the interaction between the bridge, vehicle and the track. For this reason the nature of the track on which the train travels decides which equation is used to account for excessive vibrations in the Eurocode. The South African code however bases the evaluation of the dynamic factor on the load effect being considered. Although vast research on the dynamic factor is available, additional investigation on the dynamics of the equations used in the South African design code could provide further clarity.

5.2.4 STRAP software has a powerful moving load facility that is able to generate just under a thousand load cases within a few seconds. It would be recommended that the analysis of the load effects embarked on in this study be verified using an alternative software programme. This could possibly address the unsatisfactory results encountered in the analysis of the last four 3 span continuous systems.

5.2.5 The close correlation of the ratio of shear force and bending moment for simply supported beams in the 15m to 40m range strongly suggests that the South African code supports the use of the LM71 load model by applying a factor of $\alpha = 1{,}10$ for medium span bridge design. However, the different Eurocode load model used for continuous beams poses a challenge in the case of continuous systems and further investigation in this area to critically review the South African live load model would be required.

REFERENCES

American Railway Engineering and Maintenance of Way Association, *AREMA*, (2003).Manual*: Practical Guide To Railway Engineering*. p.366-368.

Artomov V., Raspopov A. *Comparative analysis of models of railway loads C14 and LM71 for girder bridges*. Science and Transport Progress, 2014, no. 1 (49), pp. 160-166. doi: 10.15802/stp2014/22687.

Björklund, L. (2004). *Dynamic Analysis of a Railway Bridge subjected to High Speed Trains*. Masters. Royal Institute of Technology, Stockholm.

BS 5400-Part 2 Specification for Loads. http://www.scribd.com/doc/125093645/BS-5400-Part-2-Specification-for-Loads

BS NA EN 1991-2, (2003). *UK National Annex to Eurocode 1: Actions on structures. Traffic loads on bridges*. BSI, London.

Busatta, F. and Moyo, P. (2015). *Vibration Monitoring of a Large Scale Heavy Haul Railway Viaduct*. MATEC Web of Conferences, 24, p.04007.

Calgaro J,A. *Loads on bridges*. Progress in Structural Engineering and Materials, 1998, Vol 1 (4). pp. 452-461.

Chen, W., Duan, L. (1999). *Bridge Engineering Handbook*. CRC Press, *ISBN 0849374340*. pp.64-9 – 64-10.

Cook, R., Malkus, D., Plesha, M. and Witt, R. (2017). *Concepts and Applications of Finite Element Analysis*. [online] Dl.acm.org. Available at: http://dl.acm.org/citation.cfm?id=1197960 [Accessed 24 Mar. 2017].

Design Manual For Roads and Bridges BD 37/01, Composite Version of BS 5400: Part 2, Loads for Highway Bridges. (2001). ISBN 0 11 552354 5, pp.Volume 1 Section 3 Part 14.

Ellobody, E. (2014). *Finite Element Analysis and Design of Steel and Steel–Concrete Composite Bridges ISBN 9780124173033*. pp.123-126.

EN 1991-2, (2003). *Eurocode 1: Actions on structures - Part 2: Traffic loads on bridges*. CEN, Brussels.

International Heavy Haul Association (IHHA), http://www.ihha.net (2015)

James, G. (2003). *Analysis of Traffic Load Effects on Railway Bridges*. Doctoral Thesis. Royal Institute of Technology, Stockholm, Sweden.

Jonsson, H. and Ljungberg, J. (2005). *Eurocode versus Swedish national codes for steel bridges.* Masters thesis. Chalmers University of Technology.

Lukianenko, A. (2012). *Comparison of Russian norms (SNiPs) and European norms (Eurocodes) for road and railway bridges*. Bachelor's. Saimaa University of Applied Sciences, Lappeenranta.

Nautiyal, B.D. 2001. *Introduction to Structural Analysis*. New Delhi: New Age International.

Notkus A.J., Kamaitis Z. *Analysis and comparison of Eurocode and SNIP traffic load models for railway bridges*. Modern Building Materials, Structures and Techniques, 2010, pp 720 – 724.

Obrien, E., Keogh, D. and O'Connor, A. (2015). *Bridge Deck Analysis*. 2nd ed. CRC Press, pp.45 - 46.

O'Connor, C., & Shaw, P. A. (2000). *Bridge loads an international perspective*. London, Spon Press. http://www.crcnetbase.com/isbn/9780419246008.

Prokon.com. (2016). *PROKON*. [online] Available at: https://prokon.com/.

STRAP. *Structural Application Program Manual, Version 2013*

Shibeshi, R. (2015). *Dynamic analysis of steel railway bridge subjected to train loads*. MSc. University of Pretoria.

Thenbs.com. (2016). *BS 5400-2:1978 Steel, concrete and composite bridges. Specification for loads (AMD 4209) (withdrawn), British Standards Institution - Publication Index | NBS*. https://www.thenbs.com/PublicationIndex/Documents/Details?DocId=251247

Syrjä, R. (2012). *Vertical Traffic Loads on bridges according to Eurocodes*. AALTO university lecture notes, Department of Civil and Structural Engineering.

Thenbs.com. (2016). *BS 5400-2:2006 Steel, concrete and composite bridges. Specification for loads (withdrawn), British Standards Institution - Publication Index | NBS*. https://www.thenbs.com/PublicationIndex/Documents/Details?DocId=280406

Vaidyanathan, R. and Perumal, P. Volume II (2008). *Structural analysis*. India: University Science Press. pp 60 – 72

Vayas, I. and Iliopoulos, A. (n.d.). *Design of steel-concrete composite bridges to Eurocodes*. London, Spon Press. pp 89 – 92

Web.archive.org. (2018). Wayback Machine. [online] Available at: https://web.archive.org/web/20071012023401/http://www.ucw.co.za/pdf/electric_loco.pdf [Accessed 23 Jan. 2018].

Appendix A:

Table A.1: Static Mmax (kNm) for SATS NR and Eurocode LM71 loading

Span (m)	SATS NR loading	Eurocode LM 71	
	Max moment (kNm)	Max moment (kNm) α = 1,00	Max moment (kNm) α = 1,10
5	502.97	506.28	556.90
10	1934.10	1859.49	2045.44
15	3994.88	3717.53	4089.29
20	6681.66	6076.68	6684.35
25	9993.79	8936.22	9829.85
30	13931.07	12295.95	13525.55
35	18493.43	16155.78	17771.35
40	23680.84	20515.66	22567.22

Table A.2: Design Mmax (kNm) for SATS NR and Eurocode LM71 loading

Span (m)	SATS NR		EUROCODE LM 71					
	φ	M_{design}	φ_2	φ_3	M_{design} (α = 1,00)	M_{design} (α = 1,00)	M_{design} (α = 1,10)	M_{design} (α = 1,10)
					φ_2	φ_3	φ_2	φ_3
5	1.79	900.75	1.53	1.79	773.21	906.67	850.53	997.34
10	1.46	2822.18	1.31	1.46	2428.70	2713,31	2671,57	2984,64
15	1.32	5265.56	1.21	1.32	4505.84	4900.00	4956.43	5390.00
20	1.24	8255.87	1.16	1.24	7031.13	7508.36	7734.24	8259.19
25	1.18	11792.67	1.12	1.18	10008.57	10544.74	11009.43	11599.22
30	1.14	15871.75	1.09	1.14	13437.89	14008.85	14781.67	15409.74
35	1.11	20488.53	1.07	1.11	17317.71	17898.68	19049.49	19688.55
40	1.08	25638.74	1.06	1.08	21646.46	22211.86	23811.11	24433.05

Table A.3: Static Vmax (kN) for Eurocode LM71 and SATS NR load model

Span (m)	Maximum shear (static)		
	SATS NR	Eurocode LM 71	
		α = 1,00	α = 1,10
5	532.10	522.88	575.17
10	886.05	837.44	921.18
15	1170.70	1075.63	1183.19
20	1438.03	1294.72	1424.19
25	1698.42	1506.18	1656.79
30	1955.35	1713.81	1885.19
35	2210.30	1919.27	2111.20
40	2464.01	2123.36	2335.70

Table A.4: Design Vmax (kN) for Eurocode LM 71 and SATS NR loading

Span (m)	SATS NR		EUROCODE LM 71					
	φ	V_{design}	φ_2	φ_3	V_{design} (α = 1,00)	V_{design} (α = 1,00)	V_{design} (α = 1,10)	V_{design} (α = 1,10)
					φ_2	φ_3	φ_2	φ_3
5	1.53	812.65	1.53	1.79	798.57	936.41	878.42	1030.05
10	1.31	1157.28	1.31	1.46	1093.79	1221.97	1203.17	1344.16
15	1.21	1418.95	1.21	1.32	1303.72	1417.76	1434.09	1559.54
20	1.16	1663.89	1.16	1.24	1498.08	1599.76	1647.89	1759.73
25	1.12	1902.23	1.12	1.18	1686.92	1777.29	1855.61	1955.02
30	1.09	2136.94	1.09	1.14	1872.98	1952.56	2060.27	2147.81
35	1.07	2369.27	1.07	1.11	2057.30	2126.32	2263.03	2338.95
40	1.06	2599.83	1.06	1.08	2240.40	2298.92	2464.44	2528.81

Appendix B:

B.1 STRAP results – 2 span (SATS) systems

Table B.1: NR load model - 2 x 5m system

MAXIMUM BEAM RESULTS (2x5m system) 50mm increments			
Beam	**Axial**	**V2**	**M3**
* Maximum	0.000	615.733	488.858
Beam	1	2	1
Load	1	392	373
* Minimum	0.000	-623.445	-350.415
Beam	1	1	1
Load	1	355	300

hogging moment

maximum shear value

Table B.2: NR load model - 2 x 10m system

MAXIMUM BEAM RESULTS (2x10m system) 100mm increments			
Beam	**Axial**	**V2**	**M3**
* Maximum	0.000	1019.226	1578.118
Beam	1	2	1
Load	1	365	291
* Minimum	0.000	-1033.011	-1245.938
Beam	1	1	1
Load	1	310	286

hogging moment

maximum shear value

Table B.3: NR load model - 2 x 15m system

MAXIMUM BEAM RESULTS (2x15m system) 100mm increments			
Beam	**Axial**	**V2**	**M3**
* Maximum	0.000	1365.995	3358.314
Beam	1	2	1
Load	1	515	421
* Minimum	0.000	-1378.361	-2520.385
Beam	1	1	1
Load	1	460	406

hogging moment

maximum shear value

Table B.4: NR load model - 2 x 20m system

MAXIMUM BEAM RESULTS (2x20m system) 150mm increments			
Beam	**Axial**	**V2**	**M3**
* Maximum	0.000	1688.285	5745.930
Beam	1	2	1
Load	1	444	373
* Minimum	0.000	-1705.541	-4141.117
Beam	1	1	1
Load	1	407	351

hogging moment

maximum shear value

Table B.5: NR load model - 2 x 25m system

MAXIMUM BEAM RESULTS (2x25m system) 200mm increments			
Beam	**Axial**	**V2**	**M3**
* Maximum	0.000	2017.503	8780.128
Beam	2	2	1
Load	500	419	338
* Minimum	0.000	-2017.504	-6120.880
Beam	2	1	1
Load	361	369	323

hogging moment

maximum shear value

Table B.6: NR load model - 2 x 30m system

MAXIMUM BEAM RESULTS (2x30m system) 200mm increments			
Beam	**Axial**	**V2**	**M3**
* Maximum	0.000	2371.462	12416.647
Beam	1	2	1
Load	1	495	531
* Minimum	0.000	-2371.462	-8706.094
Beam	1	1	1
Load	1	443	151

hogging moment

maximum shear value

Table B.7: NR load model - 2 x 35m system

MAXIMUM BEAM RESULTS (2x35m system) 250mm increments			
Beam	**Axial**	**V2**	**M3**
* Maximum	0.000	2715.887	16705.664
Beam	1	2	2
Load	445	457	379
* Minimum	0.000	-2720.960	-11849.961
Beam	1	1	1
Load	322	414	141

hogging moment

maximum shear value

Table B.8: NR load model - 2 x 40m system

MAXIMUM BEAM RESULTS (2x40m system) 250mm increments			
Beam	**Axial**	**V2**	**M3**
* Maximum	0.000	3058.958	21600.000
Beam	1	2	1
Load	359	518	432
* Minimum	0.000	-3036.950	-15477.500
Beam	1	1	1
Load	624	472	161

hogging moment

maximum shear value

B.2 STRAP results – 2 span (Eurocode) systems

Table B.9: SW/0 load model - 2 x 5m system

MAXIMUM BEAM RESULTS (2x5m system) 50mm increments			
Beam	**Axial**	**V2**	**M3**
* Maximum	0.000	462.871	418.214 → hogging moment
Beam	1	2	1
Load	170	214	206
* Minimum	0.000	-462.871	-321.375
Beam	1	1	2
Load	166	213	403

Table B.10: SW/0 load model - 2 x 10m system

MAXIMUM BEAM RESULTS (2x10m system) 100mm increments			
Beam	**Axial**	**V2**	**M3**
* Maximum	0.000	846.160	1465.565 → hogging moment
Beam	2	2	1
Load	294	195	176
* Minimum	0.000	-846.160	-1275.175
Beam	2	1	1
Load	264	157	102

Table B.11: SW/0 load model - 2 x 15m system

MAXIMUM BEAM RESULTS (2x15m system) 100mm increments			
Beam	**Axial**	**V2**	**M3**
* Maximum	0.000	1240.575	3353.181 → hogging moment
Beam	1	2	2
Load	319	298	329
* Minimum	0.000	-1240.574	-2862.707
Beam	1	1	2
Load	305	357	508

Table B.12: SW/0 load model - 2 x 20m system

MAXIMUM BEAM RESULTS (2x20m system) 100mm increments			
Beam	**Axial**	**V2**	**M3**
* Maximum	0.000	1548.213	6063.747 → hogging moment
Beam	1	2	2
Load	372	348	378
* Minimum	0.000	-1548.212	-4824.292
Beam	1	1	2
Load	341	407	585

Table B.13: SW/0 load model - 2 x 25m system

MAXIMUM BEAM RESULTS (2x25m system) 100mm increments			
Beam	**Axial**	**V2**	**M3**
* Maximum	0.000	1725.951	8256.357
Beam	1	2	2
Load	378	398	427
* Minimum	0.000	-1725.951	-6829.121
Beam	2	1	2
Load	458	457	663

hogging moment

Table B.14: SW/0 load model - 2 x 30m system

MAXIMUM BEAM RESULTS (2x30m system) 100mm increments			
Beam	**Axial**	**V2**	**M3**
* Maximum	0.000	1926.519	9897.123
Beam	2	2	1
Load	571	651	477
* Minimum	0.000	-1926.519	-8904.969
Beam	2	1	2
Load	546	304	733

hogging moment

Table B.15: SW/0 load model - 2 x 35m system

MAXIMUM BEAM RESULTS (2x35m system) 150mm increments			
Beam	**Axial**	**V2**	**M3**
* Maximum	0.000	2231.634	11156.938
Beam	1	2	2
Load	115	468	352
* Minimum	0.000	-2231.634	-11948.390
Beam	1	1	2
Load	549	236	447

sagging moment

Table B.16: SW/0 load model - 2 x 40m system

MAXIMUM BEAM RESULTS (2x40m system) 150mm increments			
Beam	**Axial**	**V2**	**M3**
* Maximum	0.000	2514.148	12149.482
Beam	1	2	1
Load	201	501	385
* Minimum	0.000	-2518.897	-15591.651
Beam	1	1	2
Load	252	270	505

sagging moment

maximum shear value

B.3 STRAP results – 3 span (SATS) systems

Table B.17: NR load model - 3 x 5m system

MAXIMUM BEAM RESULTS (3x5m system) 100mm increments			
Beam	**Axial**	**V2**	**M3**
* Maximum	0.000	593.724	418.170
Beam	1	3	2
Load	1	297	287
* Minimum	0.000	-609.864	-369.897
Beam	1	1	1
Load	1	228	201

maximum shear value

Table B.18: NR load model - 3 x 10m system

MAXIMUM BEAM RESULTS (3x10m system) 100mm increments			
Beam	**Axial**	**V2**	**M3**
* Maximum	0.000	994.875	1348.702
Beam	3	3	1
Load	598	565	387
* Minimum	0.000	-1007.335	-1336.289
Beam	3	1	1
Load	593	410	386

maximum shear value

Table B.19: NR load model - 3 x 15m system

MAXIMUM BEAM RESULTS (3x15m system) 150mm increments			
Beam	**Axial**	**V2**	**M3**
* Maximum	0.000	1342.927	2827.939
Beam	1	3	3
Load	1	543	566
* Minimum	0.000	-1342.928	-2703.333
Beam	1	1	3
Load	1	407	579

maximum shear value

Table B.20: NR load model - 3 x 20m system

MAXIMUM BEAM RESULTS (3x20m system) 200mm increments			
Beam	**Axial**	**V2**	**M3**
* Maximum	0.000	1669.055	4808.172
Beam	1	3	3
Load	1	545	567
* Minimum	0.000	-1669.056	-4502.495
Beam	1	1	3
Load	1	393	574

maximum shear value

Table B.21: NR load model - 3 x 25m system

MAXIMUM BEAM RESULTS (3x25m system) 250mm increments				Prokon
Beam	**Axial**	**V2**	**M3**	**Mmax**
* Maximum	0.000	2011.874	~~7342.234~~	7027.54
Beam	2	3	~~2~~	2
Load	202	538	~~724~~	
* Minimum	0.000	-2017.308	~~-6723.102~~	
Beam	2	1	~~1~~	
Load	839	393	~~359~~	

maximum shear value

Table B.22: NR load model - 3 x 30m system

MAXIMUM BEAM RESULTS (3x30m system) 300mm increments				Prokon
Beam	**Axial**	**V2**	**M3**	**Mmax**
* Maximum	0.000	2352.954	~~10571.896~~	10209.75
Beam	3	3	~~2~~	2
Load	337	533	~~720~~	
* Minimum	0.000	-2352.953	~~-9314.347~~	
Beam	1	1	~~3~~	
Load	201	393	~~570~~	

maximum shear value

Table B.23: NR load model - 3 x 35m system

MAXIMUM BEAM RESULTS (3x35m system) 350mm increments				Prokon
Beam	**Axial**	**V2**	**M3**	**Mmax**
* Maximum	0.000	2683.356	~~14391.523~~	13668.19
Beam	1	3	~~3~~	2
Load	1	530	~~716~~	
* Minimum	0.000	-2700.343	~~-12281.095~~	
Beam	1	1	~~3~~	
Load	1	393	~~569~~	

maximum shear value

Table B.24: NR load model - 3 x 40m system

MAXIMUM BEAM RESULTS (3x40m system) 400mm increments				Prokon
Beam	**Axial**	**V2**	**M3**	**Mmax**
* Maximum	0.000	3042.371	~~18794.488~~	17625.81
Beam	1	3	~~2~~	2
Load	1	527	~~206~~	
* Minimum	0.000	-3042.368	~~-15658.983~~	
Beam	1	1	~~1~~	
Load	1	393	~~348~~	

maximum shear value

B.4 STRAP results – 3 span (Eurocode) systems

Table B.25: SW/0 load model - 3 x 5m system

MAXIMUM BEAM RESULTS (3x5m system) 100mm increments			
Beam	**Axial**	**V2**	**M3**
* Maximum	0.000	456.748	390.570
Beam	1	3	2
Load	133	195	198
* Minimum	0.000	-456.748	-340.007
Beam	1	1	3
Load	119	107	252

maximum shear value

Table B.26: SW/0 load model - 3 x 10m system

MAXIMUM BEAM RESULTS (3x10m system) 100mm increments			
Beam	**Axial**	**V2**	**M3**
* Maximum	0.000	843.551	1391.112
Beam	1	3	2
Load	154	498	486
* Minimum	0.000	-843.551	-1274.735
Beam	1	1	3
Load	250	157	335

maximum shear value

Table B.27: SW/0 load model - 3 x 15m system

MAXIMUM BEAM RESULTS (3x15m system) 100mm increments			
Beam	**Axial**	**V2**	**M3**
* Maximum	0.000	1217.314	3059.342
Beam	1	3	3
Load	344	448	480
* Minimum	0.000	-1217.313	-2806.747
Beam	1	1	1
Load	330	357	147

maximum shear value

Table B.28: SW/0 load model - 3 x 20m system

MAXIMUM BEAM RESULTS (3x20m system) 100mm increments			
Beam	**Axial**	**V2**	**M3**
* Maximum	0.000	1528.487	5655.701
Beam	1	3	2
Load	373	548	377
* Minimum	0.000	-1528.487	-4734.441
Beam	1	1	1
Load	317	407	170

maximum shear value

Table B.29: SW/0 load model - 3 x 25m system

MAXIMUM BEAM RESULTS (3x25m system) 150mm increments			
Beam	**Axial**	**V2**	**M3**
* Maximum	0.000	1705.083	7811.578
Beam	1	3	1
Load	259	432	283
* Minimum	0.000	-1702.018	-6708.253
Beam	1	1	3
Load	263	305	609

maximum shear value

Table B.30: SW/0 load model - 3 x 30m system

MAXIMUM BEAM RESULTS (3x30m system) 150mm increments			
Beam	**Axial**	**V2**	**M3**
* Maximum	0.000	1944.259	9469.354
Beam	1	3	1
Load	264	634	315
* Minimum	0.000	-1939.105	-8750.265
Beam	1	1	3
Load	290	203	689

maximum shear value

Table B.31: SW/0 load model - 3 x 35m system

MAXIMUM BEAM RESULTS (3x35m system) 150mm increments			
Beam	**Axial**	**V2**	**M3**
* Maximum	0.000	2252.260	10761.548
Beam	1	3	1
Load	129	701	347
* Minimum	0.000	-2246.650	-11754.856
Beam	1	1	3
Load	127	236	680

maximum shear value

Table B.32: SW/0 load model - 3 x 40m system

MAXIMUM BEAM RESULTS (3x40m system) 200mm increments			
Beam	**Axial**	**V2**	**M3**
* Maximum	0.000	2531.136	11789.909
Beam	1	3	1
Load	88	576	285
* Minimum	0.000	-2521.656	-15317.229
Beam	1	1	3
Load	150	202	579

maximum shear value

Appendix C:

C.1 STRAP results – Mmax position for 2 span (SATS) systems

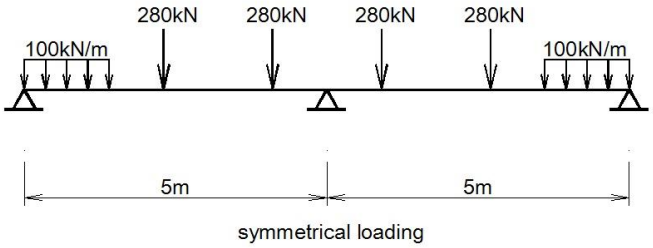

Figure C.1 Load position for M_{max} for 2 X 5m system (SATS NR load model)

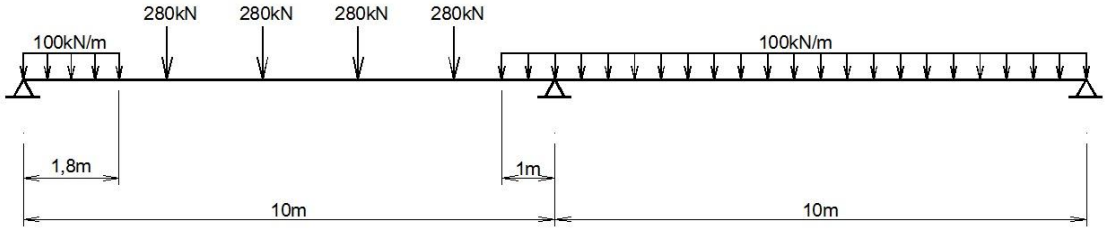

Figure C.2 Load position for M_{max} for 2 X 10m system (SATS NR load model)

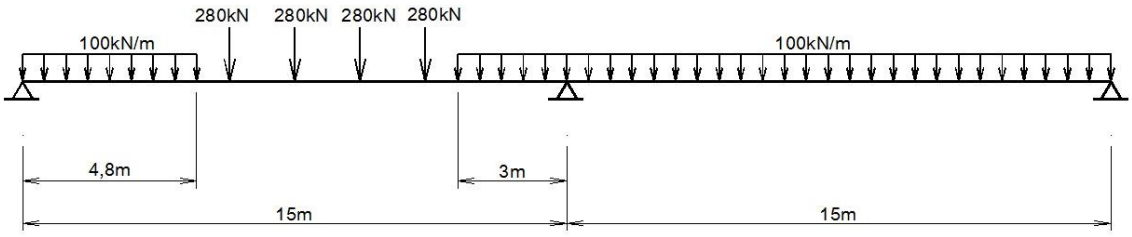

Figure C.3 Load position for M_{max} for 2 X 15m system (SATS NR load model)

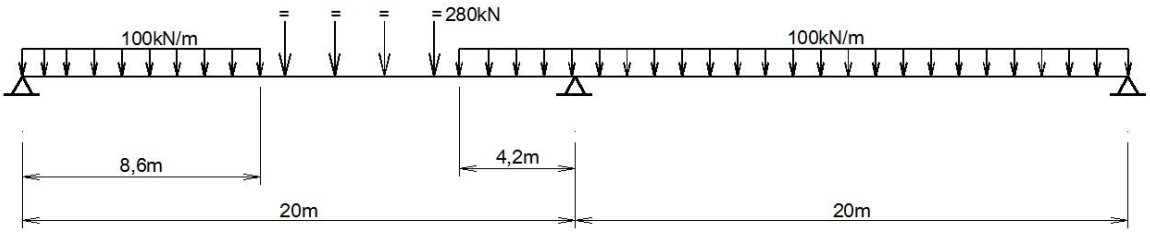

Figure C.4 Load position for M_{max} for 2 X 20m system (SATS NR load model)

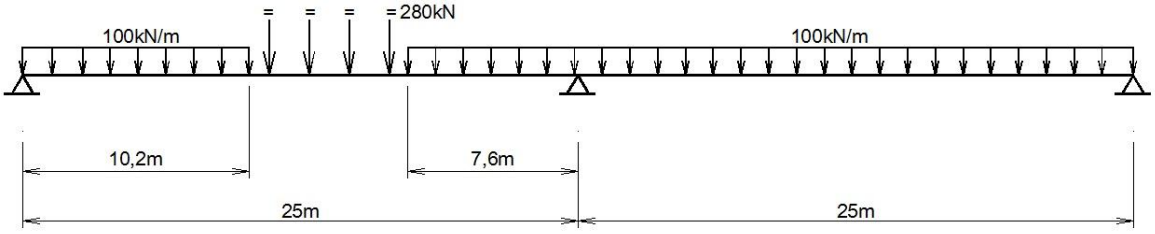

Figure C.5 Load position for M_{max} for 2 X 25m system (SATS NR load model)

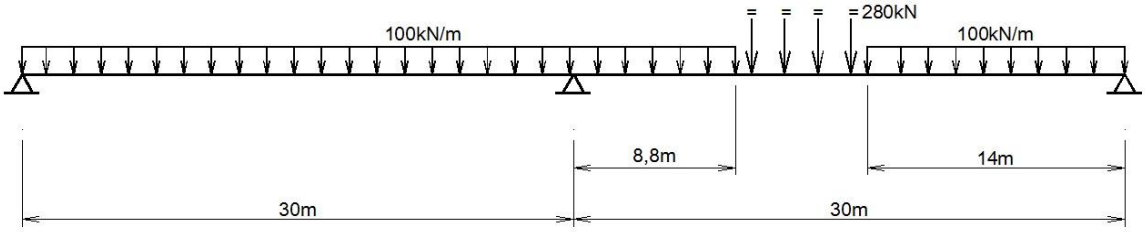

Figure C.6 Load position for M_{max} for 2 X 30m system (SATS NR load model)

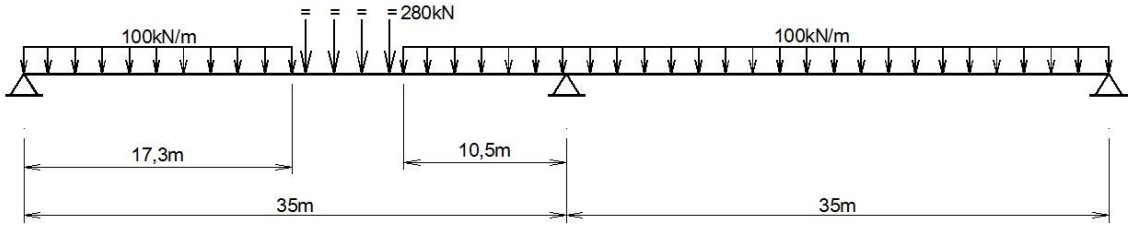

Figure C.7 Load position for M_{max} for 2 X 35m system (SATS NR load model)

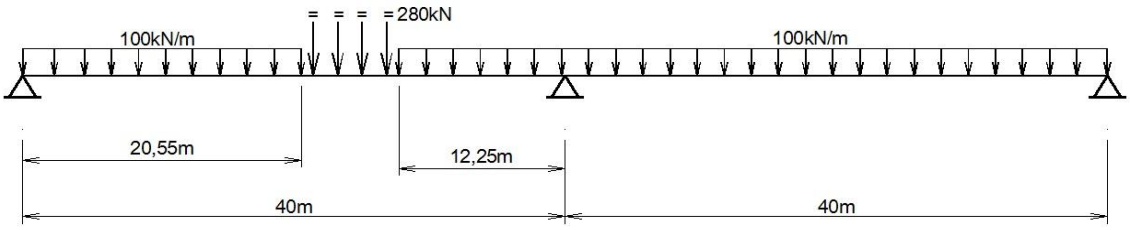

Figure C.8 Load position for M_{max} for 2 X 40m system (SATS NR load model)

C.2 STRAP results – Mmax position for 2 span (Eurocode) systems

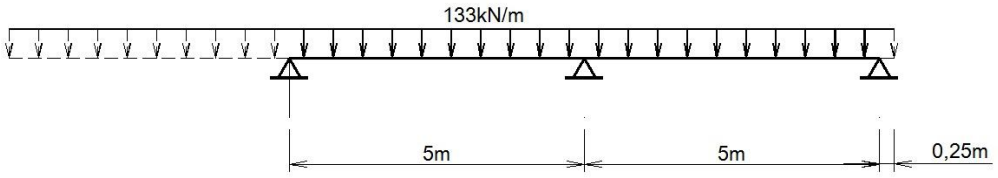

Figure C.9 Load position for M_{max} for 2 X 5m system (SW/0 load model)

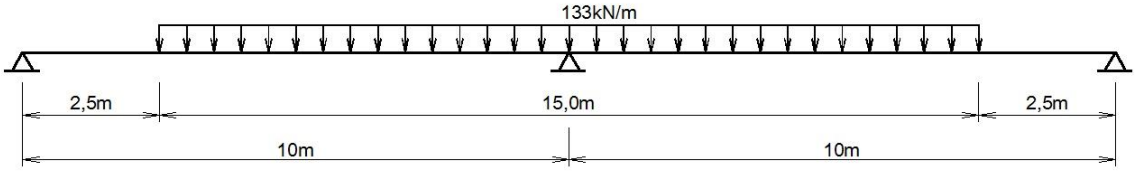

Figure C.10 Load position for M_{max} for 2 X 10m system (SW/0 load model)

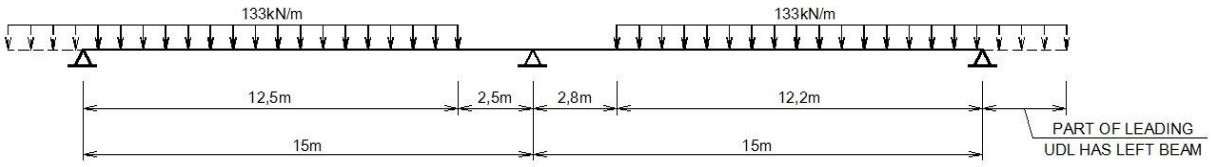

Figure C.11 Load position for M_{max} for 2 X 15m system (SW/0 load model)

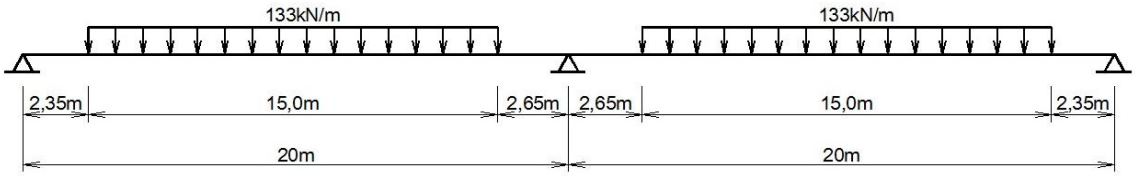

Figure C.12 Load position for M_{max} for 2 X 20m system (SW/0 load model)

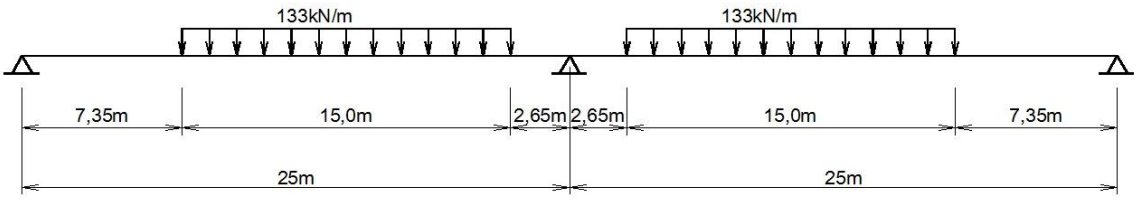

Figure C.13 Load position for M_{max} for 2 X 25m system (SW/0 load model)

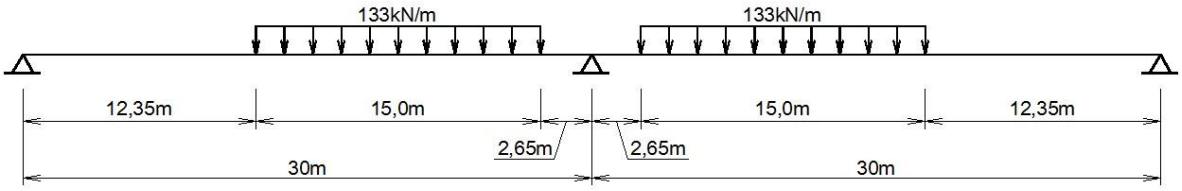

Figure C.14 Load position for M_{max} for 2 X 30m system (SW/0 load model)

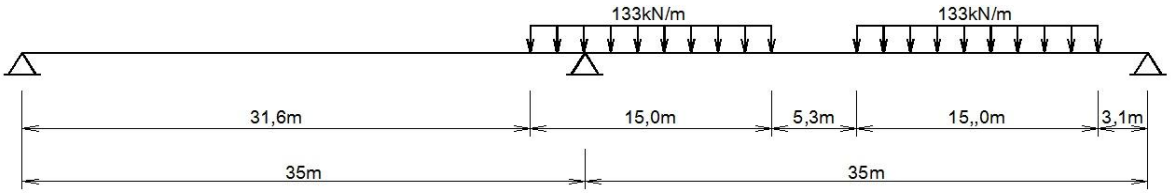

Figure C.15 Load position for M_{max} for 2 X 35m system (SW/0 load model)

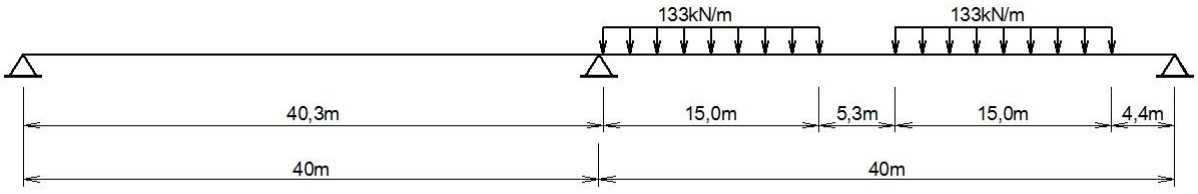

Figure C.16 Load position for M_{max} for 2 X 40m system (SW/0 load model)

C.3 STRAP results – Vmax position for 2 span (SATS) systems

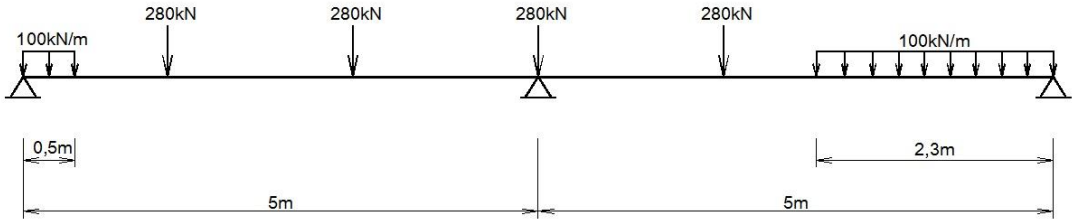

Figure C.17 Load position for V_{max} for 2 X 5m system (NR load model)

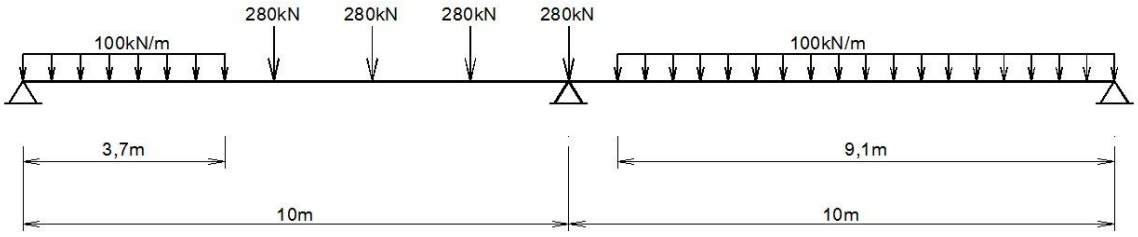

Figure C.18 Load position for V_{max} for 2 X 10m system (NR load model)

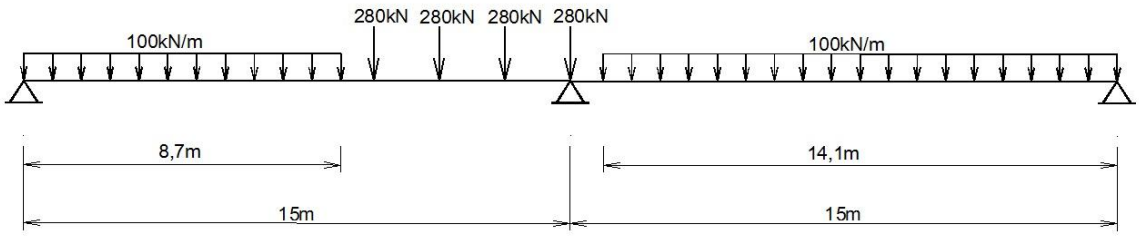

Figure C.19 Load position for V_{max} for 2 X 15m system (NR load model)

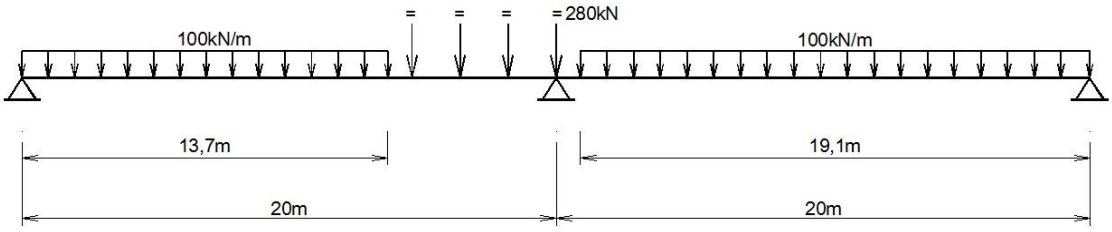

Figure C.20 Load position for V_{max} for 2 X 20m system (NR load model)

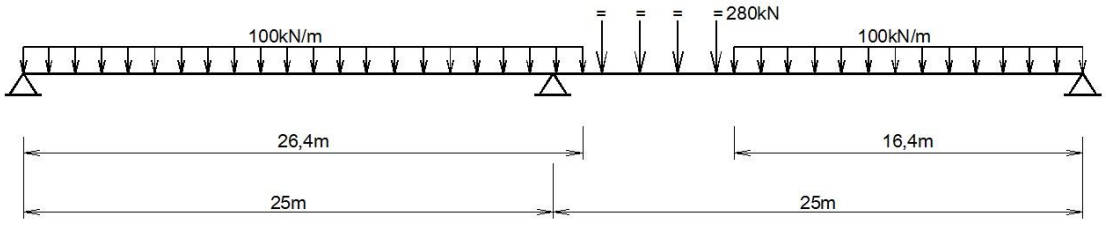

Figure C.21 Load position for V_{max} for 2 X 25m system (NR load model)

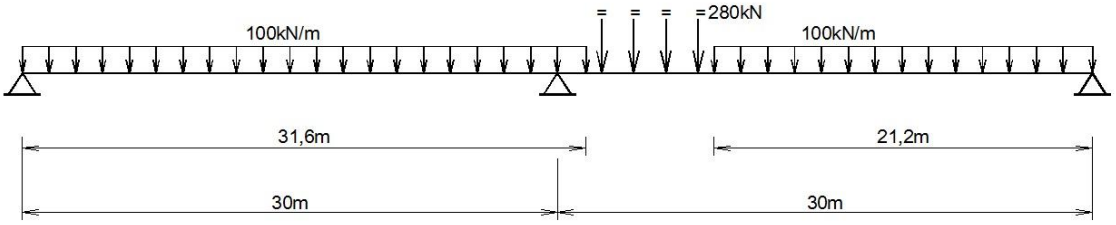

Figure C.22 Load position for V_{max} for 2 X 30m system (NR load model)

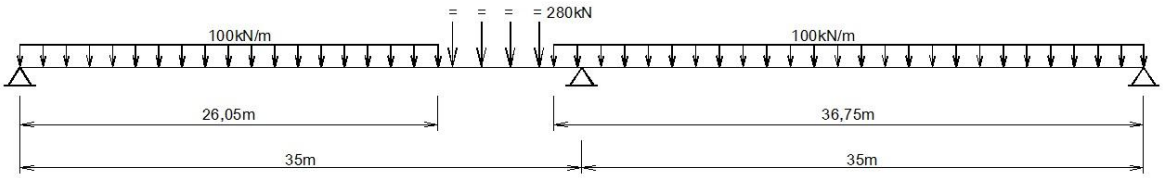

Figure C.23 Load position for V_{max} for 2 X 35m system (NR load model)

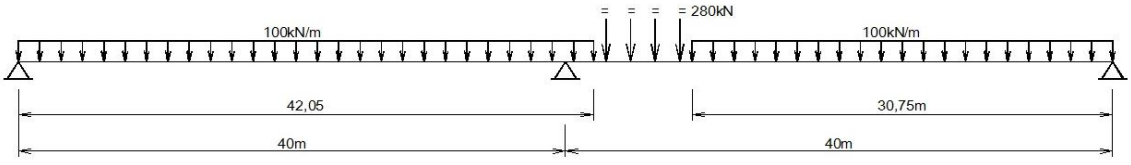

Figure C.24 Load position for V_{max} for 2 X 40m system (NR load model)

C.4 STRAP results – Vmax position for 2 span (Eurocode) systems

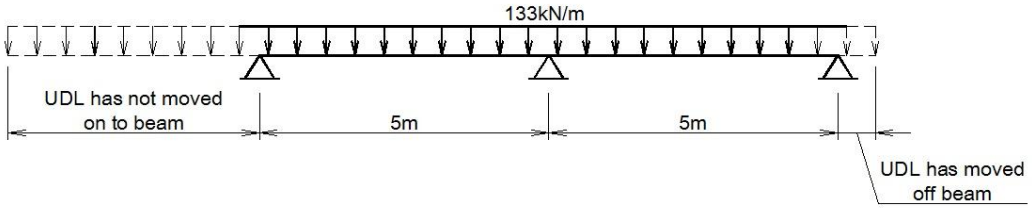

Figure C.25 Load position for V_{max} for 2 X 5m system (SW/0 load model)

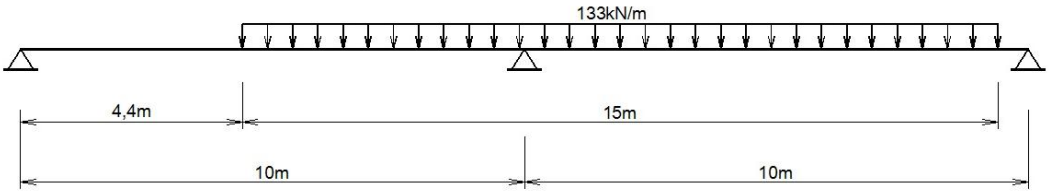

Figure C.26 Load position for V_{max} for 2 X 10m system (SW/0 load model)

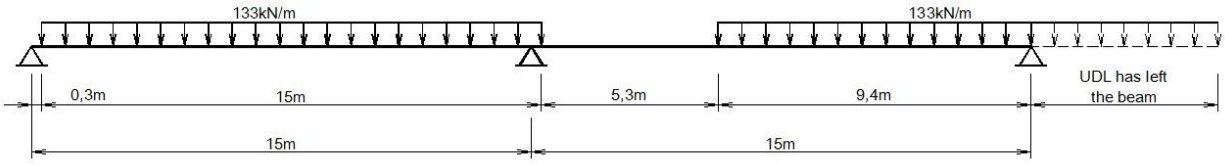

Figure C.27 Load position for V_{max} for 2 X 15m system (SW/0 load model)

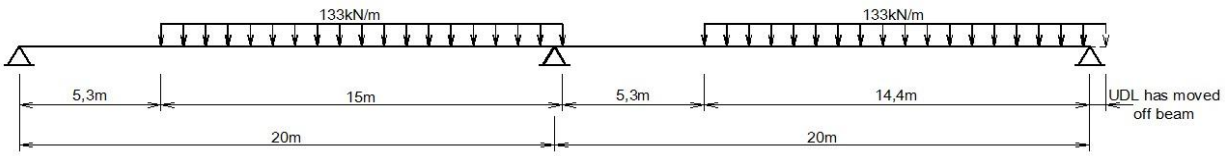

Figure C.28 Load position for V_{max} for 2 X 20m system (SW/0 load model)

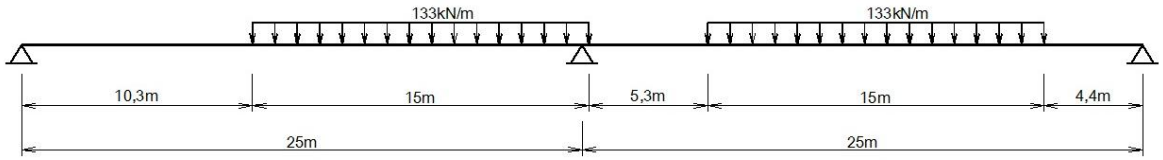

Figure C.29 Load position for V_{max} for 2 X 25m system (SW/0 load model)

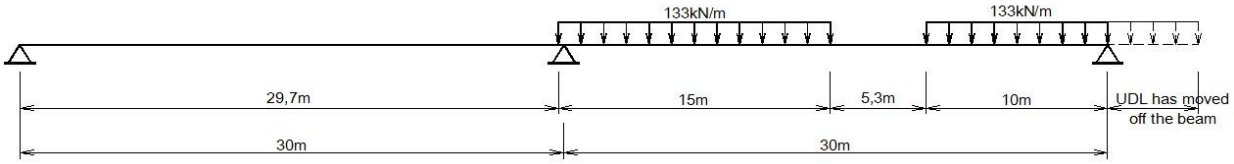

Figure C.30 Load position for V_{max} for 2 X 30m system (SW/0 load model)

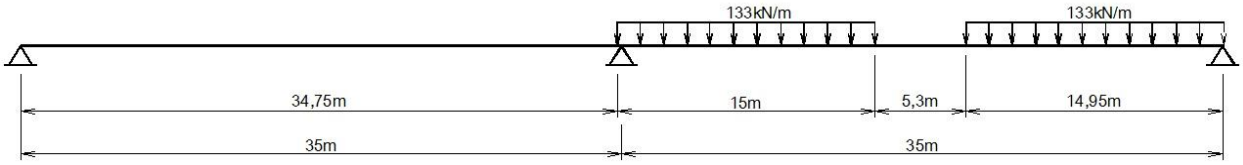

Figure C.31 Load position for V_{max} for 2 X 35m system (SW/0 load model)

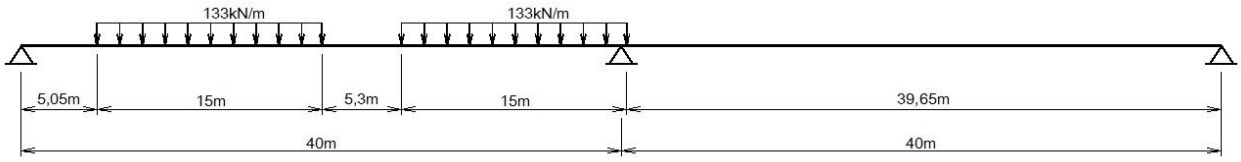

Figure C.32 Load position for V_{max} for 2 X 40m system (SW/0 load model)

Appendix D:

D.1 STRAP results – Mmax position for 3 span (SATS) systems

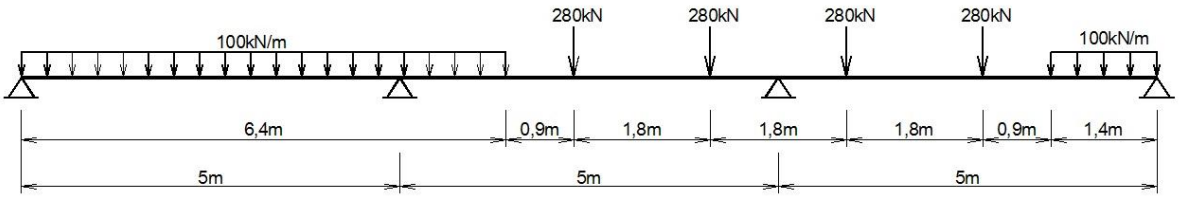

Figure D.1 Load position for M_{max} for 3 X 5m system (NR load model)

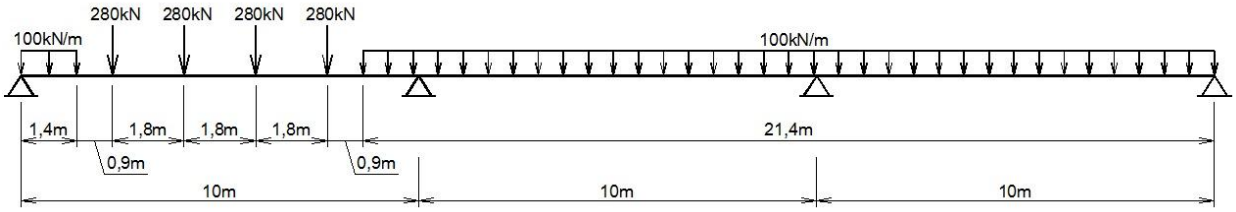

Figure D.2 Load position for M_{max} for 3 X 10m system (NR load model)

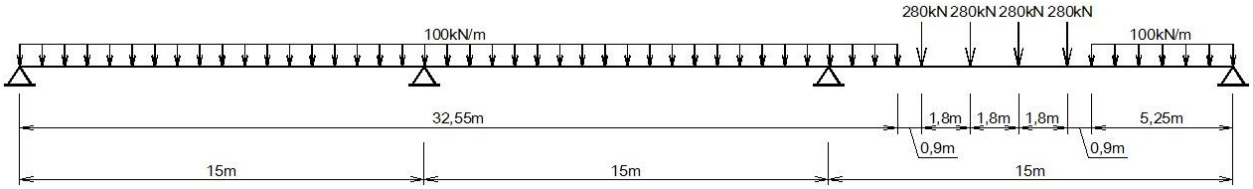

Figure D.3 Load position for M_{max} for 3 X 15m system (NR load model)

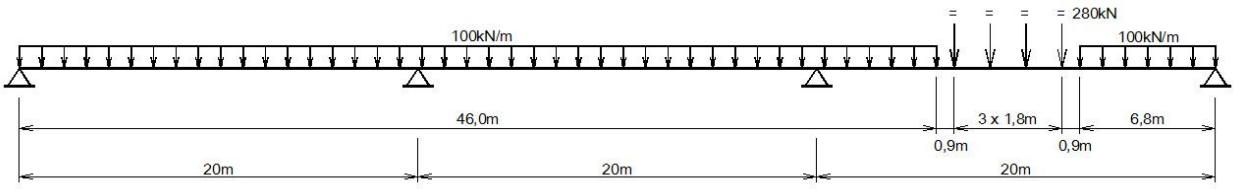

Figure D.4 Load position for M_{max} for 3 X 20m system (NR load model)

D.2 PROKON results – Mmax position for 3 span (SATS) systems

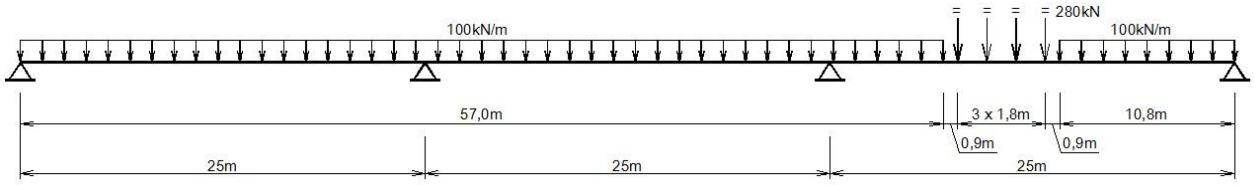

Figure D.5 Load position for M_{max} for 3 X 25m system (NR load model)

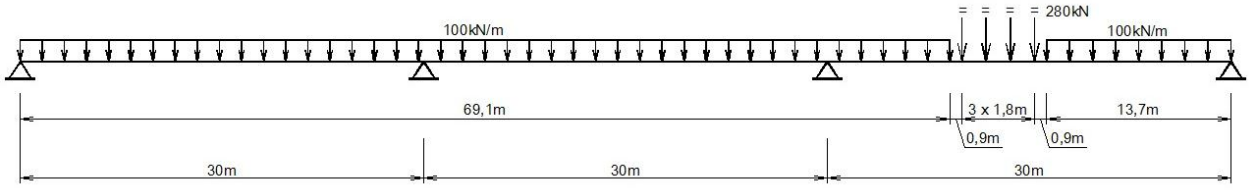

Figure D.6 Load position for M_{max} for 3 X 30m system (NR load model)

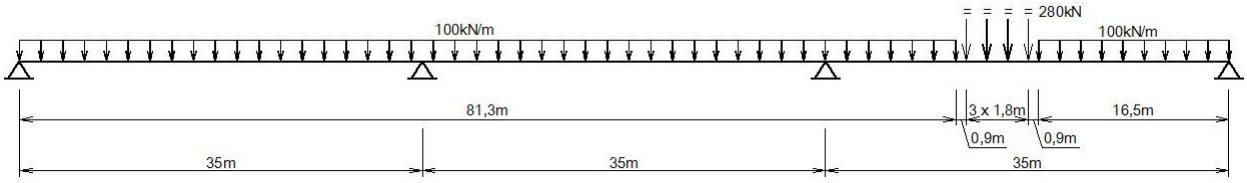

Figure D.7 Load position for M_{max} for 3 X 35m system (NR load model)

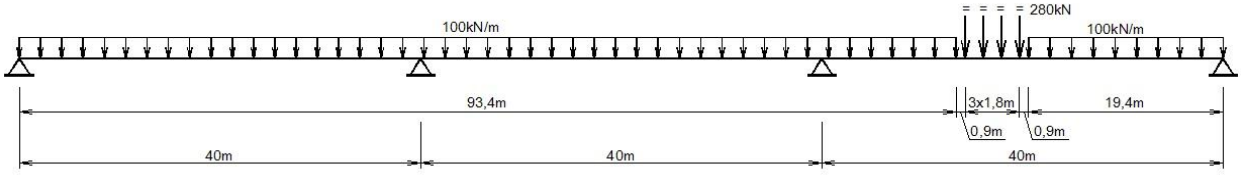

Figure D.8 Load position for M_{max} for 3 X 40m system (NR load model)

D.3 STRAP results – Mmax position for 3 span (Eurocode) systems

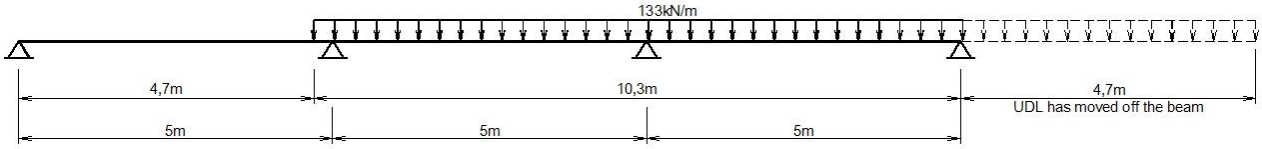

Figure D.9 Load position for M_{max} for 3 X 5m system (SW/0 load model)

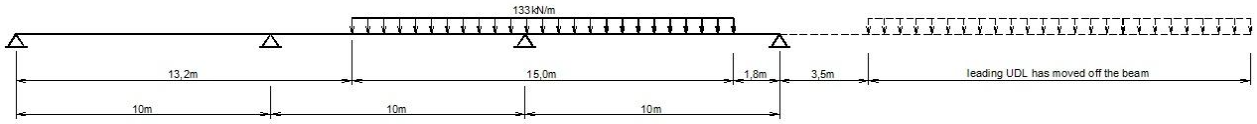

Figure D.10 Load position for M_{max} for 3 X 10m system (SW/0 load model)

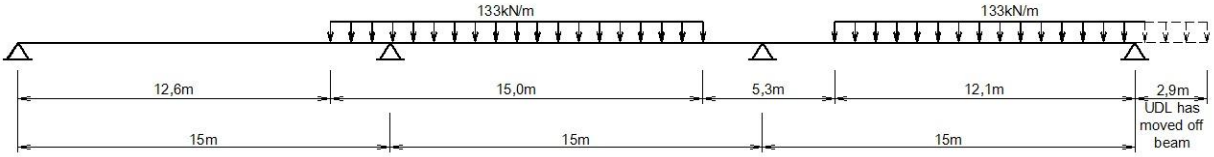

Figure D.11 Load position for M_{max} for 3 X 15m system (SW/0 load model)

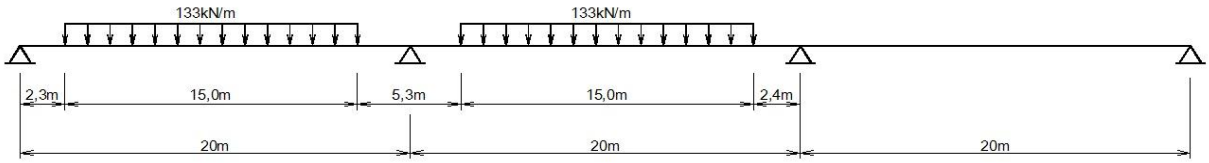

Figure D.12 Load position for M_{max} for 3 X 20m system (SW/0 load model)

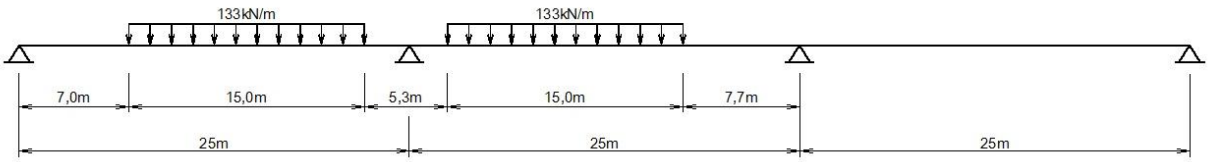

Figure D.13 Load position for M_{max} for 3 X 25m system (SW/0 load model)

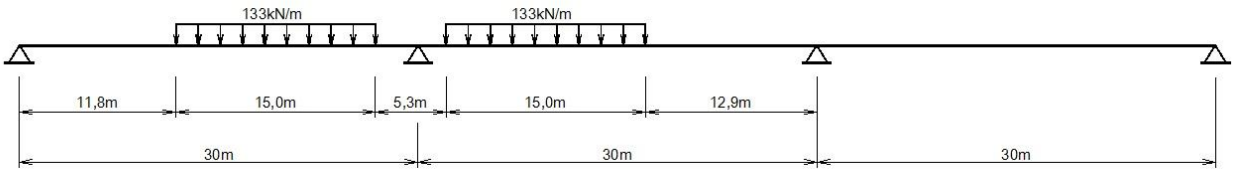

Figure D.14 Load position for M_{max} for 3 X 30m system (SW/0 load model)

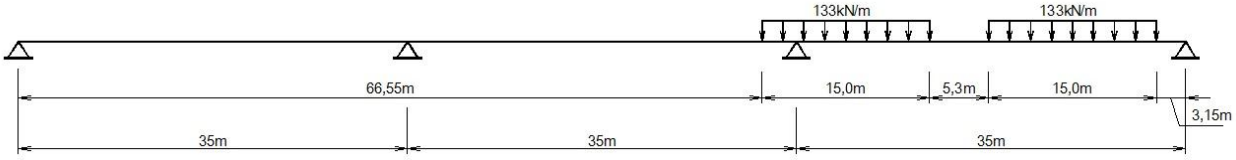

Figure D.15 Load position for M_{max} for 3 X 35m system (SW/0 load model)

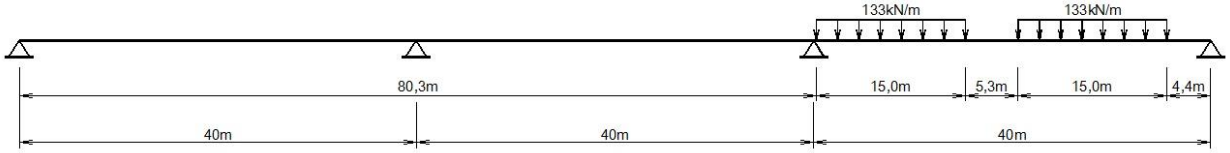

Figure D.16 Load position for M_{max} for 3 X 40m system (SW/0 load model)

D.4 STRAP results – Vmax position for 3 span (SATS) systems

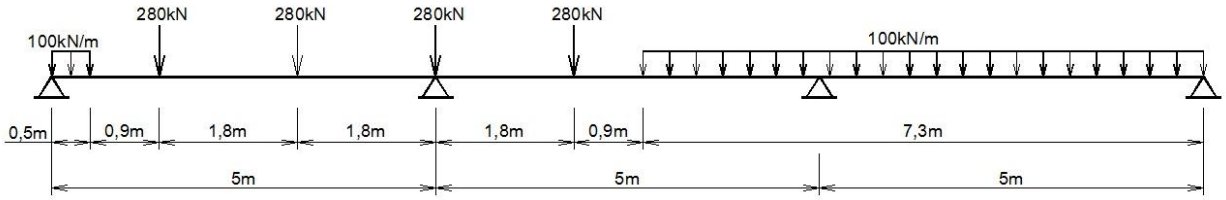

Figure D.17 Load position for V_{max} for 3 X 5m system (NR load model)

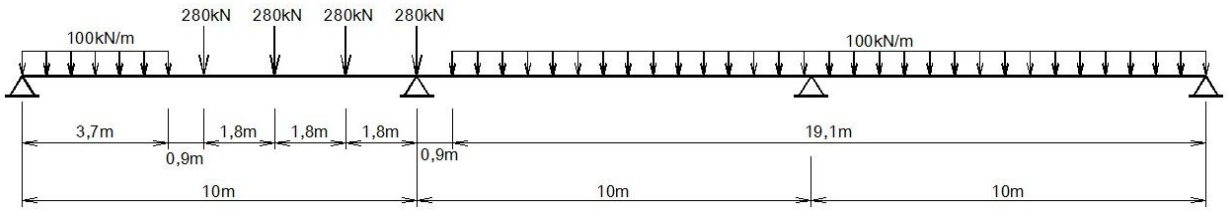

Figure D.18 Load position for V_{max} for 3 X 10m system (NR load model)

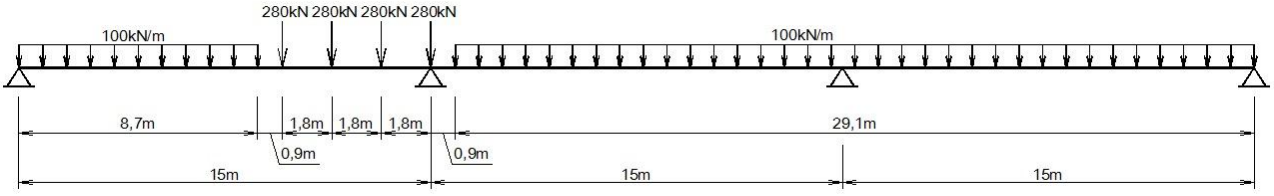

Figure D.19 Load position for V_{max} for 3 X 15m system (NR load model)

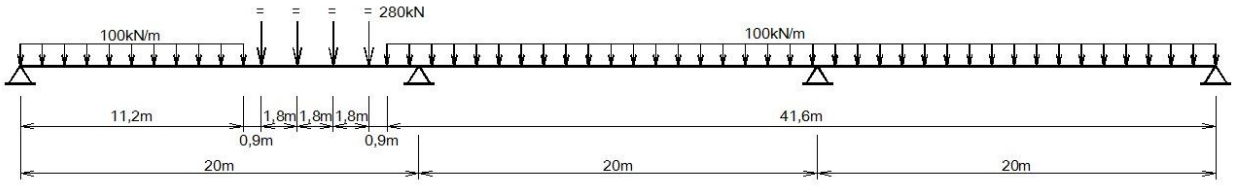

Figure D.20 Load position for V_{max} for 3 X 20m system (NR load model)

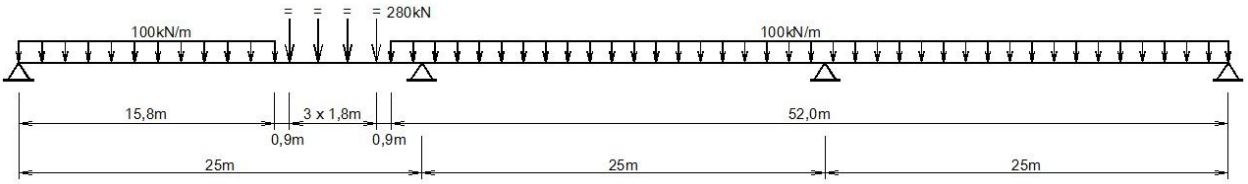

Figure D.21 Load position for V_{max} for 3 X 25m system (NR load model)

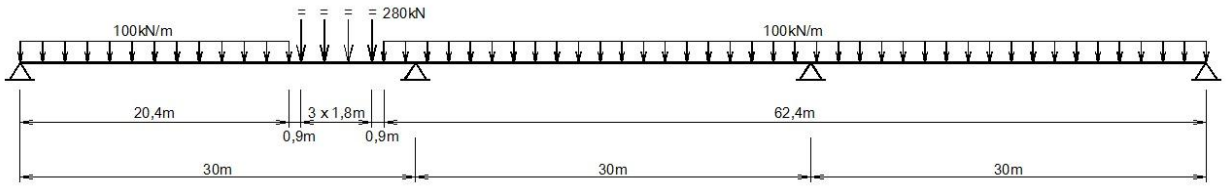

Figure D.22 Load position for V_{max} for 3 X 30m system (NR load model)

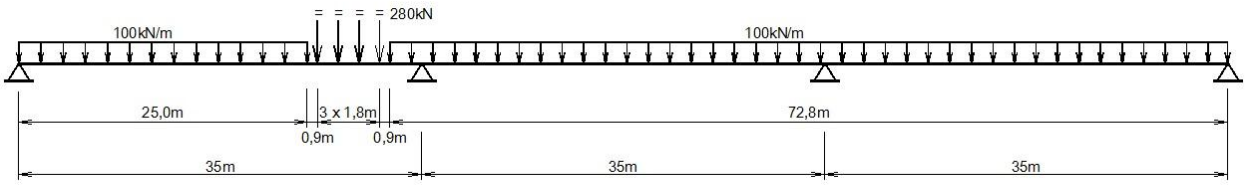

Figure D.23 Load position for V_{max} for 3 X 35m system (NR load model)

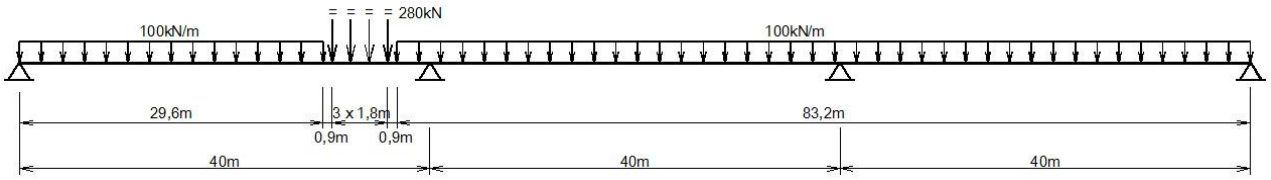

Figure D.24 Load position for V_{max} for 3 X 40m system (NR load model)

D.5 STRAP results – Vmax position for 3 span (Eurocode) systems

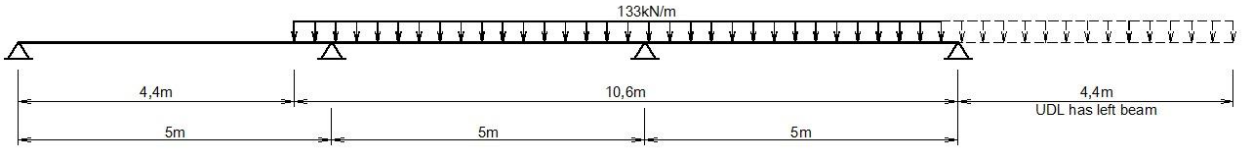

Figure D.25 Load position for V_{max} for 3 X 5m system (SW/0 load model)

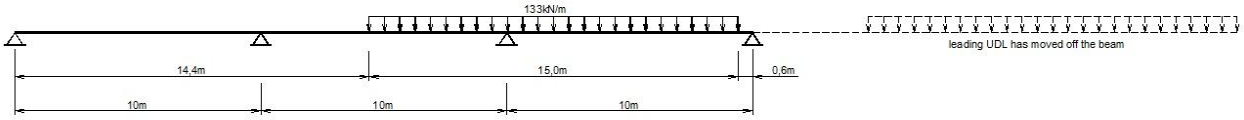

Figure D.26 Load position for V_{max} for 3 X 10m system (SW/0 load model)

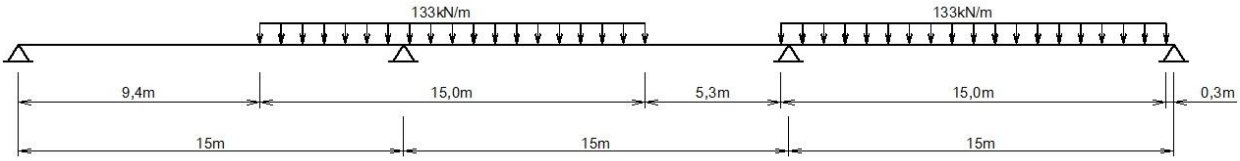

Figure D.27 Load position for V_{max} for 3 X 15m system (SW/0 load model)

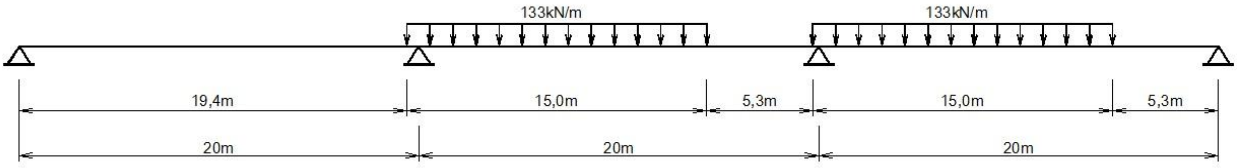

Figure D.28 Load position for V_{max} for 3 X 20m system (SW/0 load model)

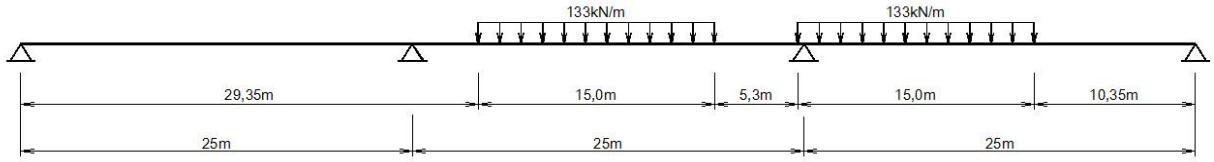

Figure D.29 Load position for V_{max} for 3 X 25m system (SW/0 load model)

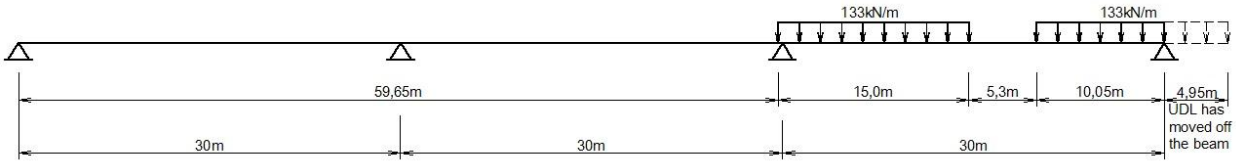

Figure D.30 Load position for V_{max} for 3 X 30m system (SW/0 load model)

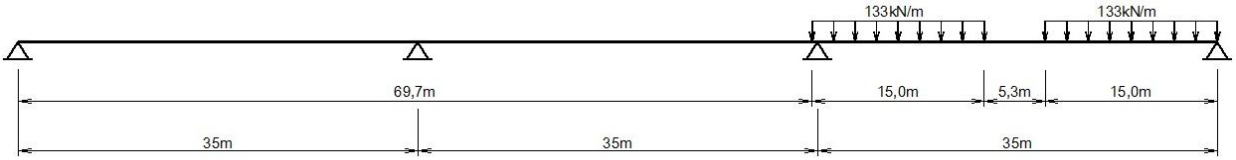

Figure D.31 Load position for V_{max} for 3 X 35m system (SW/0 load model)

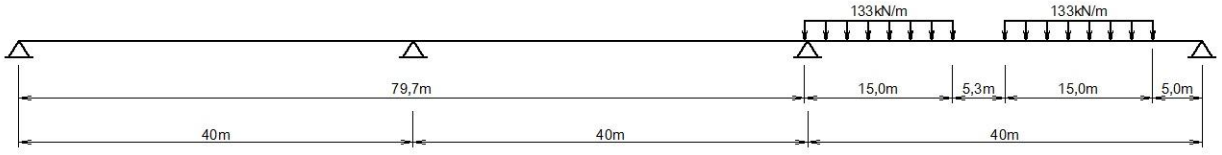

Figure D.32 Load position for V_{max} for 3 X 40m system (SW/0 load model)